NUREG–1519

Surface Interactions of Cesium and Boric Acid with Stainless Steel

U.S. Nuclear Regulatory Commission

Office of Nuclear Regulatory Research

N. Grossman-Canfield

AVAILABILITY NOTICE

Availability of Reference Materials Cited in NRC Publications

Most documents cited in NRC publications will be available from one of the following sources:

1. The NRC Public Document Room, 2120 L Street, NW., Lower Level, Washington, DC 20555-0001
2. The Superintendent of Documents, U.S. Government Printing Office, P. O. Box 37082, Washington, DC 20402-9328
3. The National Technical Information Service, Springfield, VA 22161-0002

Although the listing that follows represents the majority of documents cited in NRC publications, it is not intended to be exhaustive.

Referenced documents available for inspection and copying for a fee from the NRC Public Document Room include NRC correspondence and internal NRC memoranda; NRC bulletins, circulars, information notices, inspection and investigation notices; licensee event reports; vendor reports and correspondence; Commission papers; and applicant and licensee documents and correspondence.

The following documents in the NUREG series are available for purchase from the Government Printing Office: formal NRC staff and contractor reports, NRC-sponsored conference proceedings, international agreement reports, grantee reports, and NRC booklets and brochures. Also available are regulatory guides, NRC regulations in the *Code of Federal Regulations*, and *Nuclear Regulatory Commission Issuances*.

Documents available from the National Technical Information Service include NUREG-series reports and technical reports prepared by other Federal agencies and reports prepared by the Atomic Energy Commission, forerunner agency to the Nuclear Regulatory Commission.

Documents available from public and special technical libraries include all open literature items, such as books, journal articles, and transactions. *Federal Register* notices, Federal and State legislation, and congressional reports can usually be obtained from these libraries.

Documents such as theses, dissertations, foreign reports and translations, and non-NRC conference proceedings are available for purchase from the organization sponsoring the publication cited.

Single copies of NRC draft reports are available free, to the extent of supply, upon written request to the Office of Administration, Distribution and Mail Services Section, U.S. Nuclear Regulatory Commission, Washington DC 20555-0001.

Copies of industry codes and standards used in a substantive manner in the NRC regulatory process are maintained at the NRC Library, Two White Flint North, 11545 Rockville Pike, Rockville, MD 20852-2738, for use by the public. Codes and standards are usually copyrighted and may be purchased from the originating organization or, if they are American National Standards, from the American National Standards Institute, 1430 Broadway, New York, NY 10018-3308.

NUREG-1519

Surface Interactions of Cesium and Boric Acid with Stainless Steel

Manuscript Completed: January 1995
Date Published: August 1995

N. Grossman-Canfield

Division of Systems Technology
Office of Nuclear Regulatory Research
U.S. Nuclear Regulatory Commission
Washington, DC 20555-0001

ABSTRACT

In this report, the effects of cesium hydroxide and boric acid on oxidized stainless steel surfaces at high temperatures and near one atmosphere of pressure are investigated. This is the first experimental investigation of this chemical system. The experimental investigations were performed using a mass spectrometer and a mass electrobalance. Surfaces from the different experiments were examined using a scanning electron microscope to identify the presence of deposited species, and electron spectroscopy for chemical analysis to identify the species deposited on the surface.

A better understanding of the equilibrium thermodynamics, the kinetics of the steam-accelerated volatilizations, and the release kinetics are gained by these experiments. The release rate is characterized by bulk vaporization/gas-phase mass transfer data. The analysis couples vaporization, deposition, and desorption of the compounds formed by cesium hydroxide and boric acid under conditions similar to what is expected during certain nuclear reactor accidents.

This study shows that cesium deposits on an oxidized stainless steel surface at temperatures between 1000 and 1200 Kelvin. Cesium also deposits on stainless steel surfaces coated with boric oxide in the same temperature ranges. The mechanism for cesium deposition onto the oxide layer was found to involve the chemical reaction between cesium and chromate. Some revaporization in the cesium hydroxide-boric acid system was observed. It has been found that under the conditions given, boric acid will react with cesium hydroxide to form cesium metaborate. A model is proposed for this chemical reaction.

CONTENTS

TABLES

FIGURES

PREFACE

Since the reactor accident at Three Mile Island, there has been an awareness that retention of radionuclides in the reactor coolant system can substantially alter the inventory of the radionuclides that could be released to the environment during a severe reactor accident. Analyses published by Battelle Columbus Laboratory (BMI-2104*) show that for some of the risk-significant severe reactor accident scenarios, retention of cesium, iodine, and tellurium in the reactor coolant system would exceed 75 percent of the core inventory of those elements.

Previously deposited fission products may be revaporized if the temperature of the surfaces increases. Cesium, iodine, tellurium, and, to a lesser extent antimony are the radionuclides usually thought to be most easily revaporized. Although these radionuclides are important, the behavior of cesium is the focus of this report.

VICTORIA is a code used by the U.S. Nuclear Regulatory Commission for fission product analysis in a severe nuclear reactor accident. VICTORIA models radionuclide behavior in the reactor coolant system under severe accident conditions. The VICTORIA model is intended to predict both the release of radionuclides from degrading reactor fuel and the transport of these radionuclides through the reactor coolant system.

Recently, a group of experts on fission product transport and behavior experts reviewed information from previous experiments concerning separate effects testing, computer codes, and modeling on the primary system fission product release and transport**. Chapter 4 of that document includes a comprehensive discussion of the physical and chemical phenomena in the primary system during a severe accident, such as the vapor-phase phenomenon. Although there has been significant progress in the area of modeling fission product behavior, the experts have identified several areas of uncertainty in thermodynamics and speciation, vapor condensation, and vapor/surface and vapor/aerosol reactions.

Evidence from limited laboratory studies suggests that at temperatures of about 1100 Kelvin, deposited cesium rapidly converts to a less volatile state. Laboratory studies of radionuclide retention on surfaces are needed to provide the basis for improved surface models in VICTORIA.

---

* J. A. Gieseke et al., "Radionuclide Release Under Specific LWR Accident Conditions," draft, 1983-1986, BMI-2104 Vols. I-VIII.

** U.S. Nuclear Regulatory Commission, "Primary System Fission Product Release and Transport:A State of the Art Report on the Safety of Nuclear Installations," NUREG/CR-6193, June 1994.

LIST OF ABBREVIATIONS

BWR	boiling-water reactor
ECCS	emergency core cooling system
ESCA	electron spectroscopy for chemical analyses
PWR	pressurized-water reactor
RCS	reactor coolant system
SEM	scanning electron microscope
TMI-2	Three Mile Island Unit 2

Chemical Compounds

B_2O_3	boric oxide
Cs	cesium
$CsBO_2$	cesium metaborate
Cs_2CrO_4	cesium chromate
$Cs_2Cr_2O_4$	cesium chromite
CsO	cesium oxide
CsOH	cesium hydroxide
H_2	hydrogen
H_2O	water (steam)
H_3BO_3	boric acid
HBO_2	metaboric acid
(c)	condensed phase
(g)	gaseous phase
(s)	solid phase

CHAPTER 1

INTRODUCTION AND LITERATURE REVIEW

A severe accident in a nuclear power plant poses a risk to the public health and safety from a possible release of radioisotopes. During a severe accident, it is postulated that the fuel melts and releases fission products into the primary system. Exposure to any radioisotope is hazardous; however, some radioisotopes are more toxic than others, e.g. cesium, iodine, ruthenium.

If the primary system remains intact, little if any exposure to the public would occur. However, in the event of a primary system rupture, many of the radionuclides would be released into the containment. The amount of each radioisotope entering the containment depends in great measure on the possible retention by the surfaces of the primary system and in the remaining primary coolant. The degree of this retention thus affects the severity of any postulated further release in the event of a containment failure. Some of the factors that may affect the retention of the various radioisotopes are temperature, surface conditions, chemical environment (such as the presence of boron compounds, hydrogen, or steam), and the physical form of the radioisotope-bearing material. For example, if the form of the radioisotope is that of an aerosol or is water soluble, the containment scrubbing systems (such as sprays and de-misters) would remove a larger fraction of these materials than would otherwise be the case.

Presently, computer codes such as VICTORIA are used to estimate the fission product release from the primary system, accounting for known chemical and surface interactions. An accurate knowledge of these reactions is essential for a realistic prediction of the source term.

Following the severe accident to the nuclear power reactor at Three Mile Island Unit 2 (TMI-2), the fate of volatile radioisotopes and aerosols resulting from such an event became of greater concern. Cesium was a radionuclide of primary interest in studies of the TMI-2 accident conducted by Baston et al. Because of its radiobiological importance, the transport of cesium and its interaction with both the surfaces of the primary system and the containment structure are of interest. Cesium is a radiobiologically significant product, and an understanding of its deposition and revaporization characteristics is important in severe accident analysis. Revaporization of cesium can lead to unanticipated consequences if it were to occur at later times during an accident transient, especially in the event of containment failure. In addition, cesium reacts with the oxidized stainless steel surface of the primary system, which leads to an enhancement of corrosion of this surface. The atmosphere in a nuclear power reactor following such an incident aggravates the negative effects of the cesium. For example, hydrogen and steam increase the volatility of cesium hydroxide and boric acid and could affect the cesium inventory retained on the surface.

The objective of this research is to investigate the effects of vapor deposition of cesium and cesium compounds onto an oxidized stainless steel surface at high temperatures and pressure near one atmosphere (1 atm) with and without boric acid present. This study determines the degree to which boric acid reduces the volatility of cesium-bearing compounds in a hydrogen and steam atmosphere through the formation of less volatile compounds. Experiments have already shown that under some severe accident conditions that cesium in a steam environment will form cesium hydroxide, and that this reaction product is more likely in a steam-hydrogen, high-temperature environment (NUREG-0772). Deposition and revaporization of various forms of cesium hydroxide and boric acid are important phenomena that take place on the surface. Under certain conditions, boric acid will react with cesium hydroxide to form cesium metaborate, which is less volatile than cesium hydroxide in the presence of hydrogen and steam. The vapor-vapor and the vapor-solid reactions on the oxidized stainless steel surface are to be evaluated in the course of this investigation.

The effects on the source term from the cesium hydroxide and boric acid interactions is most important in the reactor coolant system pipes. Stainless steel is widely used in the reactor upper internals, piping systems, and the steam generators. During severe accident conditions, the growth of oxide film layers on core structures, primary piping, control rods, and cladding is accelerated. The reaction of cesium with an oxidized layer can also modify the release. Analysis of structure samples from the upper plenum of the TMI-2 reactor vessel after the accident revealed some evidence of cesium hydroxide retention (Baston et al.).

Models describing the chemical interactions provide assistance in analyzing the magnitude of the effects of the stainless steel on the chemical form of fission products released. The surfaces under investigation are the stainless steel and the associated oxide layer and these are of most interest after the cesium hydroxide and boric acid are introduced to the surface in vapor form.

This is the first study to investigate the deposition and revaporization of boric acid and cesium hydroxide on an oxidized stainless steel surface in the presence of low partial pressures of hydrogen and steam at high system temperatures. Since revaporization is dependent on the chemical form of deposited compounds, the chemical compounds involved in the deposition and revaporization will be thoroughly investigated.

These mechanisms are studied using two different sets of experimental apparatus. The first set was an oxidized stainless steel reaction cell into which steam and hydrogen were fed and allowed to interact with the walls. A mass spectrometer was connected to the reaction cell to analyze the vapors formed. The second set was an apparatus constructed to determine mass changes on the surface. This apparatus utilized a reaction chamber that had steam and hydrogen continuously flowing inside where an oxidized stainless steel sample resided. Cesium hydroxide and boric acid were fed into the reaction chamber and the reaction cell

of the two sets of apparatus in order for the compounds to mix with the steam and hydrogen in the reaction areas.

Following reactor accidents, deposition of fission products onto the oxidized surfaces would be caused by various mechanisms such as vapor deposition, formation of aerosols and their deposition, thermophoresis, and chemisorption. In this study, the major mechanisms are those due to vapor deposition, aerosol formation and deposition, and chemisorption. The measurement techniques used in this study cannot distinguish the mechanism of deposition. The chemical species and their physical forms (gas, liquid, or solid) are identified for this investigation.

1.1 Deposition and Revaporization of Cesium and Boric Acid

Under severe accident conditions in a nuclear reactor, once the volatile fission products leave the fuel, the interaction with oxidized stainless steel surfaces will include condensation and chemical interaction of some vapor species with nearby surfaces (NUREG-0772). The interactions of those volatile compounds with the structural materials have not been fully characterized. In NUREG/CR-6193, the authors specifically note that boric acid reacts chemically with the stainless steel surface, an interaction that can affect the release of cesium. The authors indicate that this system needs to be further characterized. A significantly better understanding of the kinetics of the volatile vapors and their reaction products is needed.

Retention of radionuclides in the reactor coolant system may not be permanent. Because of convection and radioactive decay, heat loads on deposited radionuclides may be sufficiently intense that deposited materials revaporize later in an accident (Elrick & Sallach). Heating of the surfaces resulting from decay of deposited radioactive materials may provide enough energy to revaporize the fission products deposited on the surface in this process (Kazikowski et al.). The timing and extent of revaporization depend critically on the chemical form of deposited materials. Powers and Bieniarz showed that cesium revaporization is substantially inhibited when the element is involved in reactions that form cesium metaborate on structural surfaces. They found that revaporization could essentially be stopped if cesium formed a mixture of 10-percent cesium metaborate in addition to the cesium hydroxide and boric acid on the surface. They also found that cesium metaborate is less volatile than cesium hydroxide in the presence of hydrogen and steam.

The rate of revaporization is determined by the vapor pressure of the deposit, which is strongly dependent on temperature. If the partial pressure of the deposit is higher than that in the bulk gas, the deposit will revaporize. Vapor deposition (and revaporization) is strongly controlled by the pressure of the bulk gas.

In recent years, interest in revaporization of deposited radionuclides has increased for two reasons:

First, revaporization impacts the source term, and current analysis shows that the decay heat from the deposited radionuclides causes a larger temperature increase on the surface than was formerly believed. Analyses of core degradation during severe reactor accidents have shown that, for many risk-significant accident sequences, natural circulation flow patterns develop within the reactor coolant system. The natural circulation flows transfer heat from the degrading core to primary surfaces of the balance of the reactor coolant system. Heat is generated in the same areas in which radionuclides have been deposited, thus resulting in elevated temperatures in the region of deposition. The revaporization release or late in-vessel release could occur at a constant rate over a 10-hour period after core damage. This slow revaporization can replace the radioactive materials lost, due to natural aerosol processes (e.g., sedimentation, deposition and thermophoresis), from the containment atmosphere.

Second, radionuclide deposition and the potential for revaporization have received increased attention because of the results of the NRC study on severe accident risks (NUREG-1150). This study showed that "bypass" accidents could be risk dominant. Bypass accident sequences are those that involve flow from the reactor coolant system directly to the external environment. This could occur by way of the secondary side of steam generators or through auxiliary buildings without passing through the containment atmosphere. The containment is one of the major barriers of defense in depth against radionuclide release. In such accident sequences, the source term* attenuation normally expected to take place in the containment does not occur. For these risk-dominant accidents, the major attenuation is provided by retention on the surfaces in the reactor coolant system. To the extent that revaporization can occur, the source term attenuation by retention on these surfaces would be reduced.

Transport of material in aerosol form in the reactor vessel is of concern in a severe accident scenario. Absorption of the aerosol on the internal vessel walls and structures could enhance corrosion that can cause premature failure (Kazikowski et al.). This arises in part as a result of certain reactions that involve increased volatilization of such materials as chromium, nickel, or iron.

1.2 Cesium Hydroxide and Boric Acid Chemistry in a Severe Reactor Accident

One of the main objectives of this study is to investigate the deposition behavior of the cesium compounds that are deposited onto the oxidized stainless steel surfaces. Previous studies have investigated environments that contained only vapor species. This study addresses the equilibrium and non-equilibrium states that arise from an environment containing both the vapor and condensed phase species.

---

*The expression "source term" used in this work denotes the fission product inventory leaving the reactor coolant system.

There are conflicting suggestions on the deposition of cesium onto an oxidized stainless steel surface in the presence of boric acid. The Powers and Bieniarz model suggests that part of the cesium inventory is removed from the reactor coolant system as cesium metaborate. Bowsher et al. suggest that boric acid is the gettering agent for cesium on an oxidized stainless steel surface, and removes part of the cesium inventory from the reactor coolant system.

Boric acid is typically found in the emergency core coolant systems (ECCSs) (Quick et al.) in a pressurized-water reactor (PWR). In a boiling-water reactor (BWR), boron is used as a neutron absorber in boron carbide absorber pins. Boron is also added to the water of the ECCS in a BWR. The boron carbide in the absorber pins is not expected to be a major factor in fission product speciation. In a four-loop PWR, there are approximately 12,700 ft^3 of coolant in the primary system, including the pressurizer and surge line, and the boron inventory in the core varies between 80 and 500 kg (Camp). Typically, the boric acid concentration in the coolant ranges from 850 to 3000 ppm. The total mass of boric acid in the primary system can be calculated on the basis of the dimensions and concentrations for a typical PWR. The mass of boric acid in the primary system in a four-loop reactor is approximately 1853 kg, assuming a concentration of 1500 ppm.

Although not all of the boron in the coolant will be vaporized along with the water, the reactivity of boron in the atmosphere will dominate during a reactor accident. At low temperatures and high oxygen potential, boric acid will dominate; at high temperatures and low water content of the atmosphere, metaboric acid is the more abundant boron-carrying species as shown by Minato's calculations. It is expected that part of the inventory of cesium hydroxide will convert to cesium metaborate, or that cesium-bearing species will be deposited on the surface in the reactor coolant system, and more of these species will remain in the containment. If the containment fails, or as in the case of a containment bypass scenario, the fission products would be released into the environment.

Boron can be effective in reducing the volatility of harmful radionuclides during a severe accident at lower temperatures. In a source term analysis, boron is assumed to react with cesium to form cesium metaborate. Calculations by Gotzmann showed that cesium is less volatile as cesium metaborate than as cesium hydroxide, the most abundant cesium-carrying species. Although Ball et al. also conclude that cesium in a metaborate form is less volatile than as cesium hydroxide, the relative volatility has not been quantified. Most of these theoretical calculations were based on tabulated data from sources such as JANAF tables (Stull & Prophet) and Cordfunke and Konings.

The increased temperature and steam in a severe accident scenario affect the stoichiometry of fission products. The dependence of the molecular form of compounds on the temperature is important for accurate source term analysis. Some studies (Ackerman et

al., 1975; Alexander and Ogden, 1990; Alexander et al., 1985 & 1986) have investigated the specific effects of the environment on certain molecules. When the system is at elevated temperatures, increased steam may be formed by the following reaction by way of the production of cesium metaborate: $CsOH_{(g)} + HBO_{2(g)} = CsBO_{2(g)} + H_2O$.

Cesium metaborate, a much less reactive substance than cesium hydroxide, is formed through various reactions involving steam and hydrogen. This cesium metaborate is substantially less volatile than cesium hydroxide, and could reduce the source term release.

It has been shown in "separate effects" experiments that boric acid used in the coolant of PWRs reacts with the dominant species, cesium iodide and cesium hydroxide, to produce the less volatile species cesium metaborate (Hobbins et al., 1991). At 300 °C, cesium hydroxide is known to cause corrosion of stainless steel. Also, as previously stated, the presence of steam will increase the volatility of most metal oxides and increase the corrosion rate. Therefore, at high temperatures representative of severe accidents, cesium retained within the oxide layers and boric acid-containing aerosols both have corrosion effects on the stainless steel. This effect could contribute to an early failure of the stainless steel structure (NUREG/CR-5214). Cesium metaborate could be formed through the reaction of cesium hydroxide and boric acid. Cesium metaborate is less volatile than cesium hydroxide and could alter the transport and release by forming cesium metaborate and water as follows: $CsOH_{(g)} + HBO_{2(g)} = CsBO_{2(g)} + H_2O$.

Cesium is usually thought to be transported in the vapor phase as cesium hydroxide. At the hydrogen/steam ratio of 1.0, the dominant form of cesium is predicted to be cesium hydroxide (Hobbins et al., 1987). CORSOR-M (NUREG/CR-4173), a severe accident fission product code, predicts almost total release of cesium from UO_2 fuel in about 10 minutes at 2200 Kelvin. Based on calculations using the SCDAP code (a thermal-hydraulic core degradation and fission product release code) by Hobbins et al. (1991), 16 percent of cesium-137 was retained in the lower plenum of the TMI-2 vessel, and 21 percent was retained in the upper debris.

From the vapor form, the deposited cesium hydroxide is quite volatile and readily revaporizes. Any retention of cesium hydroxide in the reactor coolant system could readily be reduced as surfaces heat up. Cesium hydroxide is quite reactive at elevated temperatures and it is possible that deposited cesium hydroxide will react to form a less volatile material. Several possible reactions can be assumed. A most important possibility is that deposited cesium may react with boric oxide to form any of a number of cesium metaborates. Generally, the aerosol formation involving cesium metaborate reactions will take the form of $2CsOH + nB_2O_3 = (CsBO_2) \cdot (n-1)B_2O_3 + H_2O$.

Different reactions between boric acid and cesium hydroxide will occur during the course of a severe accident. All of these reactions are dependent on the environmental conditions in the reactor

coolant system. Boric oxide is the residue formed from boric acid when the water in the coolant is boiled away at accident initiation. It is expected to be abundantly present on surfaces in the reactor coolant system (Bowsher et al.). The various reactions between cesium hydroxide and boric acid that form cesium metaborate may actually result in a greater release of cesium to the containment atmosphere in the form of cesium metaborate. If more cesium hydroxide is converted into cesium metaborate aerosol, more cesium would be released into the containment.

There are, however, competitive reactions for borates. Cesium is not the only fission product that will react with the boric acid inventory. Certain investigations have suggested that borates enhance the corrosion of stainless steel in the presence of steam by reacting with chromium oxide on the stainless steel surfaces. The corrosion will be affected if certain compounds leave the surface upon vaporization or desorption. Although the effects of fission products on corrosion are not studied in this investigation, it is important to note that fission products do contribute to the accelerated corrosion of the surfaces. Elrick and Sallach have shown that the composition of oxides on stainless steel depend on oxygen potential. The variation of oxygen potential with location, controls the distribution of each species on a stainless steel surface (Wang & Olander). The chemical equilibrium models for surface vaporization/desorption developed from the laws of thermodynamics can help provide an understanding of the release kinetics of fission products. These models can be used to study the interaction of radionuclides with the oxide film layer formed on stainless steel surfaces.

Oxide layers form on the stainless steel as a result of its interactions with steam. At different temperatures and in different environments, the formation of the oxide layer on the surface can affect the reaction with the fission products and, thereby, the retention of these radionuclides. Cesium hydroxide on the surface of oxidized stainless steel might react with phosphorus impurities in the steel to form cesium phosphates or with manganese oxide to form cesium manganates. Cesium hydroxide might also react to form cesium ferrites, cesium chromites, or cesium chromates. The maximum amount of the radionuclides that will be retained in the oxide layer depends on various system parameters (e.g., pressure and temperature). Similarly, the rate at which the fission products migrate to the surface can affect their retention, the diffusion rate through the oxide layer, and the reactions the radionuclides undergo with the impurities in the oxide layer.

As conditions change, fission product species may evaporate, revaporize, chemically combine with the structural material, leave the surface as an aerosol, or decompose. Rapid temperature increases lead to an imbalance between the equilibrium partial pressure and the actual partial pressure over the condensed phase. This leads to a net vaporization flux of fission products. The excess of equilibrium partial pressures provide the driving force for fission product release and transport.

Modeling release data for a potential nuclear reactor accident have been based primarily on evaluation of deposition after an experiment has been conducted. Elrick and Sallach used a facility in which steam and hydrogen are introduced to the test coupons downstream. The vaporized fission products were mixed with superheated steam and carried through a reaction tube to the condenser. The test coupons in the area of the reaction tube were removed and analyzed. Although the analysis of the test coupons showed that fission product cesium can react with the oxide layer in the stainless steel, there were no real-time measurements. However, because of the time-dependent complex physical and chemical processes that take place during the time the fission products reside in the primary system, the cesium/boric acid system has not been well characterized in the high-temperature steam-hydrogen environment. A literature search has indicated that neither the free energy nor the nature of the species itself is known for cesium and boric acid in a mixed environment of steam and hydrogen at 900 to 1200 Kelvin. This is compounded when the interactions with condensed species on oxidized stainless steel surfaces are considered.

Powers and Bieniarz noted that it is important to predict the possible chemical transformation of deposited radionuclides before accurate estimates of revaporization can be made. Radionuclides deposit in the reactor coolant system after they escape the core. The chemical form strongly influences the vapor pressures and chemisorption potential for cesium, and ultimately influences the transport and retention within the pressure vessel and the RCS.

1.3 Survey of Selected Thermodynamic Data on Fission Products Obtained by Mass-Spectrometric Methods

Understanding deposition/revaporization in the past usually involved studying samples after the material had been treated by high temperatures and H_2-H_2O environments. At Battelle, Alexander and Ogden (1990) developed an accurate method (with reproducible results) for real-time vapor measurements of release and transport using mass spectrometry. In some of their earlier work, Alexander and Ogden (1986) were able to measure (by using mass spectrometry) the vapor pressure of cesium as low as 7.0×10^{-7} atm in samples composed of a urania matrix at 2200 Kelvin.

There have been many measurements made by mass spectrometry for different applications. The mass spectrometer has been found to be an effective tool for investigating and understanding the vaporization process because of the real-time data measurements. The revaporization process and different chemical forms of deposited cesium can be observed using this technique. Alexander and Ogden (1990) have developed a convenient method to prepare and analyze specimens using the mass spectrometer system at Battelle. The mass spectrometer system measures vapor pressures as a function of temperature of the materials under investigation. In this section, selected mass spectrometric studies that apply to severe nuclear reactor accident phenomonology are discussed.

Using mass spectrometric methods to investigate thermodynamic properties of compounds and elements has shown good agreement among different laboratories (Ackerman et al., 1975; Ackerman and Rauh; Chupka et al., Thorn and Winslow; Matsui; Kanno et al.).

Although the mass spectrometer system provides a sensitive instrument for determining vapor pressures in systems that are in equilibrium, it is also valuable to investigate the quantity and the nature of surface deposition in the reaction cell. Such studies are described in Chapters 4 and 5.

1.4 Value of a Thermodynamic Study of Fission Product Simulants

A typical application of the thermodynamic method is the prediction of the equilibrium state of a system at a particular temperature and pressure. The equilibrium products of the reactions can be determined without any knowledge of the detailed nature of the course of the reactions. The final state of a system is predicted from the knowledge of the general principles of thermodynamics and their applications, while considering the restrictions imposed upon the system. It is not always necessary to know the intermediate steps when the temperature and pressure of a system are constant. Usually, order-of-magnitude agreement is all that can be expected of such calculations. The values of interest are the initial and final system states. This is how problems in thermodynamics are generally approached.

A thermodynamic study of cesium and boric acid chemistry will increase the current understanding of the characteristics in the RCS that are important for analyzing transport and retention of certain fission products. Such a study will characterize the equilibrium between solid and vapor compounds and the equilibrium partial pressures and will involve the relative abundance of the various compounds and the equilibrium partial pressures. This study examines the effects of temperature and oxygen potential (related to steam-to-hydrogen partial pressure ratio) on the composition and activities of stainless steel surfaces with and without cesium and borates present.

An appropriate first step in such a study is to define a set of measurements that will provide the necessary data base. The species present in the vapor can be identified by using a mass spectrometer. Thermochemical and kinetic data can be derived and formulated to characterize the speciation under the conditions utilized. The key to modeling the behavior of cesium on surfaces is to have available a database on the chemical activities of surface species as functions of temperature and oxygen potential.

The activity of a species is a measure of the interaction of chemical species with the other species. The activity measurement determines how reactive the species are in a solution. Chemical activities of particular chemical species that are formulated among cesium, boric acid, water, and hydrogen are assumed to be unity when they appear in the condensed state in such predictive codes as VICTORIA. This assumption tends to overpredict the release of some

fission products. The assumption of ideal chemistry (i.e., no chemical surface interactions) tends to overpredict the fission product inventory of certain fission products in the nearby atmosphere. By contrast, the calculations in this study are equilibrium calculations among species in the gas phase or in equilibrium with a condensed phase.

VICTORIA models radionuclide behavior (release, transport, and deposition) in the core and the reactor coolant system under severe accident conditions. The primary basis for modeling chemistry in VICTORIA is through the calculation of thermodynamic equilibrium-all chemical phases are assumed to be ideal. VICTORIA solves systems of conservation equations that describe the transport, phase, and chemical changes that elements and molecules experience. The evolution of these changes are modeled as the materials interact with one another in response to changing pressures, temperatures, and the transport mechanism. The input to the code requires an initial elemental distribution, the variation of pressures, temperatures, and geometry.

An accurate predictive capability for radionuclide retention and revaporization in the reactor coolant system is needed to better quantify the magnitude of the fission product releases to the environment following a severe accident at a nuclear power plant. VICTORIA does not now have very sophisticated models of surfaces and the transformation of deposited radionuclides on these surfaces that will be needed to accurately predict revaporization.

Equilibrium calculations that do not assume all the species are in their standard state (ideal chemistry) will results in more accurate VICTORIA calculations.

Temperatures between 700 and 1200 Kelvin were chosen to demonstrate the effect of temperature on the volatility and vaporization of fission product species. The total pressure of the system in this investigation is due to the partial pressures of water and hydrogen and is controlled to about 1 atm.

The standard representation for a thermodynamic analysis of a chemical reaction is a plot of the natural logarithm of the product of the pressures of the output products divided by that of the reactants on one axis and the inverse of the temperature of the system on the other. The relationship of products divided by reactants is commonly defined as the equilibrium constant of the reaction, and this type of plot is an Arrhenius plot. This type of curve indicates that the system is in equilibrium for temperature ranges in which the slope is constant.

The boric acid species are in both solid and vapor phases. Because of the conservation of mass in this closed system, the portion of the products that is not in vapor form is assumed to be condensed on the stainless steel. The physical state dependence on the temperature determines if the reaction products are in a condensed state, in crystal or vapor, or are a combination of both. Analysis of the free energy of formation begins with listing the reactions

that have the dominant species of boron and cesium that are present in the current environmental conditions. Under the conditions covered in the scope of this analysis, the following reactions are possible (Camp; Cubicciotti) (the phase of the species is identified as solid (*s*) or vapor (*g*)):

- $CsBO_{2(g)} + \frac{1}{2}H_2 = Cs_{(g)} + HBO_{2(g)}$
- $CsOH_{(g)} = CsOH_{(g)}$
- $CsBO_{2(g)} = CsBO_{2(g)}$
- $Cs_{(g)} + CsO_{(g)} + H_2O = 2CsOH_{(g)}$
- $CsOH_{(g)} = CsO_{(g)} + \frac{1}{2}H_2$

1.5 Summary

Interest in certain volatile chemical species arises because the stainless steel surfaces of the reactor coolant system heat up during the course of a reactor accident due to fission product deposition. As temperatures rise, the deposited materials can revaporize. That is, the important mitigation of the source term to containment provided by deposition in the RCS may only be temporary. Rapid revaporization of deposited materials may mean that the deposition in the reactor coolant system has little effect on the magnitude of the release of volatile radioisotopes into containment. Slower revaporization may create a late-time source term to containment, potentially after containment failure. Revaporization is risk significant in the late in-vessel release phase of severe reactor accidents.

The revaporization of materials deposited onto surfaces in the reactor coolant system depends on the chemical form adopted by these deposited materials. Nonideal chemical interactions of cesium-containing species are possible and could both enhance deposition of these species on stainless steel surfaces within the RCS and impede or prevent revaporization of cesium later in a severe reactor accident.

An evaluation of the cesium deposition and revaporization under these conditions is needed. The source term predictions could be inaccurate without the consideration of cesium bonding to the oxidized surface. This investigation will determine the deposition rate of cesium-containing species onto an oxidized stainless steel surface at high system temperatures and low pressure. The net volatility effect of boric acid on cesium hydroxide will be investigated. This study will also evaluate the chemical environment that causes cesium to deposit onto the oxidized surface and will model the chemistry of that effect.

CHAPTER 2

REACTION CELL SYSTEM EXPERIMENT

This work includes an investigation of the formation of the products from the reaction of cesium hydroxide and boric acid in the vapor phase in a hydrogen and steam environment. A set of measurements was made using a mass spectrometer attached to the reaction cell which was constructed of stainless steel for this purpose. Cesium hydroxide and boric acid were fed into a reaction cell which contained steam and hydrogen, each at approximately a partial pressure of 1.0 atm. The formation of all possible combinations of reaction products under these conditions is investigated. The possible combinations of reactants include: CsOH (mass = 150), CsO (149), Cs_2CrO_4 (382), $CsBO_2$ (176), Cs (133), H_3BO_3 (62), HBO_2 (44), Cs_2O (282), $CsO_{2(g)}$ (165), CsH (134), HBO (28), BO (27), BO_2 (54), and B_2O_3 (70). The vapor phase of the products resulted from both compound formations (due to CsOH and H_3BO_3) and their interactions with the oxide film on the wall of the reaction cell. Thermodynamic investigations utilizing mass spectrometry are used to characterize the overall chemical reactions of cesium hydroxide and boric acid with oxidized stainless steel in a high-temperature, hydrogen-steam environment through identification of the products formed during the experiment. Temperature dependence of partial pressures can be measured over a broad range of temperatures in a single experiment with negligible loss of material in the spectrometer. Even species formed in minor concentrations can be measured with the same accuracy as those formed in major concentrations.

A thermodynamic investigation of compound formation and vaporization behavior of compounds requires a defined set of test conditions as a key to an interpretation of the data collected. Necessary conditions for an equilibrium experiment are constant pressure and temperature. The measurements were all performed under the presumption that the conditions in the reaction cell are at equilibrium. The vapor products formed in the reaction cell leave the reaction cell through a very small orifice (0.025-cm radius) in the top of the cell. Because the orifice is so small compared with the other dimensions of the reaction cell, the closed system is considered uncompromised. The orifice of the reaction cell leads directly to the mass spectrometer. Reactions between these reactants occurred in a temperature range between 600 and 1200 Kelvin. A mass spectrometer was adapted to identify the products formed from these reactants. The intensity peaks are analyzed to calculate the equilibrium vapor pressure of each product at selected temperatures. Analysis of these data led to the finding that some partial pressures decreased with increasing temperature, which implies the reactants may not follow the ideal gas relationship. An ideal gas is one that obeys the equation of state $PV = nRT$. For the case in which the gas is in thermal equilibrium with the surroundings, the pressure will increase with the temperature for constant volume. Therefore, the results of the

data indicating decreasing pressure with temperature suggests that material was being "lost" in the reaction cell.

Upon further investigation, the surfaces of the reaction cell were found to affect the revaporization of the products. If vapors condense on a heated surface in an ideal chemical system, the material can be expected to revaporize in the absence of chemical reactions on the surface. Because of the results from the mass spectrometer measurements, the surface of the reaction cell was analyzed using a scanning electron microscope (SEM) and an electron spectroscopy for chemical analysis (ESCA) instrument to identify the deposits. Following this, the rate of mass deposition was investigated using a mass electrobalance.

2.1 Reaction Cell Apparatus

The reaction cell was constructed of stainless steel to simulate to a great extent the surface conditions found in the primary system of a nuclear power plant. The reaction chamber is held near 1 atm total pressure, with the total pressure equal to the sum of the partial molar pressures of hydrogen gas and the water vapor (steam) that pass into the reaction chamber, each about 1.0 atm. The interior dimensions of the cell were 6.35 cm in length and approximately 0.5 cm in diameter. An orifice having a radius of 0.025 cm was placed in the top of the cell. Crucibles for the boric acid and the cesium hydroxide were attached to the cell with inlets immediately above the bottom plane. To control the environment during the experiment, there is a continuous flow of hydrogen and steam into a mixing pipe attached to the reaction chamber. The pipe is heated to prevent condensation on the flow path which could affect the hydrogen and steam ratio and perturb the testing atmosphere. Figure 2.1 is a schematic drawing of the hydrogen and steam flow path, the reaction chamber, and the flow path of the vapor to be analyzed.

Cesium hydroxide vapor enters the reaction cell from a separately heated reservoir. An externally controlled heater is wrapped around the cesium hydroxide crucible. The boric acid volatilizes at a lower temperature than the cesium hydroxide. The heat conducted from the reaction chamber is sufficient to volatilize the boric acid. Each duct into the reaction cell is heated to minimize condensation prior to entry into the cell.

A separate externally controlled heater is used to control the temperature within the reaction cell. Additionally, the cell is insulated to reduce heat loss and minimize temperature transients.

The concentrations of the gaseous species formed are determined with the use of a mass spectrometer (Figure 2.2 is a block diagram of the mass spectrometer). Figure 2.3 is a photograph of the NUCLIDE 12-90 mass spectrometer system used in this research. The photograph shows the mass spectrometer, all three pumping stages, and part of the control panel. The NUCLIDE 12-90 model has been used successfully for other thermodynamic activity measurements such as U-Zr alloys (Kanno et al.). The mass spectrometer offers

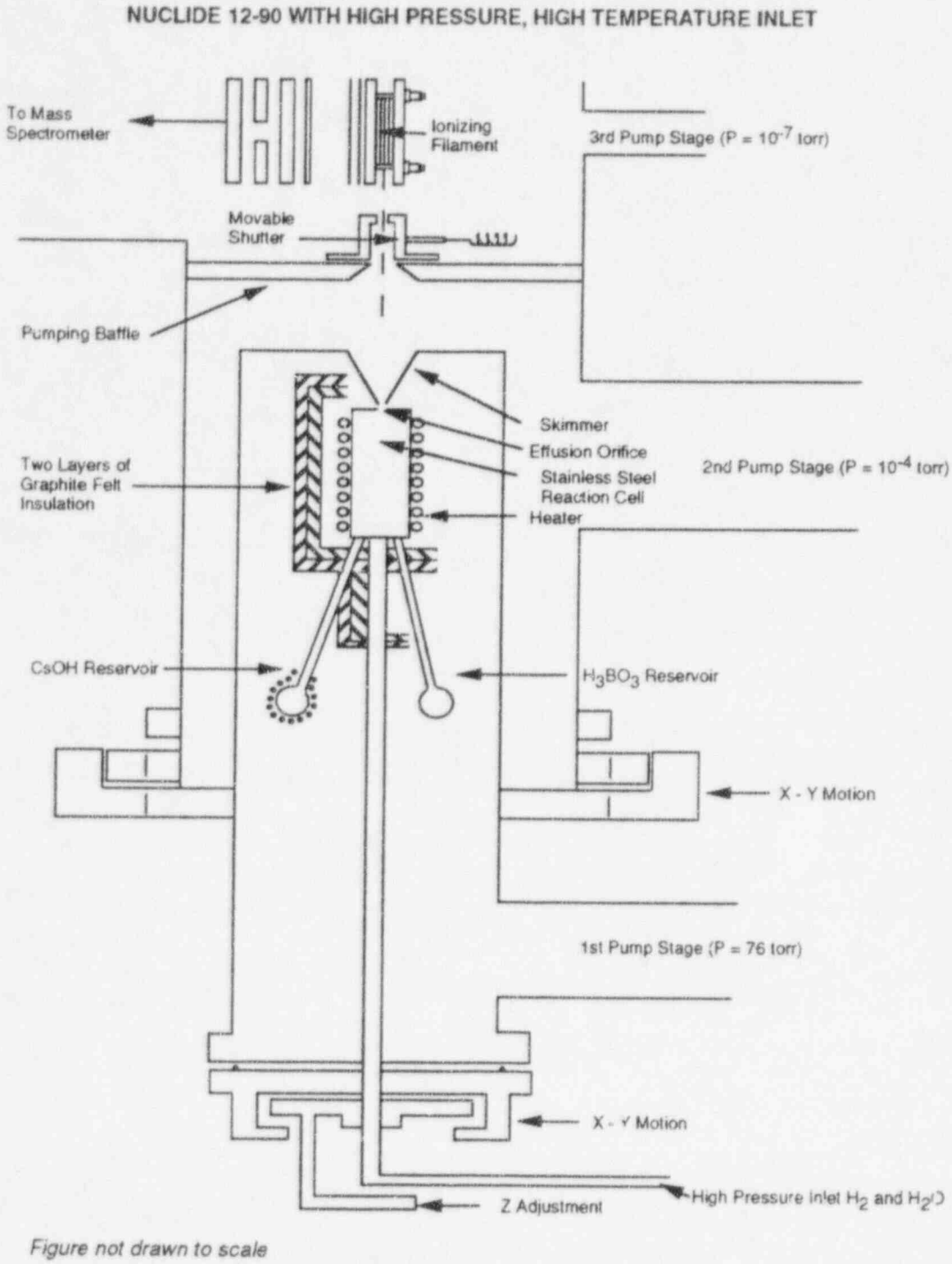

Figure 2.1 Schematic Representation of Flow Path

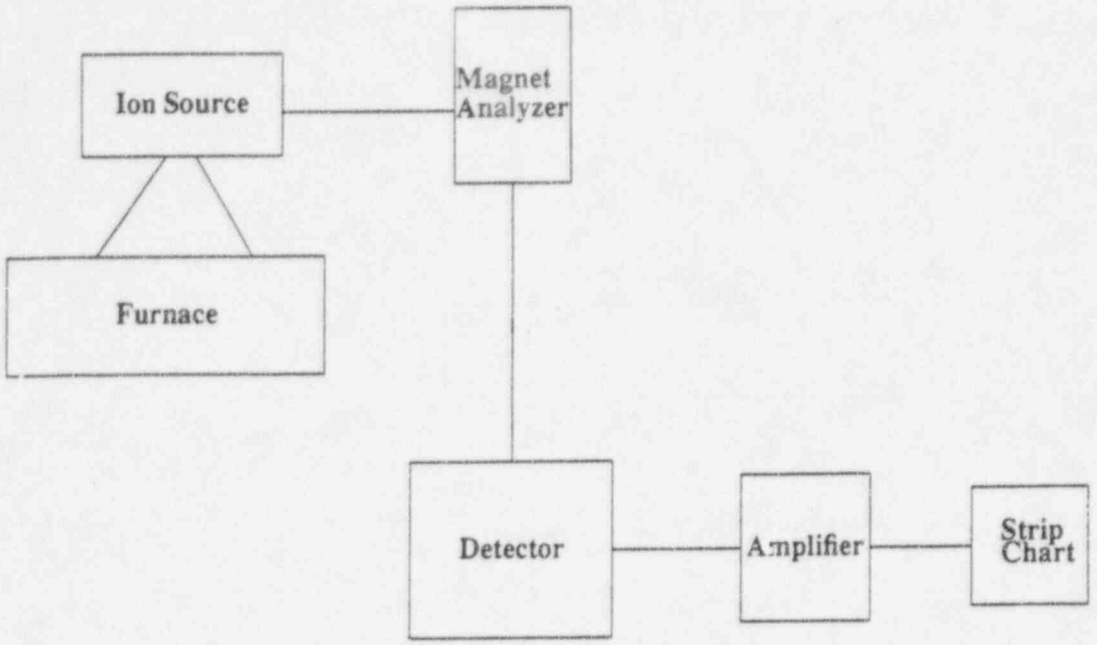

Figure 2.2 Block Diagram of Mass Spectrometry System

real-time measurements due to its capability of both continuous monitoring and species identification during an experiment. The mass spectrometry method consists of the following steps:

(1) Isolate a representative sample of the gaseous phase of the system investigated in the form of a molecular beam.
(2) Ionize the atoms of the beam, forming ions from the neutral species in the beam.
(3) Measure the mass of the species formed by ionization.
(4) Identify the ions and the neutral species from which they were formed.
(5) Determine the flux in the molecular beam from the ion intensity, and derive thermodynamic and kinetic quantities from the flux.

The vacuum system of the mass spectrometer system is divided into three pumping stages. Figure 2.4 is a photograph of the three pumping stage systems and the magnets on the mass spectrometer behind the pumps (wrapped in black duct tape). The reaction chamber is in the center of the photograph located in the vertical white column, and is part of pumping stage II. Directly below the sample chamber is pumping stage I. At the lower left corner is the flange for pumping stage III.

Stage I vacuum pumping maintains the pressure at 76 torr. The pressure inside stage II is 10^{-4} torr. This stage is physically isolated from stage I, except for a small orifice, to maintain the vacuum integrity. The reaction cell is placed inside pumping stage II. The beam emerging from the testing cell is a large number of neutral molecules that move virtually collision free in an

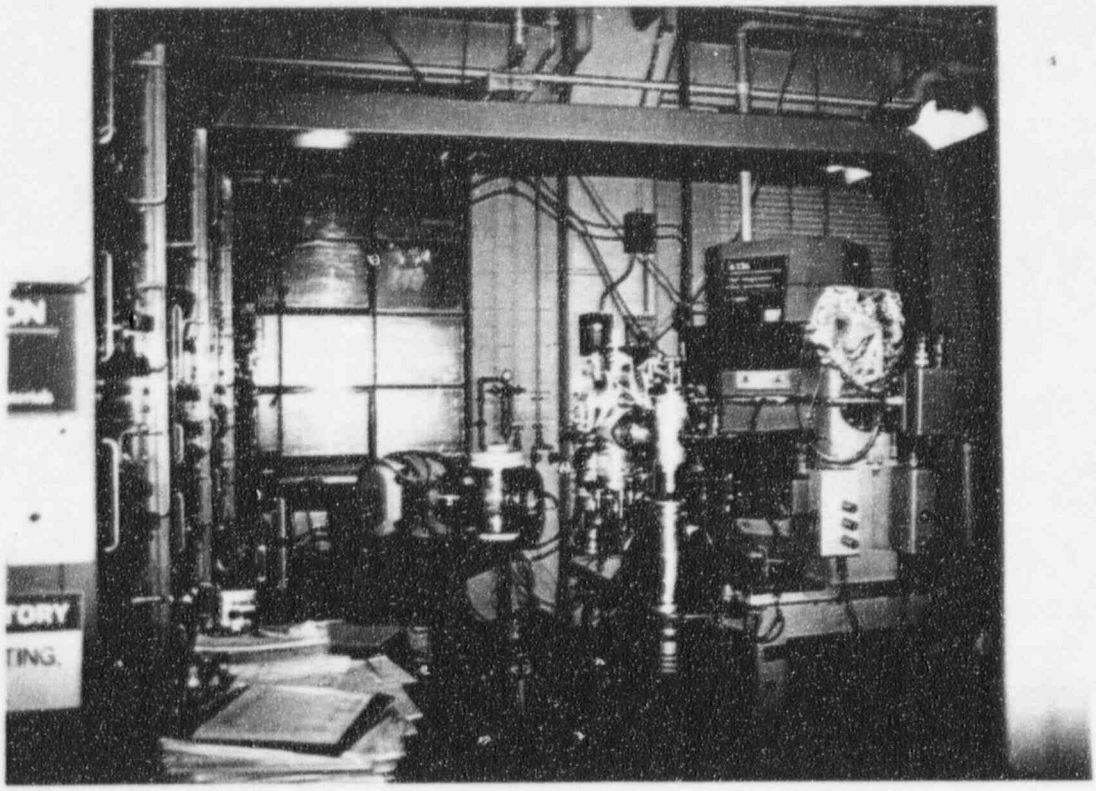

Figure 2.3 NUCLIDE 12-90 Mass Spectrometer

evacuated space. This molecular beam provides a continuous flow field that is collimated at the skimmer. The skimmer is a device that aids in collimating the beam and removing molecules that may have altered momenta from collisions with the surface of the orifice. The velocity of the molecules in the axial direction (effusive flow) does not change as the flow path continues to the ion source. The neutral molecules are ionized by an electron beam. The resulting ions are accelerated and then pass through a magnetic field and into an electron multiplier detector. The detector current is amplified and directly recorded by a strip chart recorder. A moveable slit called the shutter is located between the skimmer and the ion source, as seen in Figure 2.1. The ionizing filament is inside pumping stage III, and the pressure there is maintained at 10^{-7} torr.

A liquid nitrogen cold trap in the pumping system condenses and freezes those condensible gases that enter the evacuated system. Stage I pressure is monitored by a CONVECTRON which operates in a manner similar to a thermocouple gauge. The pressure in stage II is monitored by an external digital readout vacuum gauge.

Pumping stage III is monitored very carefully during the experiment for any changes in pressure. As a result of differences in the pumping speed or leak rates, there could be differences between the composition of the beam and the background in the detector chamber under steady-state sampling conditions.

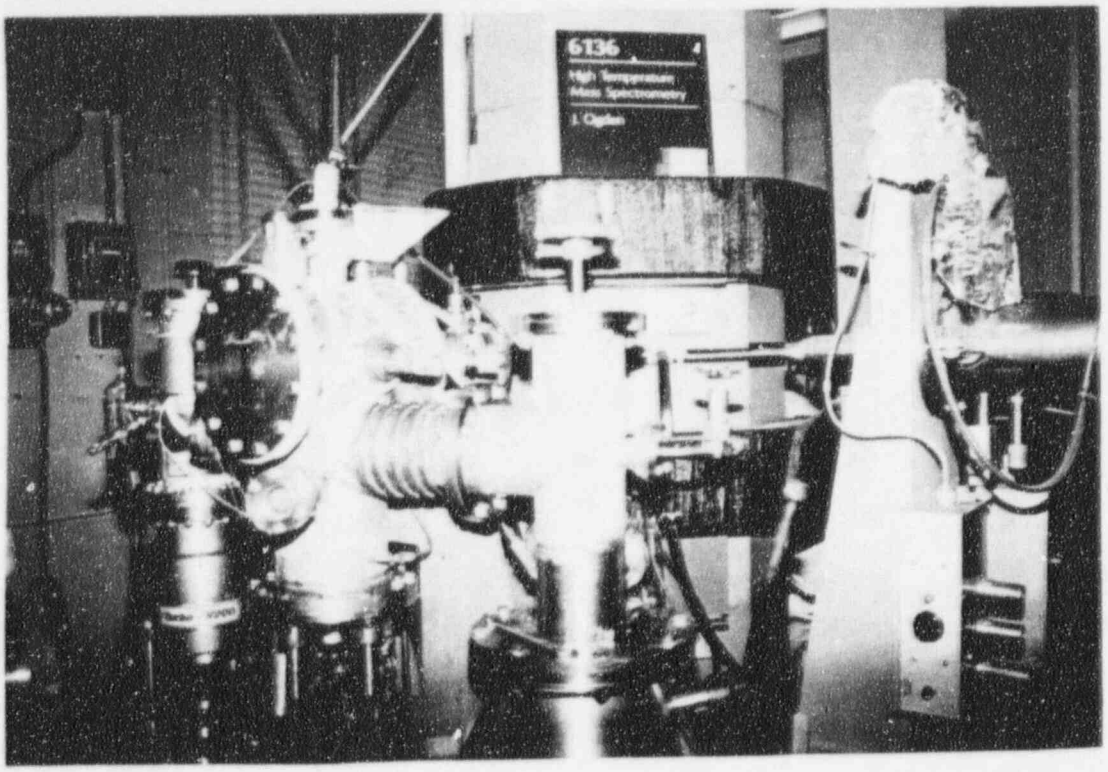

Figure 2.4 Pumping Stages and Magnets of Mass Spectrometer

The ionization does not appear to cause dissociation of the molecules and thereby provide erroneous results.

2.2 Pretreatment of the Stainless Steel Reaction Cell

Before conducting the experiment, the reaction cell was pretreated to simulate the stainless steel surface of the RCS piping system during a severe accident (Hobbins et al., 1991); Kazikowski et al.; Powers & Bieniarz). To prepare the reaction chamber, an oxidized film layer was grown on the stainless steel surface using the apparatus shown in Figure 2.5, previously described by Alexander et al. (1993). The procedure involves connecting a heater to two lines that are both in contact with the ends of the reaction cell (the details of the inside configurations are shown in Figure 2.6). Thermocouples are connected to the heater tape and to the copper feed-through to monitor the temperature of the system. Heater tape is wrapped around the water line entering the bottom portion of the closed system for insulation. The electric power supplied to the heater from a Variac is used to regulate the temperature. The hydrogen supply line into the furnace is located near the water line. There is a pressure gauge for monitoring the pressure of the gases inside the apparatus. A cover at the top of the chamber is cooled by an independent water line. The tempera-ture selected for oxidizing the surface was 973 Kelvin, and the pressure of the gases inside the apparatus was 2 atm. The sample is connected to the furnace and the heaters, as shown in Figure 2.6. The stainless steel cell is in the furnace during the heatup period. The desired temperature and pressure were set, and the furnace remained at the

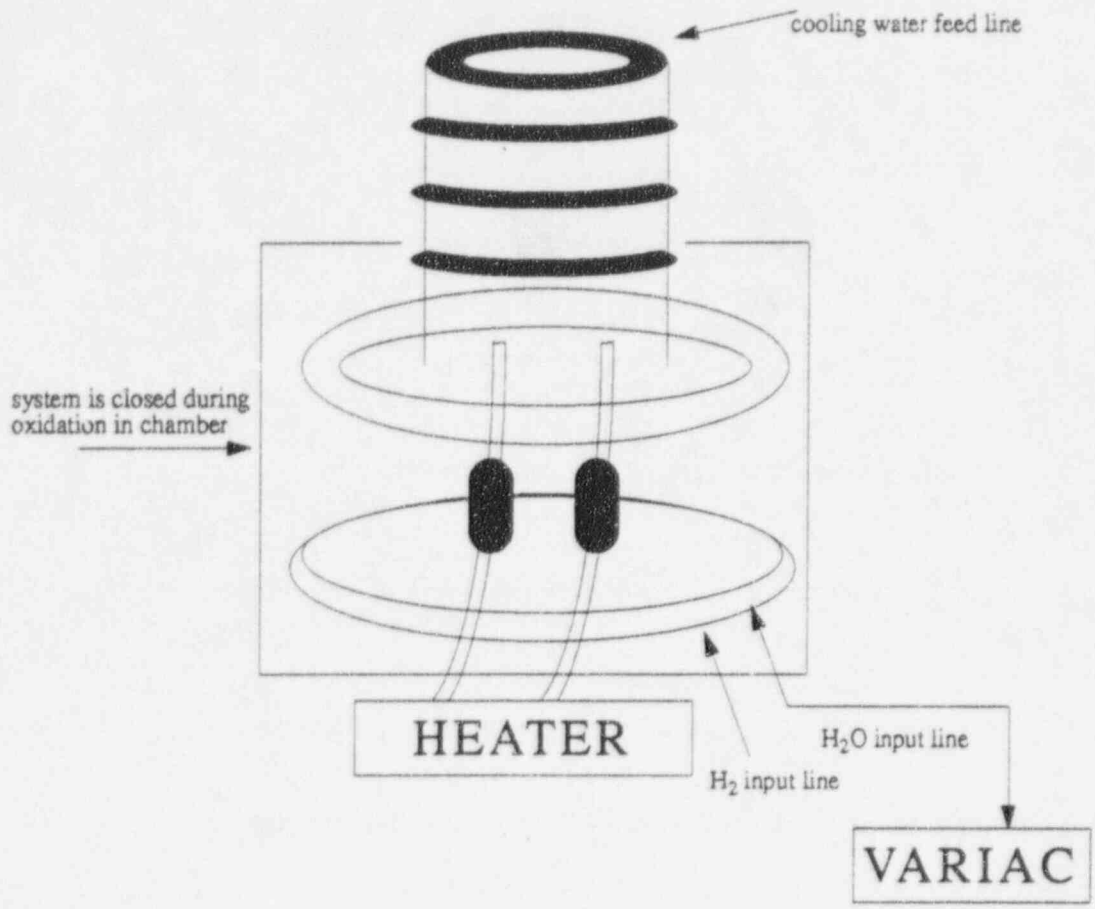

Figure 2.5 Oxidation Apparatus

same conditions for 60 minutes. The film growth has been characterized by Alexander et al. (1993) as

$$d = 0.012t^{\frac{1}{2}} + 0.0025$$

where

d = thickness of the film in micrometers
t = time in seconds

The desired film layer in this system is 0.72 μm. All of the oxide films have been grown using the same furnace and experimental parameters to simulate the chemical reactions taking place on the surface only.

Figure 2.7 is a photograph of the pretreated oxidized reaction cell. The top cylindrical portion, the center duct leading to the chamber, and the input lines from the cesium hydroxide and boric acid all have a grayish tone to their surfaces as a result of the oxidation process.

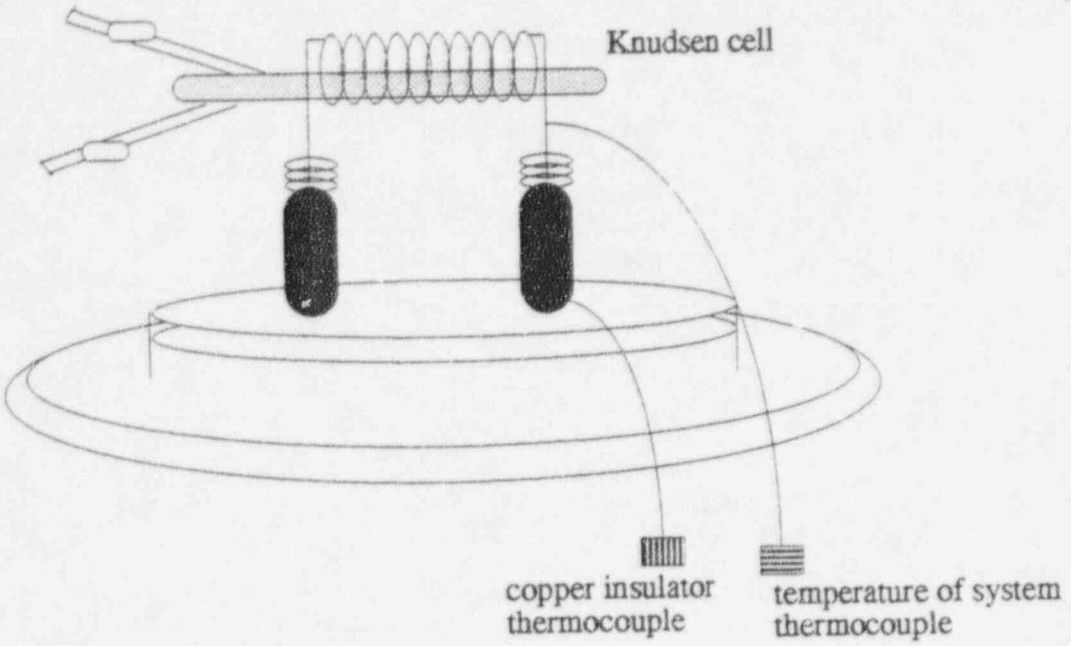

Figure 2.6 Interior of Oxidation Apparatus

2.3 Measurement of Partial Vapor Pressures Using Mass Spectrometry

The mass spectrometer signal (I) is proportional to the number density (n) of ionizable species/unit volume. For ions formed by electron impact, the intensity measured on the collector in the mass spectrometer can be calculated. By relating machine characteristics and the intensity signals from the strip recorder connected to the mass spectrometer, the vapor pressure of a species can be determined.

The number of atoms, N_j, for species j that crosses the electron beam is directly proportional to the intensity read on the collector of the mass spectrometer. The signal intensity for ions formed by electron impact for species j is I_j. The intensity, $I = \alpha n$, where α is a constant of proportionality. Since $P = nkT$, then $P = (IkT)/\alpha$. Under the conditions of these experiments, α is nearly constant with n.

At each temperature during the experiment, the strip chart was used to record the intensity of the selected species. The detection process begins early in the experiment by identifying intense background peaks of H_2O. Water molecules can be detected at low temperatures, and this provides a good indication of whether the vapor path is unobstructed. The temperatures were recorded manually on the strip chart during the measurements.

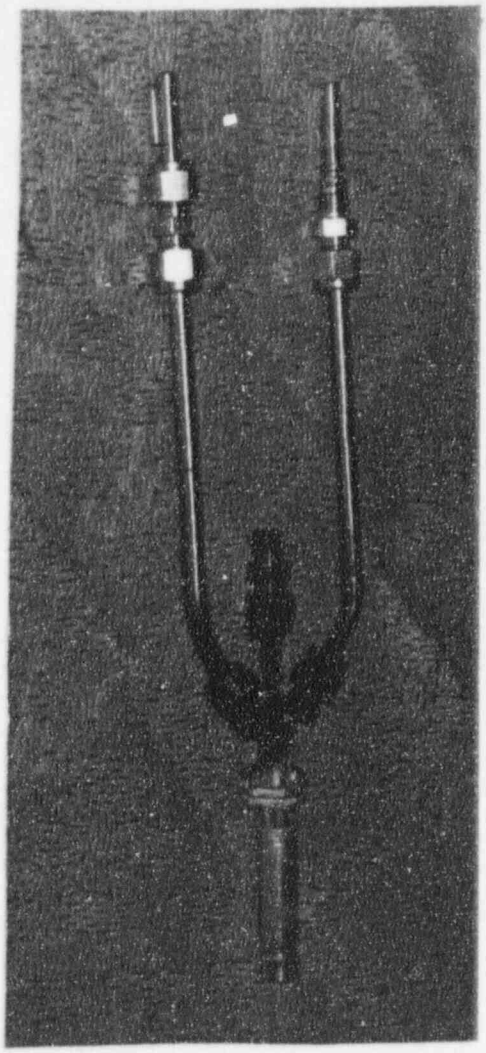

Figure 2.7 Pretreated Oxidized Reaction Cell

2.4 Interpretation of the Partial Pressure Measurements for Thermodynamic Data

The information recorded by the mass spectrometer was interpreted to identify chemical species and the pressure of the neutral species exiting from the cell. The thermochemical calculations were performed using the ionization data from the mass spectrometer experiments.

Thermodynamic data were derived by evaluating the neutral species in the molecular beam. Other physical data on species formation in the mass spectrometer can be calculated. For example, the Gibbs free energies, enthalpies, and entropies of formation can be derived for specific experimental conditions.

In the event of equilibrium reactions, enthalpies (ΔH_T^0) (^{0} denotes the magnitude taken with respect to a reference state) can be obtained by use of the Clausius-Clapeyron equation when equilibrium is reached between the gas and condensed phase of the materials (Klotz & Rosenberg). The enthalpy can be obtained from known values of vapor pressure as a function of temperature, or vapor pressures may be predicted as a function of temperature,as shown in the following equation:

$$\ln P = -\frac{\Delta H}{RT} + \text{constant}$$

where

P = partial pressure of the substance (atm)
ΔH = enthalpy of vaporization (J/mole)
R = gas constant (8.31451 J/K-mol)
T = absolute temperature of closed system (Kelvin)

For the system to remain in equilibrium, T and P cannot be varied independently. In the system which is the subject of this investigation, equilibrium conditions are not attained. Thus, a different model was needed that characterizes a system of both vapors and solids (because the vapors are in equilibrium with each other but not necessarily in equilibrium with the condensed material.

The high-temperature products in the system were characterized during the vaporization process. The end products were identified and their vapor pressure was determined from the intensity. In this system, two gases (H_2 and H_2O) were swept past the species in the reaction chamber. However, the gases did not flow at a velocity that would interfere with the equilibrium of the vapors formed in the system.

The neutral gases emerging from the reaction cell were ionized by impact with electrons and related by the following empirical equation (Drowart & Goldfinger):

$$\frac{\text{no. molecules effusing}}{\text{time}} = \frac{nus}{4}$$

where

n = molecular density of the species
u = average speed
s = effusion orifice area through which the vapor leaves the Knudsen cell

These quantities are related by the following equations:

$$n = \frac{p}{kT}\left(\frac{\text{mol}}{\text{cm}^3}\right) \text{ also } u = \left(\frac{8kT}{\pi m}\right)^{\frac{1}{2}}$$

where
m = mass of molecule
k = Boltzmann's constant

2.5 Calibration of Sampling System

The mass spectrometer sensitivity value (S) was obtained by performing a calibration experiment in which 4.6 mg of silver contained in a tungsten effusion cell was heated in order to vaporize the silver. A silver sample was chosen to be vaporized for calibration since the thermodynamic properties of silver are well known (Stull & Prophet; Hultgren et al.). A sample of silver was placed in the Knudsen cell and vaporized. The silver intensity was measured as a function of time using the same ionizing electron energy and emission current as was used in the cesium hydroxide–boric acid experiments. Z represents the evaporation of the silver in units of g/sec-cm^2. The expression for Z (derived in Appendix A) yields the following result:

$$Z = 44.343\ P(\text{atm})\sqrt{\frac{M}{T}}$$

The calibration process requires the measurement of the total mass of the calibration material at the beginning of the experiment. By integrating Z over the total run time of the mass spectrometer, and using the relationship $P = SIT$, the sensitivity constant can be derived. The formulation of the integral over time is

$$Q_{\text{total mass}} = \int_0^t aZdt = 44.3\int_0^t aP\sqrt{\frac{M}{T}}dt$$

In this equation, a represents the orifice area. The integral is evaluated numerically and the sensitivity constant can be determined by

$$\sum_0^i aZ_i\Delta t_i = \sum_0^i 44.3aP\sqrt{\frac{M_i\Delta t_i}{T_i}} = [(50)(6.25\times10^{-4}\pi44.3\sqrt{107.87}]S\sum_0^t I_i\sqrt{T_i}$$

The total run time (~50 minutes) was multiplied by the summation over time.

The Knudsen cell was heated to approximately 1000 Kelvin before any silver began to evaporate. The response of the mass spectrometer

The Knudsen cell was heated to approximately 1000 Kelvin before any silver began to evaporate. The response of the mass spectrometer was examined at five temperatures in the range of 1123 to 1393 Kelvin during the calibration process. The changes in temperature were such that the system was assumed to remain in equilibrium.

The observation that the calibration constant was not affected by temperature ensures the consistency of the partial pressures (Behrens & Rinehart). If the properties of the instrument remain constant, the measurements are presumed to have a 5-to-10-percent accuracy. The value obtained in this calibration was 2×10^{-12}. This calibration yielded the calibration constant and provided a mechanism to test for variations among different temperatures. This calibration process was adapted from the work of Behrens and Rinehart.

2.6 The Experiment

Vaporization at high temperatures offers the advantage of studying the molecules as they form at high temperatures in the environment inside the experimental system. The species to be directly identified and measured are the products of high-temperature chemical interactions. The results of the high-temperature sampling system allows the characterization of the reaction products of cesium hydroxide and boric acid as a function of the system temperature.

The mass spectrometer readings are analyzed to identify the effects of temperature on the chemical reactions that occur when the vapors are in equilibrium with each other. The cesium hydroxide and boric acid in the presence of steam and hydrogen form a variety of vapor compounds. The reactions that form the different compounds do not necessarily occur at all the temperatures investigated. The experiment is designed to continuously measure the effect of a single variable (i.e., temperature) at fixed conditions. With this technique, the compounds formed at each temperature can be observed. The temperature can be varied during one continuous experimental run for a series of measurements that are isothermal and isobaric. During each measurement, the pressure and temperature have been constant over a period of time.

The reaction chamber is mounted on the flange that separates pumping stages I and II. Figure 2.8 is a photograph of the mounted reaction chamber on the flange for stage I. Thermocouples connected to both of the reservoirs monitor the temperature of these species during the experiment. The tube in the center toward the top is where the carrier gas connecters are attached. Some of the molecular compounds are deposited into the oxide layer and others leave the chamber and are collected in a nitrogen cold trap at the end of the third pumping stage. The nitrogen freezes and condenses water vapor and any other gases that enter the evacuated system. At the center of the flange is a pipe that leads directly to the chamber. Heater coil wrapped around the reaction chamber is the primary source of heat in the experiment. The thermocouple wires

to the top, center, and bottom of the chamber are visible in Figure 2.8.

The vapor samples to be measured are entrained by the carrier gases and carried into the detector at a rate sufficiently low so that equilibrium conditions prevail. The carrier gas flows past the sample in an isothermal region in the cell and the products are carried into the mass spectrometer. The intensity signal was measured as a function of mass numbers. Mass numbers which correspond to all known, possible combinations of the elements and their isotopes present in the system, including the constituents of the container and all possible impurities, were scanned. This procedure was performed for each temperature in the study. The masses of the elements and molecular constituents encountered in this investigation were such that no confusion arose in the identification of the species.

It is important that the stainless steel and the samples of interest in the reservoirs do not react with the carrier gas. This is not a concern in this system because the flow of hydrogen and steam are at the lower limits of their detectability. At such a low flow rate, the carrier gas does not affect the chemical equilibrium of the species under investigation.

The assumption in the experiment is that the vapor behaves like an ideal gas, where the vapors do not interact with one another. Some preliminary experiments were done on different tube sizes between the cell and the reservoirs. The main problem encountered before the final configuration of the experimental setup, was that boron would volatilize at a faster rate than cesium hydroxide. Boron would vaporize before the temperature in the stainless steel reaction vessel was high enough for any reactions to occur. The tube between the reservoirs that extends through the center of the reaction chamber up to the skimmer is where the hydrogen and steam enter the stainless steel cell (Figure 2.1).

The distance between the effusion cell and the skimmer is small enough so only a negligible loss of vapor from the cell to the analyzer could occur during an experiment. All reactants in the reaction cell that will vaporize travel to the ionizer of the mass spectrometer.

As the vapor gas mixture flows through the reaction cell, parts of the vapor condense at the cooler sections of the capillary and the vaporized species-gas mixture is carried into the analyzer. The flow of gas could affect the activity of the condensed phase of the species if it is not low enough.

The first experiment was conducted in the temperature range of 300 to 1200 Kelvin. The mass settings on the spectrometer were set to look for the mass of specific compound formations and elements (see para. 1, p. 13). Although the products from certain reactions may be present inside the reaction cell, the temperature of the reaction cell may not be high enough to vaporize the products. There will not be any detection of a molecule if its partial

Figure 2.8 Reactor Chamber Mounted on Pump Flange

pressure is lower than the detectability limit. The flow of hydrogen and steam from their supplies was adjusted so that the total pressure in the reaction cell was near 1 atm. This pressure would supply a sufficient quantity of hydrogen and oxygen to initiate the reactions. The total time of one series of temperature changes and related measurements was approximately 3 hours.

Species in the vapor form to be directly identified and measured are due to the compound formations from cesium hydroxide, boric acid, steam, and hydrogen. The vapor products of primary interest in this experiment are the end products of the various chemical reactions and not the intermediate species. The temperature intervals between measurements are varied based upon the intensity peaks. If products from a reaction have strong intensity signals

at certain temperatures, the temperature steps will be finer than if the products are not as abundant. In the regions of higher abundance, where the step between measurements is 1 or 2°C, the temperature step could be as coarse as 50°C. The step sizes taken between temperature intervals are based on the vaporization temperature of the products of interest. At temperatures above this value, smaller temperature steps are used so that the vapor pressure changes can be closely monitored.

2.7 Revaporization From the Reaction Cell

An additional experiment was conducted in order to revaporize any deposited material that remained after the course of the reaction cell experiment. Smaller quantities of cesium compounds were observed in the previous measurements, so an effort was made to vaporize cesium, cesium hydroxide, and cesium metaborate material retained on the surface. The reaction cell was cut into smaller pieces for the surface analysis testing and the revaporization experiment. Five pieces of the reaction cell, each with a surface area of about 0.5 cm^2, were placed into a Knudsen cell connected to the mass spectrometer for analysis. The samples were not treated before they were placed into the Knudsen cell. The Knudsen cell revaporization experiment had the same temperature range as the vaporization experiments performed on the reaction cell, but the pressure in this system was subatmospheric. The pressure was 10^{-7} torr (1.33×10^{-10} atm) in pumping stage II of the reaction cell-mass spectrometer apparatus. The Knudsen cell was evacuated and the evaporation of the gases from the surfaces formed a molecular beam exiting the orifice of the reaction cell.

The cell was heated to approximately 1200 Kelvin and the intensity was determined for each species which had been detected in the earlier measurements. Figure 2.9 shows the pathway for vapor flow in the Knudsen cell. The tungsten heater in the cell is wrapped around the sample cell. The vapor travels upward through the orifice of the effusion cell which is 0.5 mm in diameter, out through the shutter, into the ionizer. The ionized particles travel into the ion beam analyzer where the signals can be detected by the data acquisition system.

Elemental cesium was observed to be the most abundant revaporized product. After examination of the stainless steel surface by ESCA, it appeared that not all the deposits on the surface did revaporize. This means it is possible that some of the molecules may have chemically combined to the oxide layer or to the stainless steel surface, or to both, and are not readily revaporized.

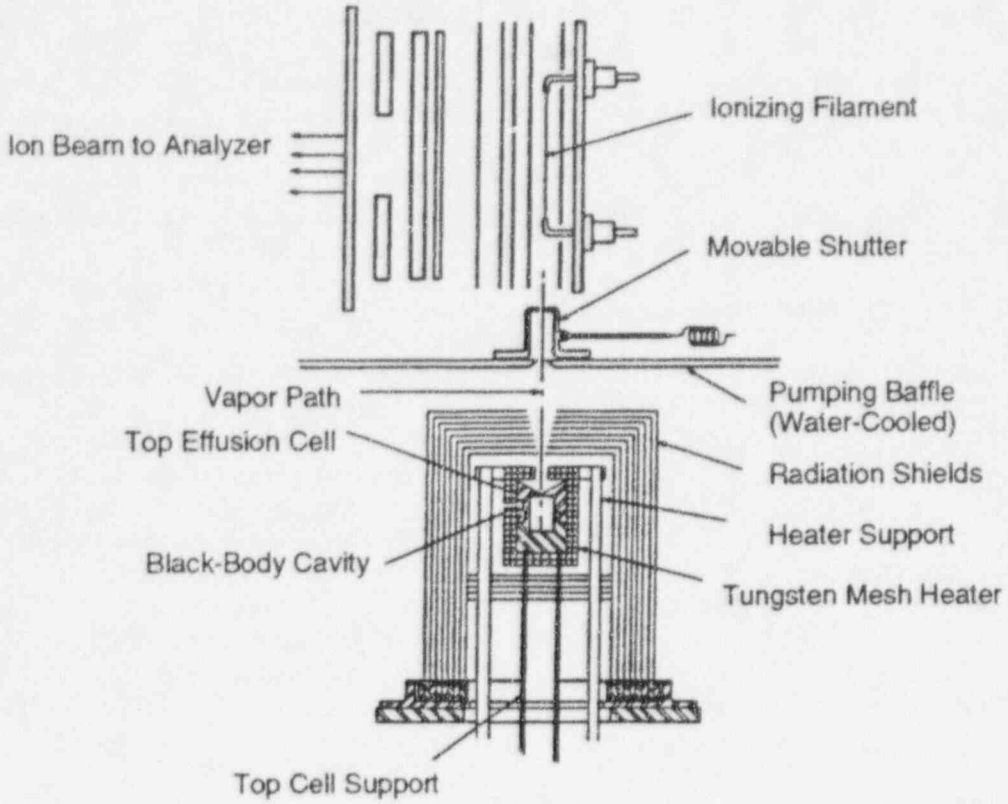

Figure not drawn to scale

Figure 2.9 Current Design of Mass Spectrometer Inlet (Source: Alexander et al., 1986, reprinted with authors' permission)

CHAPTER 3

MEASUREMENTS IN THE REACTION CELL SYSTEM

The data from the reaction cell measurements are presented in this chapter. Data from the mass spectrometer are presented in this chapter and compared with tabulated data. In addition, surface analysis from electron spectroscopy for chemical analysis (ESCA) and the scanning electron microscope (SEM) of the reaction cell are presented following the mass spectrometer data. The data show the dependence of the partial pressure for each of six different vapors measured as a function of temperature. These partial pressures are for vapor products from the reactants that are assumed to be in equilibrium. The data from this investigation are compared to data derived from Cordfunke and Konings and to calculations performed using VICTORIA.

There are several published sources for thermochemical data such as Cordfunke and Konings, the JANAF tables (Stull & Prophet), and Hultgren et al. Of these, Cordfunke and Konings was the only source to contain all of the species studied in this investigation. The tables in Cordfunke and Konings present the Gibbs free energies of the species at different temperatures. The partial vapor pressures were calculated using the following relationship:

$$\Delta G = \Delta G_{products} - \Delta G_{reactants}; \quad \frac{\Delta G}{RT} = \ln P$$

A model of the reaction cell was prepared for VICTORIA to simulate the reactions occurring and the pertinent experimental parameters. Cordfunke's experiments involved the study of the equilibrium between the condensed and vapor phase of isolated species. Since the algorithm in VICTORIA accounts for chemical reactions in the vapor phase, the results from VICTORIA would not be expected to agree with those of Cordfunke. However, since both Cordfunke and VICTORIA assume ideal gas conditions in the vapor, the overall trend of partial pressures versus temperature are similar. The results from the calculation are presented on the graphs to compare with the tabulated data and the results of this experiment.

The partial pressure data obtained by the mass spectrometer experiments performed here were expected to be different from Cordfunke's results. This was due, in great measure, to the expectation that there would be a large interaction in the vapor phase between the boric acid contained in the cell and the cesium-bearing species. It was not anticipated that the oxidized stainless steel surface would play a major role in the reactions taking place in the cell. Cordfunke's measurements were done in a Knudsen effusion cell at low vacuum conditions with cell materials carefully chosen so there would be no interaction between the species and the crucible walls. The cell material and conditions in the reaction cell of this experiment were selected to more nearly simulate the primary system of a light-water reactor. For each

This page was left blank intentionally.

experiment performed, the partial pressures of each of the species found in the cell were measured to compare with the model in VICTORIA calculations.

In addition, the thermodynamic activity, a_i, is presented in tables for each species investigated. For a gaseous phase in equilibrium with a condensed phase, the thermodynamic activity a_i of the component i can be defined as the ratio of the partial pressure of the component in the mixture (P_i) to the vapor pressure of the pure compound at the same temperature (P^o_i):

$$a_i = \frac{P_i(\text{experiment})}{P_i^o}$$

3.1 Results

The input to the VICTORIA code was divided into six nodes that would simulate the experiment. The reaction cell nodalization is shown in Figure 3.1. In the experiment, there was a continuous input of cesium hydroxide, boric acid, hydrogen, and steam flowing through the reaction cell. The input into node 1 comprised the four items listed above; the input into the other five nodes comprised the four items listed above and the output of the previous node. The input for node 2 was the same as for node 1 and the output of node 1. The algorithm in VICTORIA allows the code to compute the partial pressures of all the products based on all the possible reactions that can take place from the reactants given as input, in addition to the pressure and temperature of the system being simulated. Because there was a continuous flow of cesium hydroxide, boric acid, hydrogen, and steam throughout the experiment, the results for metaboric acid and boric acid are in good agreement with the measured values. These results will be discussed in the next sections.

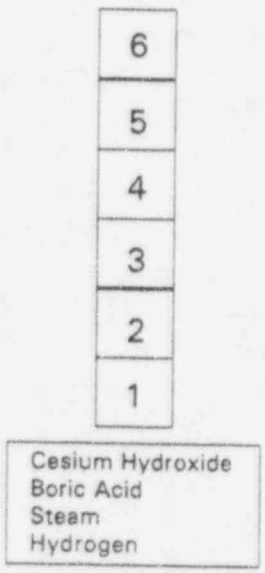

Figure 3.1 Nodalization of Reaction Cell for VICTORIA Input

3.1.1 Cesium Hydroxide (CsOH)

The data for CsOH are presented on an Arrhenius plot, Figure 3.2. The experimentally observed vapor pressures are represented by filled circles. The values of Cordfunke and Konings for vaporization and the results from the VICTORIA code are also presented. The values of Cordfunke and Konings are for pure solid CsOH which is volatilizing and shows an increase in vapor pressure with temperature. The experiment began with pure CsOH in the condensed phase which was transported by hydrogen and steam into the reaction cell when the material vaporized. The observed decrease in vapor pressure with an increasing temperature shows a departure from ideal gas behavior in this experiment. The implication must be drawn that a chemical system is more complex than a simple system of pure CsOH in equilibrium between gaseous and solid phases.

In Table 3.1, the calculated activities for each observed temperature are presented. The activity is the activity of CsOH in the steam-hydrogen-cesium hydroxide-boric acid system. The variables in the table follow: P_{exp} is the measured partial pressure and $P_{Cordfunke}$ is the partial pressure calculated from the values of Cordfunke and Konings. All pressure values are expressed in atmospheres. The activity values are all relative to the standard state values (Cordfunke's values).

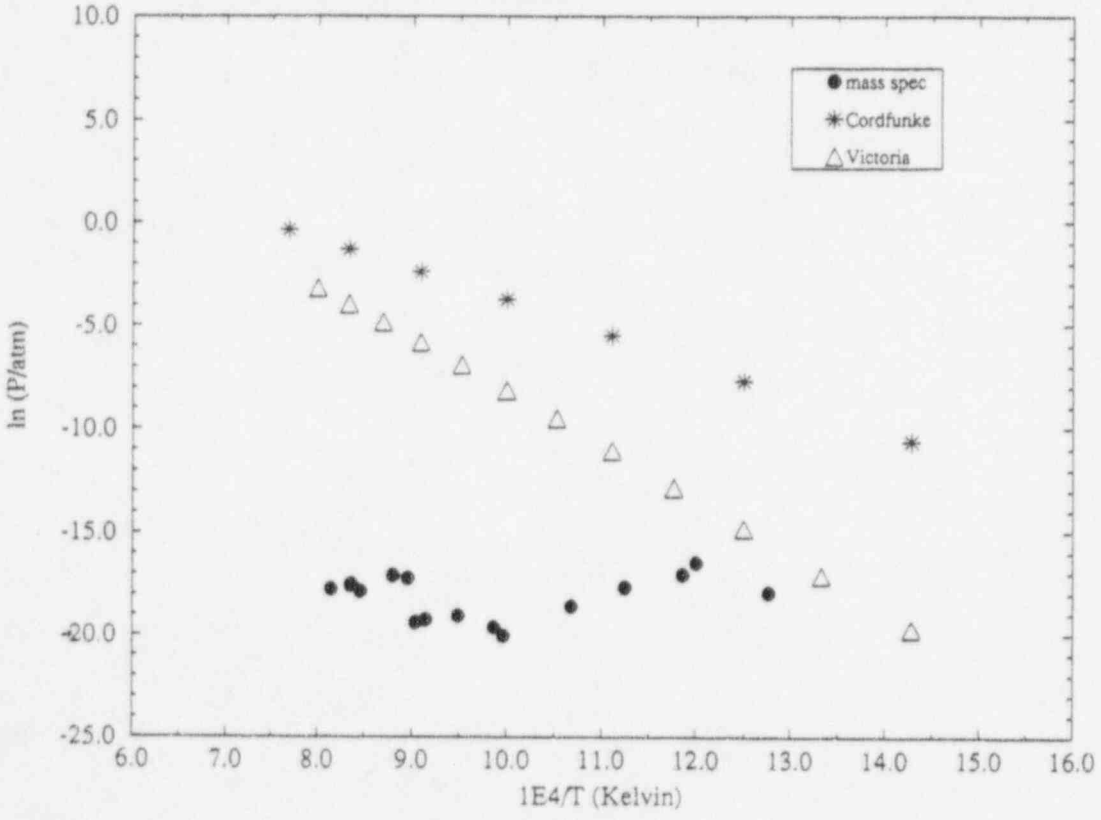

Figure 3.2 Cesium Hydroxide Vapor Pressure

Table 3.1 Vapor Pressures and Activity of CsOH in the Cell

T(K)	P_{exp}	$P_{Cordfunke}$	a(CsOH)
783	1.64×10^{-8}	1.90×10^{-4}	8.63×10^{-5}
833	7.16×10^{-8}	7.70×10^{-4}	9.30×10^{-5}
843	4.05×10^{-8}	9.90×10^{-4}	4.09×10^{-5}
889	2.13×10^{-8}	2.97×10^{-3}	7.17×10^{-6}
936	8.42×10^{-9}	8.14×10^{-3}	6.91×10^{-6}
1003	2.01×10^{-9}	2.91×10^{-2}	8.79×10^{-8}
1013	3.04×10^{-9}	3.46×10^{-2}	8.70×10^{-8}
1054	5.27×10^{-9}	6.88×10^{-2}	7.66×10^{-8}
1093	4.37×10^{-9}	1.25×10^{-1}	3.49×10^{-8}
1106	3.87×10^{-9}	1.52×10^{-1}	2.55×10^{-8}
1116	3.35×10^{-8}	1.76×10^{-1}	1.99×10^{-7}
1136	3.86×10^{-8}	2.34×10^{-1}	1.65×10^{-7}
1195	2.51×10^{-8}	5.07×10^{-1}	4.95×10^{-8}
1197	2.39×10^{-8}	5.20×10^{-1}	4.60×10^{-8}
1227	1.96×10^{-8}	7.48×10^{-1}	2.62×10^{-8}

3.1.2 Boric Acid (H_3BO_3)

Boric acid vapor was measured in the products of the reaction cell. The measurements from the mass spectrometer, data from Cordfunke and Konings, and the VICTORIA results in the temperature range of interest are shown in Figure 3.3. The activity values for H_3BO_3 in the cell are presented in Table 3.2. The measured values for H_3BO_3 vapor pressure and the results of VICTORIA are in fairly good agreement, and both differ from Cordfunke and Konings. This is because H_3BO_3 was continuously supplied throughout the experiment, so the vapor pressure was approximately constant. The input for VICTORIA was similar, H_3BO_3 was continuously supplied; therefore, there was a steady vapor pressure during the experiment. If there had been a finite supply of H_3BO_3 during the experiment, the results would be similar to the values of Cordfunke and Konings.

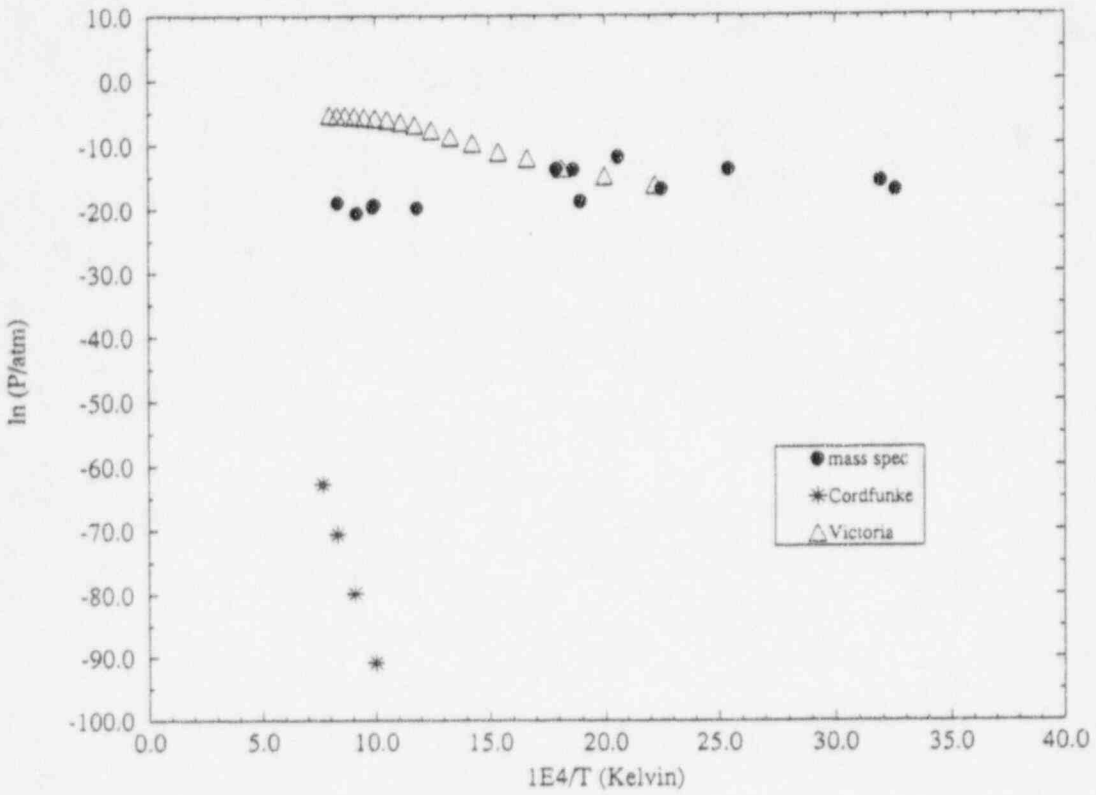

Figure 3.3 Boric Acid Vapor Pressure

Table 3.2 Vapor Pressures and Activity of H_3BO_3 in the Cell

T(K)	P_{exp}	$P_{Cordfunke}$	$a(H_3BO_3)$
307	3.68×10^{-8}	7.13×10^{-7}	0.1
313	1.57×10^{-7}	6.31×10^{-7}	0.2
393	9.83×10^{-7}	1.77×10^{-7}	5.0
444	4.62×10^{-8}	1.00×10^{-7}	0.4
527	6.85×10^{-9}	5.01×10^{-8}	0.1
536	9.18×10^{-7}	4.70×10^{-8}	19.0
557	1.00×10^{-6}	4.10×10^{-8}	24.0
843	2.53×10^{-9}	1.25×10^{-8}	0.2
1003	4.01×10^{-9}	8.61×10^{-9}	0.4
1012	3.04×10^{-9}	8.47×10^{-9}	0.3
1089	1.09×10^{-9}	7.39×10^{-9}	0.1
1197	5.99×10^{-9}	6.28×10^{-9}	0.9

3.1.3 Cesium Metaborate ($CsBO_2$)

Cesium metaborate is one of the products identified in the vapor phase by the mass spectrometer and it is a product of a reaction of cesium hydroxide, boric acid, hydrogen, and steam. The results are presented in Figure 3.4.

The vapor pressures and activity values for $CsBO_2$ in the cell are presented in Table 3.3.

It is noted that measurable vapor pressures for $CsBO_2$ do not appear at temperatures lower than 843 Kelvin. This would infer that below this temperature the $CsBO_2$ is a solid and has low vapor pressure. The reactivity of $CsBO_2$ is increasing as the $CsBO_2$ formed in the cell is vaporizing; the activity is decreasing.

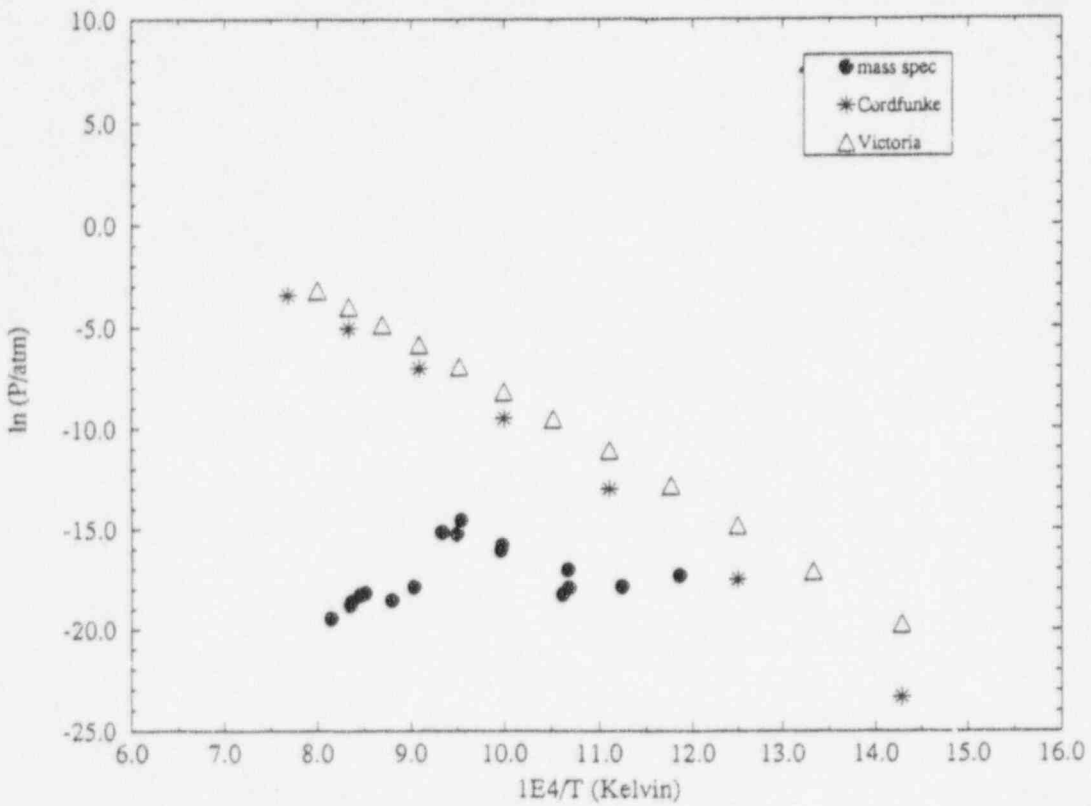

Figure 3.4 Cesium Metaborate Vapor Pressure

Table 3.3 Vapor Pressures and Activity of $CsBO_2$ in the Cell

T(K)	P_{exp}	$P_{Cordfunke}$	$a(CsBO_2)$
843	2.00×10^{-8}	1.49×10^{-7}	1.30×10^{-1}
889	1.78×10^{-8}	1.00×10^{-6}	1.78×10^{-2}
935	1.68×10^{-8}	5.60×10^{-6}	3.00×10^{-3}
936	4.12×10^{-8}	5.81×10^{-6}	7.09×10^{-3}
941	1.22×10^{-8}	6.93×10^{-6}	1.76×10^{-3}
1002	1.40×10^{-7}	5.18×10^{-5}	2.70×10^{-3}
1003	1.10×10^{-7}	5.34×10^{-5}	2.06×10^{-3}
1048	4.82×10^{-7}	2.02×10^{-4}	2.39×10^{-3}
1053	2.47×10^{-7}	2.33×10^{-4}	1.06×10^{-3}
1071	2.73×10^{-7}	3.83×10^{-4}	7.13×10^{-4}
1106	1.77×10^{-8}	9.59×10^{-4}	1.80×10^{-5}
1116	1.12×10^{-9}	1.23×10^{-3}	9.11×10^{-7}
1136	9.09×10^{-9}	2.02×10^{-3}	4.50×10^{-6}
1174	1.29×10^{-8}	4.89×10^{-3}	2.63×10^{-6}
1182	1.18×10^{-8}	6.00×10^{-3}	1.97×10^{-6}
1195	8.37×10^{-9}	8.00×10^{-3}	1.05×10^{-6}
1197	7.18×10^{-9}	8.00×10^{-3}	8.98×10^{-7}
1227	3.68×10^{-9}	1.50×10^{-2}	2.45×10^{-7}

3.1.4 Cesium (Cs)

Cesium was detected by the mass spectrometer. The results are presented in Figure 3.5. The activity values for Cs in the cell are presented in Table 3.4.

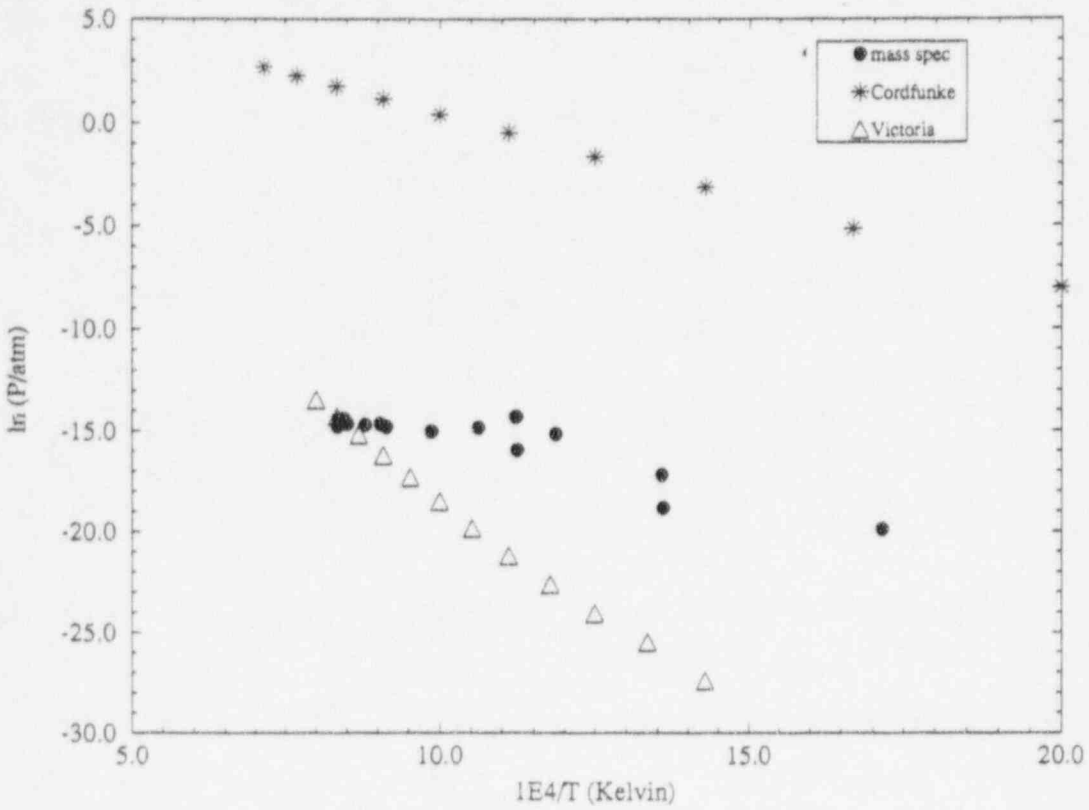

Figure 3.5 Cesium Vapor Pressure

Table 3.4 Vapor Pressures and Activity of Cs in the Cell

T(K)	P_{exp}	$P_{Cordfunke}$	a(Cs)
583	2.33×10^{-9}	3.20×10^{-3}	7.28×10^{-7}
736	6.62×10^{-9}	6.91×10^{-2}	9.58×10^{-8}
737	3.46×10^{-8}	7.02×10^{-2}	4.93×10^{-7}
784	5.41×10^{-7}	1.42×10^{-1}	3.81×10^{-6}
843	2.61×10^{-7}	3.06×10^{-1}	8.53×10^{-7}
889	1.20×10^{-7}	5.19×10^{-1}	2.30×10^{-7}
890	6.05×10^{-7}	5.24×10^{-1}	1.15×10^{-6}
941	3.58×10^{-7}	8.87×10^{-1}	4.04×10^{-7}
1013	2.94×10^{-7}	1.70	1.73×10^{-7}
1093	3.77×10^{-7}	1.15	3.28×10^{-7}
1106	4.42×10^{-7}	3.48	1.27×10^{-7}
1116	1.83×10^{-7}	3.73	4.91×10^{-8}
1174	4.40×10^{-7}	5.46	8.06×10^{-8}
1182	5.56×10^{-7}	5.74	9.69×10^{-8}
1197	5.63×10^{-7}	6.33	8.89×10^{-8}
1227	3.31×10^{-7}	7.50	4.41×10^{-8}

3.1.5 Cesium Oxide (CsO)

Cesium oxide was also detected in the reaction cell. The partial pressures are compared in Figure 3.6. The activity values for CsO in the cell are presented in Table 3.5.

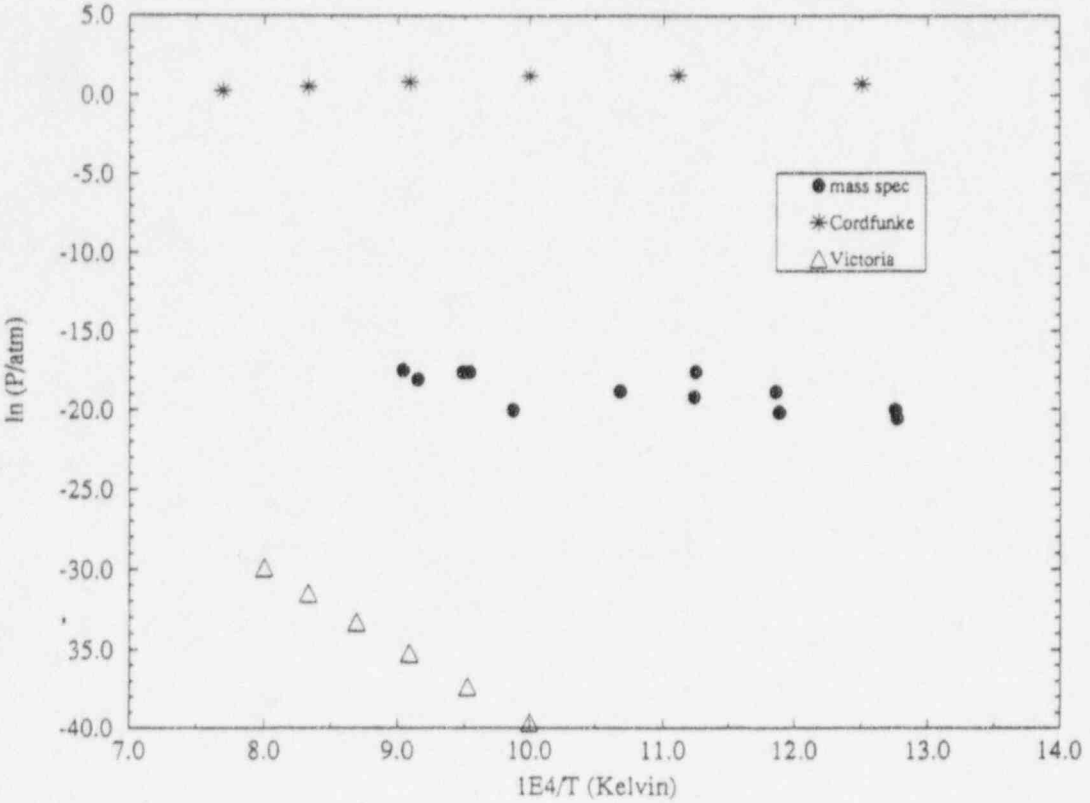

Figure 3.6 Cesium Oxide Vapor Pressure

Table 3.5 Vapor Pressures and Activity of CsO in the Cell

T(K)	P_{exp}	$P_{Cordfunke}$	a(CsO)
783	1.17×10^{-9}	1.93	6.06×10^{-10}
784	1.96×10^{-9}	1.94	1.01×10^{-9}
841	1.68×10^{-9}	2.79	6.02×10^{-10}
843	6.32×10^{-9}	2.82	2.24×10^{-9}
889	2.22×10^{-8}	3.65	6.08×10^{-9}
890	4.45×10^{-9}	3.67	1.21×10^{-9}
936	6.55×10^{-9}	4.62	1.42×10^{-9}
1013	2.03×10^{-9}	6.49	3.13×10^{-10}
1048	2.20×10^{-8}	7.45	2.95×10^{-9}
1054	2.21×10^{-8}	7.63	2.90×10^{-9}
1093	1.42×10^{-8}	8.79	1.62×10^{-9}
1106	2.54×10^{-8}	9.19	2.76×10^{-9}

3.1.6 Metaboric Acid (HBO_2)

Metaboric acid was detected in the higher temperature regions. The mass spectrometer measurements, the data of Cordfunke and Konings, and VICTORIA results are presented in Figure 3.7. The activity values are presented in Table 3.6.

The VICTORIA prediction for HBO_2 is steady over the temperature range; however, it is higher than the fairly steady experimental values. The VICTORIA prediction is based on the input to the code. VICTORIA predicted the same trend for HBO_2 as the measured values, and the departure is within approximately 1.5 orders of magnitude, which is reasonable.

Metaboric acid appears to have a fairly constant pressure over temperatures above 1000 Kelvin. One of the reactions H_3BO_3 undergoes at high temperatures is hydrolysis. A boric acid molecule loses a water molecule, and the result is metaboric acid and steam: $H_3BO_3 = HBO_2 + H_2O$.

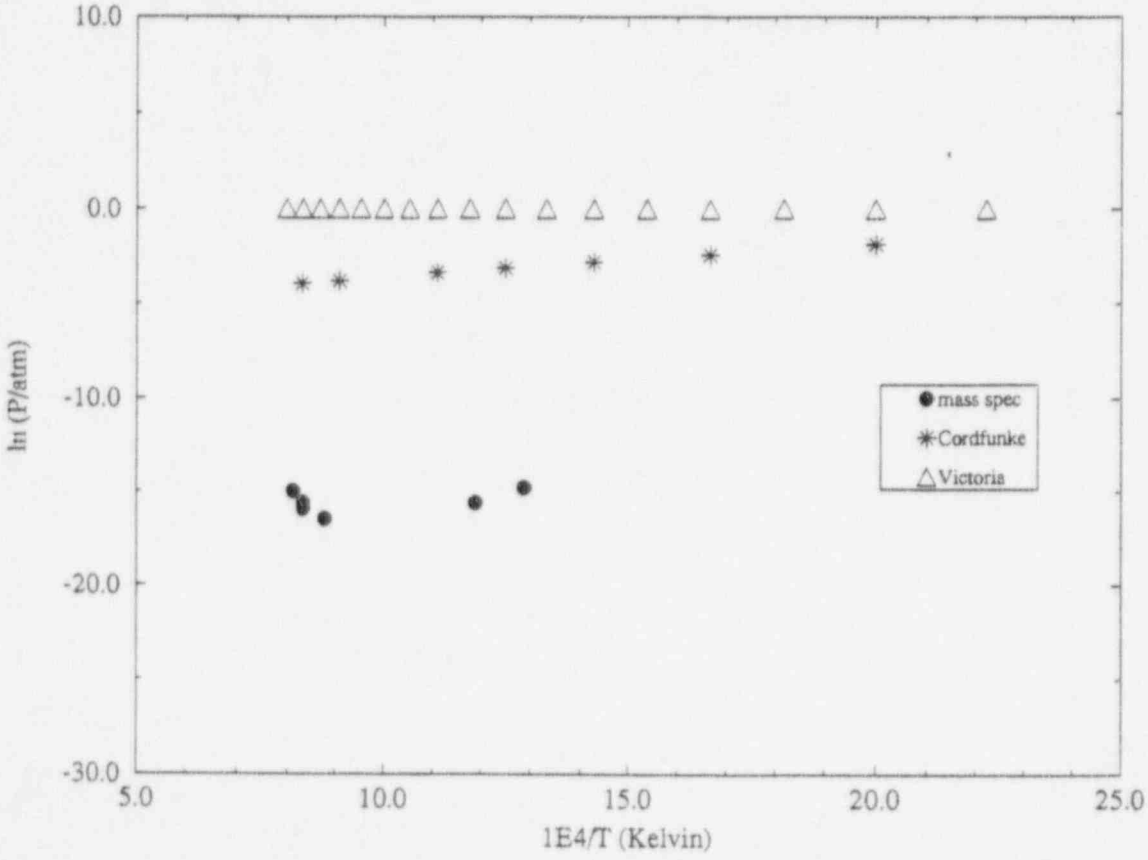

Figure 3.7 Metaboric Acid Vapor Pressure

Table 3.6 Vapor Pressures and Activity of HBO_2 in the Cell

T(K)	P_{exp}	$P_{Cordfunke}$	$a(HBO_2)$
776	3.72×10^{-7}	.08	4.65×10^{-6}
841	1.63×10^{-7}	.05	3.26×10^{-6}
1136	6.82×10^{-8}	.03	2.27×10^{-6}
1197	1.20×10^{-7}	.02	6.00×10^{-6}
1198	1.62×10^{-7}	.02	8.10×10^{-6}

3.2 Equilibrium Reaction Constants

The hypotheses for the reactions that take place inside the reaction chamber are based on the vapor pressure data of the individual species. The trends in pressure of the different species monitored during the experiment played the largest role in deducing the possible chemical reactions. For example, the vapor pressure of $CsBO_2$ increased in some temperature regions and decreased in others. Examining the vapor pressure of $CsBO_2$ and CsOH in the same temperature regions, shows an increase in $CsBO_2$ when there is a decrease in the vapor pressure of CsOH. This behavior was postulated in Chapter 1 and becomes clear in the graphical representation of an Arrhenius plot.

Some of the reactions of interest are in Chapter 1. The graphs of the reaction equilibrium constants in this section compare the Cordfunke and Konings data (straight line) and the data from this investigation (filled boxes).

One of the major reactions of interest is the vaporization of $CsOH_{(c)}$. The chemical reaction, the equilibrium constant, and the equation using the Gibbs free energy from Cordfunke and Konings are given below:

$$CsOH_{(c)} = CsOH_{(g)}$$

$$\ln K = \left[\ln\left\{\frac{p(CsOH)}{\alpha(CsOH)}\right\}\right]$$

$$\ln K = \frac{-1}{RT}\{\Delta G[CsOH_{(g)}] - \Delta G[CsOH_{(c)}]\}$$

For the partial pressure of a solid, α denotes the value of Cordfunke and Konings. The partial pressures are compared in Figure 3.8.

The data of Cordfunke and Konings show a steady increase in the equilibrium constant with increasing temperature. The trend of the results from this experiment differs from the trend of the Cordfunke and Konings data. The equilibrium constant is decreasing

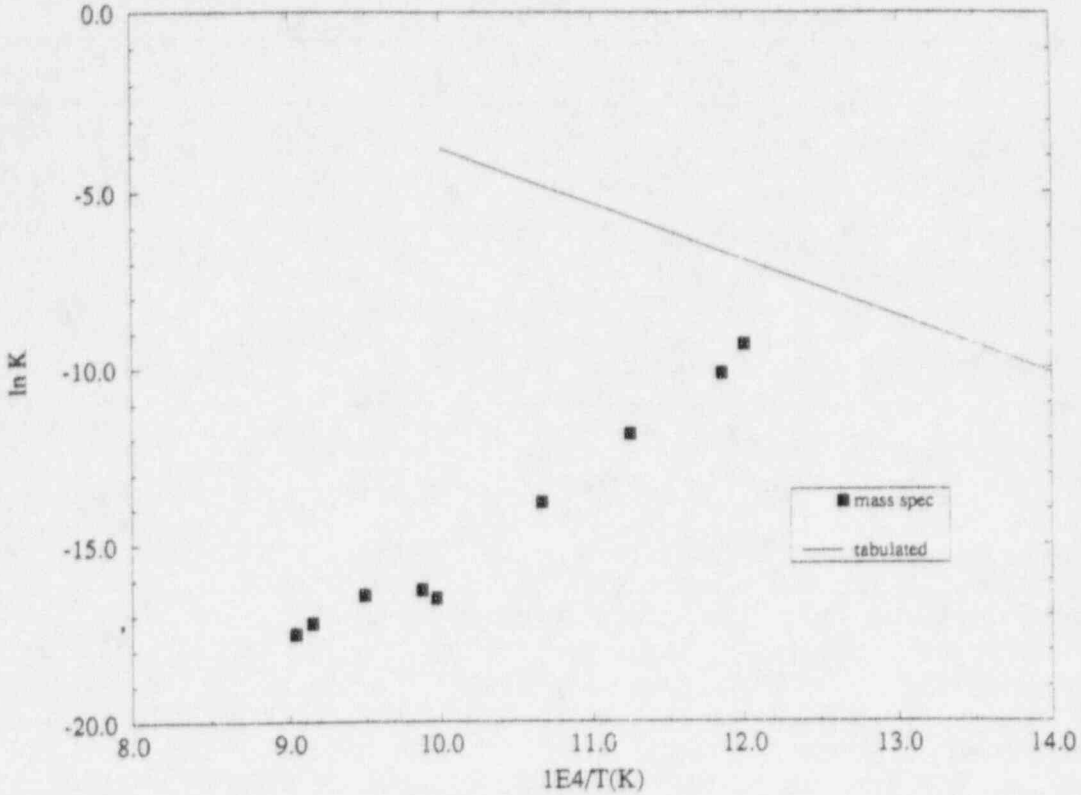

Figure 3.8 Equilibrium Reaction Constant for $CsOH_{(c)} = CsOH_{(g)}$

as the temperature increases for the data from the present investigation. This indicates that as the temperature increases, the formation of $CsOH_{(g)}$ is less favored. This behavior violates the ideal gas laws. This creates the strong inference that at the higher temperatures of this investigation there are reactions between the CsOH, H_3BO_3 and the oxidized stainless steel surface.

The next equilibrium reaction of interest is the phase change of $CsBO_2$. $CsBO_2$ is a product detected during the high temperatures of the reactants CsOH and H_3BO_3. The chemical reaction, equilibrium constant, and the equation for the Gibbs free energy are given below:

$$CsBO_{2(c)} = CsBO_{2(g)}$$

$$\ln K = \ln\left\{\frac{p(CsBO_2)}{a(CsBO_2)}\right\}$$

$$\ln K = \frac{-1}{RT}\{\Delta G[CsBO_{2(g)}] - \Delta G[CsBO_{2(c)}]\}$$

In Figure 3.9 the Cordfunke and Konings data show that the equilibrium constant favors the production of the vapor form of $CsBO_2$ as the temperature increases. The experimental data show

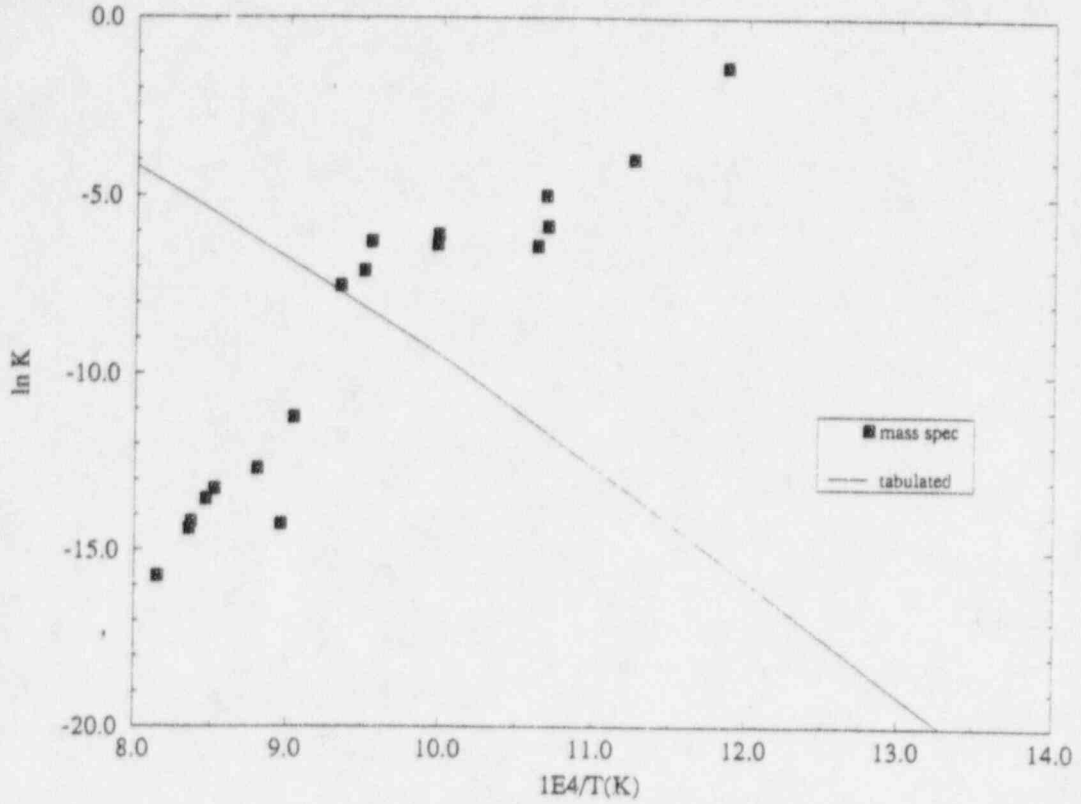

Figure 3.9 Equilibrium Reaction Constant for $CsBO_{2(c)} = CsBO_{2(g)}$

that the pressure of the $CsBO_2$ gas reduces as the temperature increases.

This shows either that the reaction constant at the higher temperature favors the production of the condensed phase of $CsBO_2$ or that other more favored reactions are occurring which remove Cs. This is another indication that there may be a strong surface interaction with the oxide layer.

CsO was also detected in the reaction cell. CsO is produced when the hydrogen portion of the CsOH molecule dissociates:

$$CsOH = CsO + \frac{1}{2}H_2$$

Figure 3.10 is a graph of the equilibrium constant for this reaction. Cordfunke and Konings' equilibrium constant value is considerably lower than the equilibrium constant in the other reactions. The experimental data show that the vapor pressure of CsO is constant over the temperature range of the experiment.

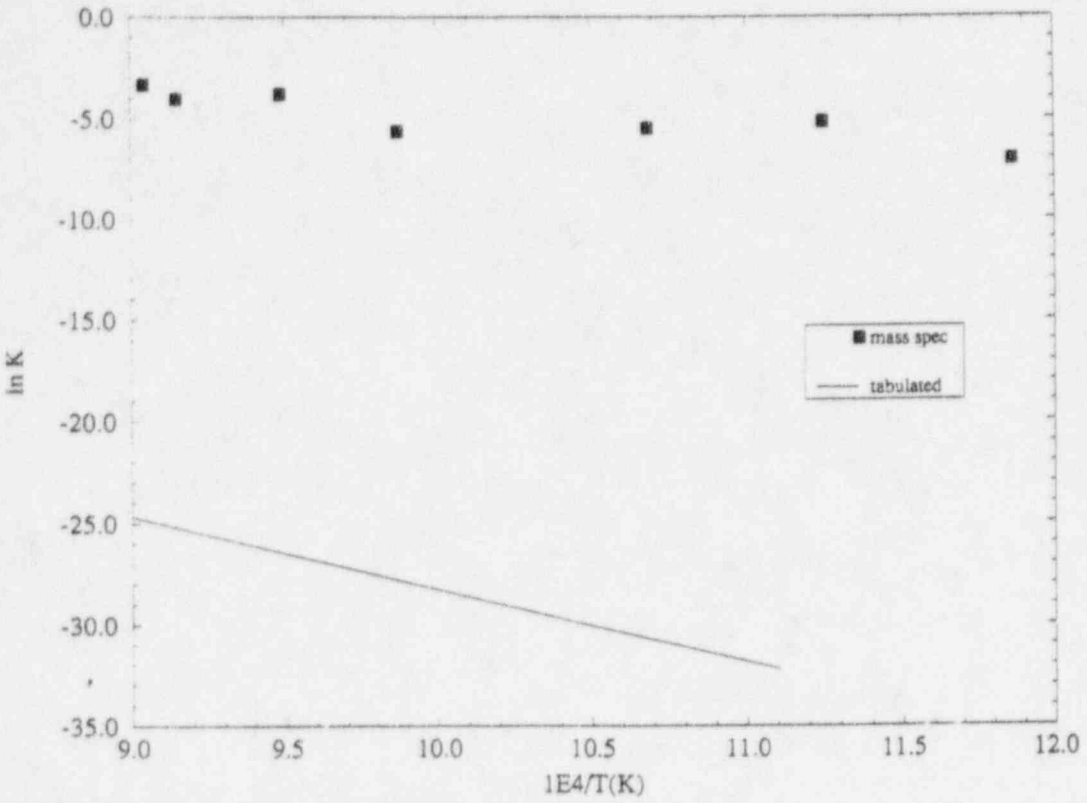

Figure 3.10 Equilibrium Reaction Constant for CsOH = CsO + 1/2H_2

Another reaction involving cesium oxide is

$$Cs_{(g)} + CsO + H_2O = 2CsOH_{(g)}$$

$$\ln K = \ln\left\{\frac{p(CsOH)^2}{p(Cs)p(CsO)p(H_2O)}\right\}$$

$$\ln K = \frac{-1}{RT}\{\Delta G[2CsOH] - \Delta G[H_2O + CsO + Cs]\}$$

Cordfunke and Konings' data favor the production of Cs, CsO, and steam at the high temperatures and favors the formation of CsOH at low temperatures. Figure 3.11 is the Arrhenius plot of the equilibrium constant for this reaction. The equilibrium constant of the experimental data is two to three orders of magnitude less than that of the Cordfunke and Konings data. On the basis of these results, it is expected that the lower vapor pressure measurements are due to some of the compounds binding to the surface layer of the stainless steel. The equilibrium constant remains reasonably constant at all the temperatures, so the generation of Cs and CsO from CsOH also remains fairly constant.

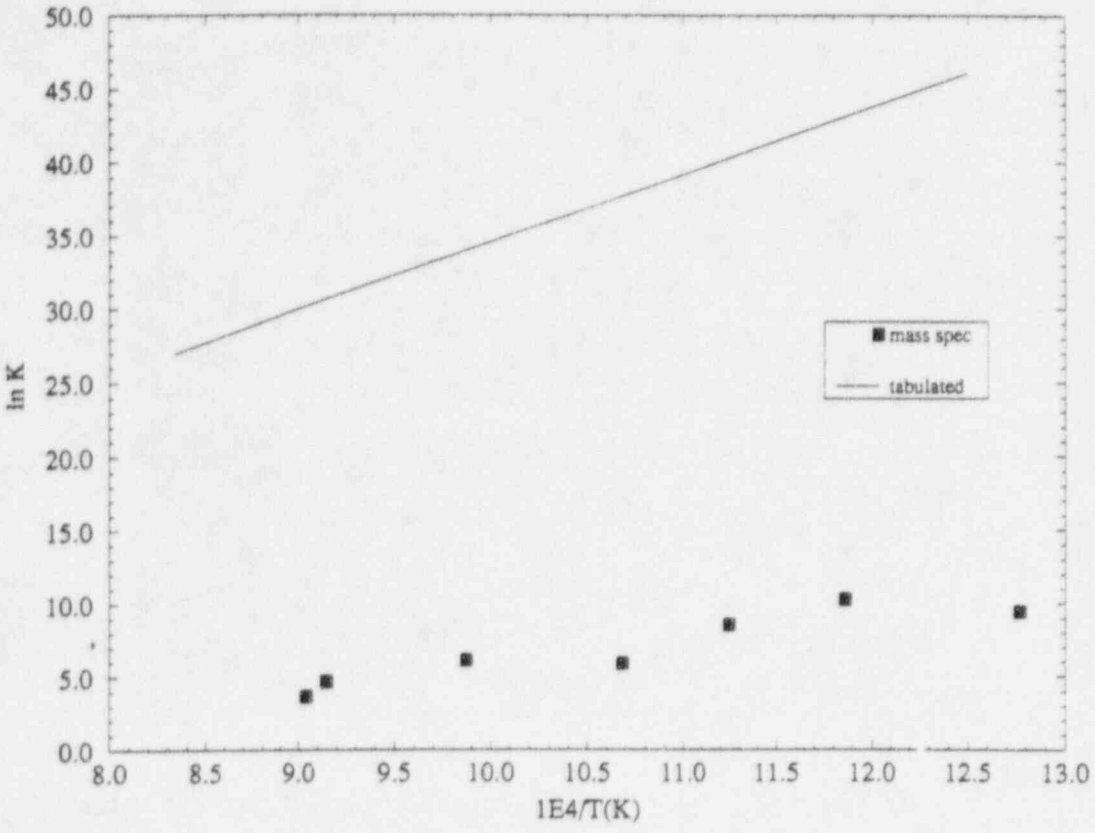

Figure 3.11 Equilibrium Reaction Constant for $Cs+CsO+H_2O = 2CsOH$

3.3 Scanning Electron Microscopy Inspection of the Stainless Steel

Figure 3.12 is a photograph of the sampling chamber after a reaction cell partially melted during one experiment. This afforded an opportunity to investigate the interior wall of the cell after an experiment had been conducted. The stainless steel reaction cell was cut into several smaller pieces to examine the surface. The surfaces of the partially melted reaction cell in Figure 3.12 were examined by using a scanning electron microscope (SEM) to look for any vapor deposition and aerosol deposition into the oxide layer and to see the surface damage caused by the corrosive environment. The original oxide layer is formed at the expense of the stainless steel and grows an additional amount during the experiment. The micrographs show the degradation of the stainless steel surface. Figures 3.13 through 3.15 show the surface of three different samples at increasing levels of magnification. Figure 3.13 is at the lowest magnification, 156 times (156X). Under the top layer is a porous surface, that is, the oxide layer. Inside the porous layer is a granular substance. Figure 3.14 is at a magnification of 417X. A closer examination of the cracked surface reveals the structure. Figure 3.15 is at a magnification of 1.02kX. The deposits observed on the surface could not be identified with a SEM analysis. It was later determined by other means that there was a surface condensation of boric acid and cesium hydroxide.

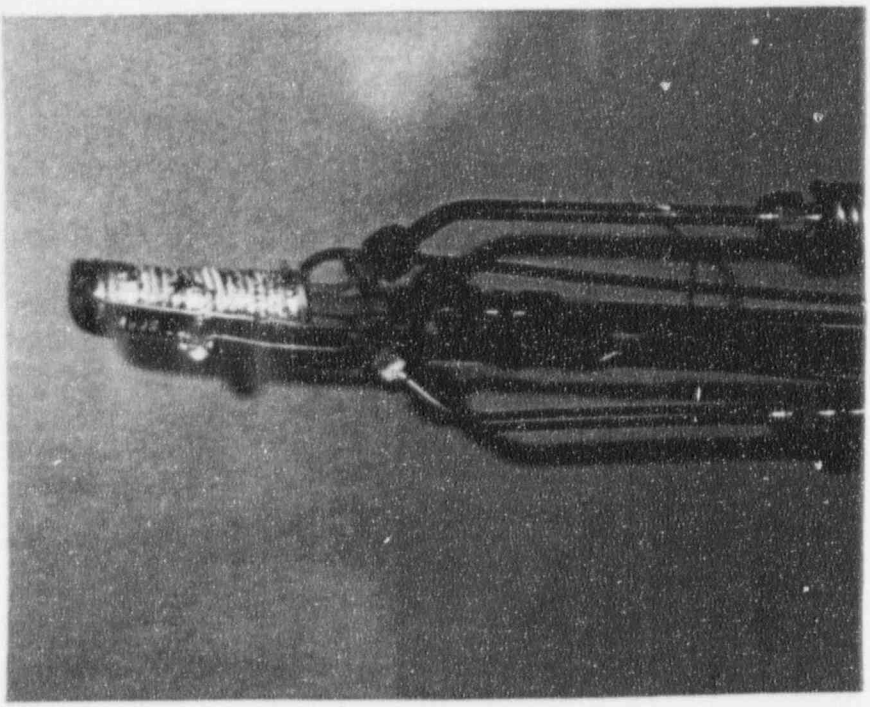

Figure 3.12 Partial Melting of Sample Chamber After Experiment

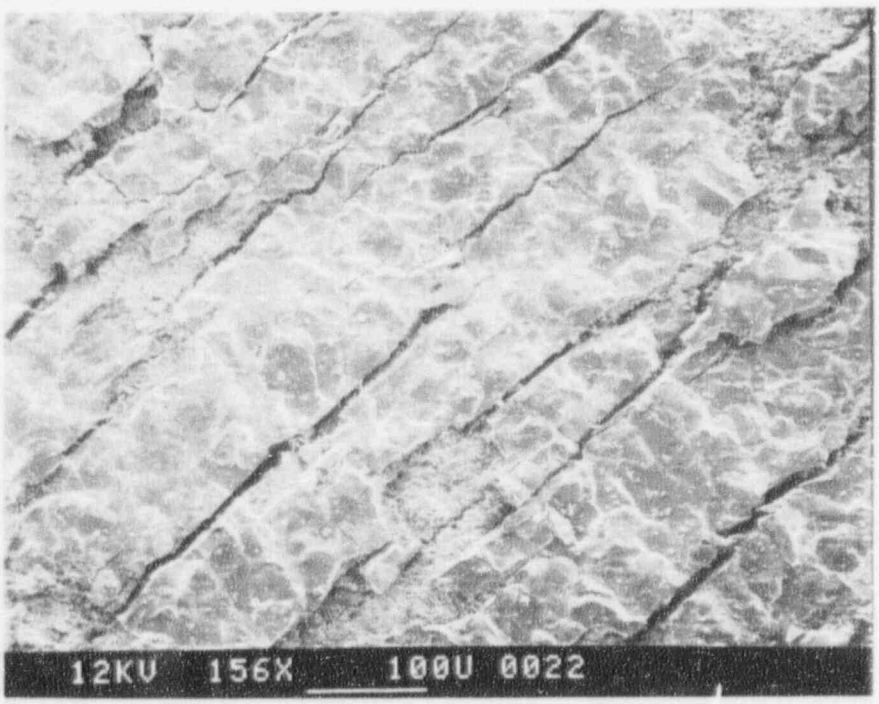

Figure 3.13 Reaction Cell Surface Magnified 156X

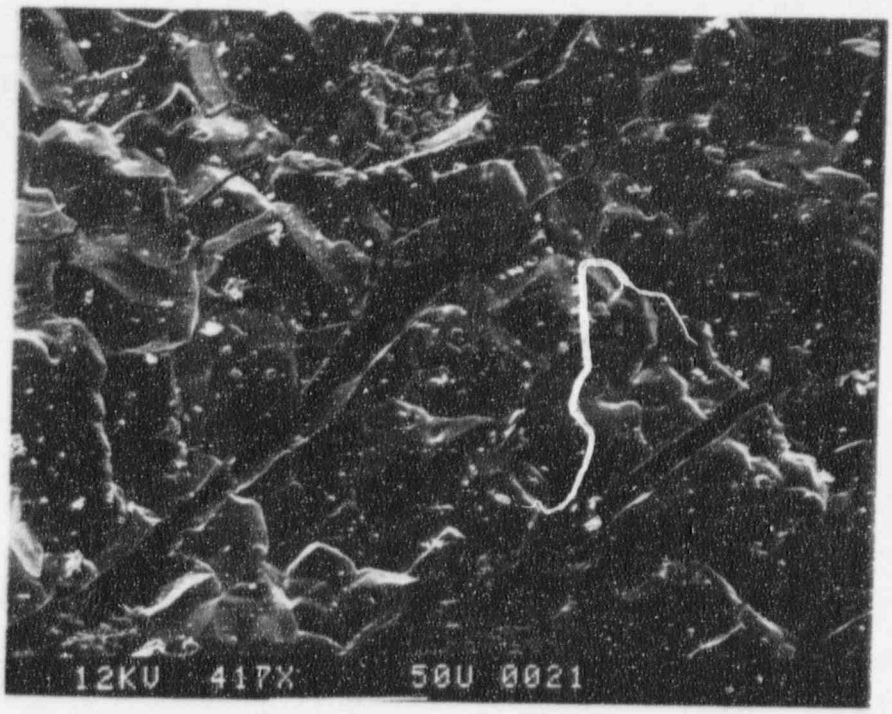

Figure 3.14 Reaction Cell Surface Magnified 417X

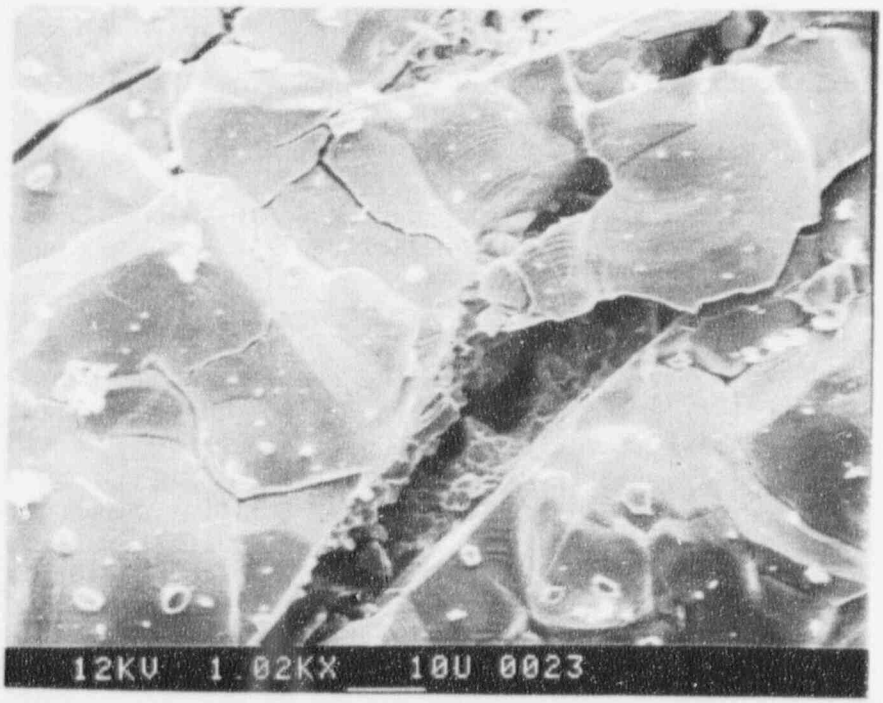

Figure 3.15 Reaction Cell Surface Magnified 1.02kX

3.4 Electron Spectroscopy for Chemical Analysis (ESCA)

ESCA is a tool used to study the outer electron configurations of atoms in chemical compounds by use of X-rays to produce Auger electrons in molecules. Auger electrons are observed from the specimens when they are irradiated by X-rays. The shifts of inner atomic levels due to chemical structures are features of ESCA analysis. The sensitivity of ESCA is high. The electron line spectrum maps out individual atomic levels of the molecular compounds that have been deposited on the stainless steel surface.

The excitation energy of the atoms is converted to kinetic energy for a given electron. The measurement of the energy of an Auger line allows the identification of the element involved. The interest in ESCA analyses is to identify the chemical environment of the deposits on the stainless steel after the vaporization experiment.

The composition of the sample as a function of depth beneath the surface can be determined by progressively removing thin layers of material from the surface and then analyzing the surface composition between removals. A specified thickness of the surface can be removed by "sputtering" in the ESCA apparatus. The sputtering of the surface does not cause damage to the layer of material beneath the surface to be investigated.

The surfaces placed in the ESCA apparatus were samples from the partially melted reaction chamber shown in Figure 3.12. The sample was not pretreated (i.e., coated) before being mounted in the ESCA apparatus. The instrument resolution depth allowed the outer 30 angstroms (Å) of the surfaces to be scanned. The elements at the outer surface of the oxide layer were identified.

Figure 3.16 is a scan of the energy of the Auger electrons coming from the surface over a range of kinetic energy from 250 eV to 1250 eV. The continuous spectrum is the background signal due to the Auger electrons; the amplitude of the peaks in the spectrum can be related to the percent abundance of a certain orbital shell of an atom relative to the other materials on the surface. The different electron orbital shells each has a unique kinetic energy, which allows the process for identifying the species. On the stainless steel surface, Ni, Cr, and C were identified; these are all characteristic of the oxidized stainless steel composition. A characteristic of oxidized stainless steel is for the nickel and chromates to migrate onto the surface and into the oxide layer.

Cesium was also identified on the surface and had the largest signal. In addition, the other elements detected were Cr, Ni, and B. Figure 3.17 shows the spectrum of the surface after the top layer sputtered away. The scan showed peaks for Ni, Cr, and Cs. These results show that the deposition of cesium was embedded at least 50 Å into the oxide layer. The abundance of Cs and Cr on the surfaces is presented on the ESCA scan. The abundance ratios of Cs and Cr are near 4:1. The ESCA scans of the outer surface, and after sputtering 50 Å from the top layer, are in near agreement

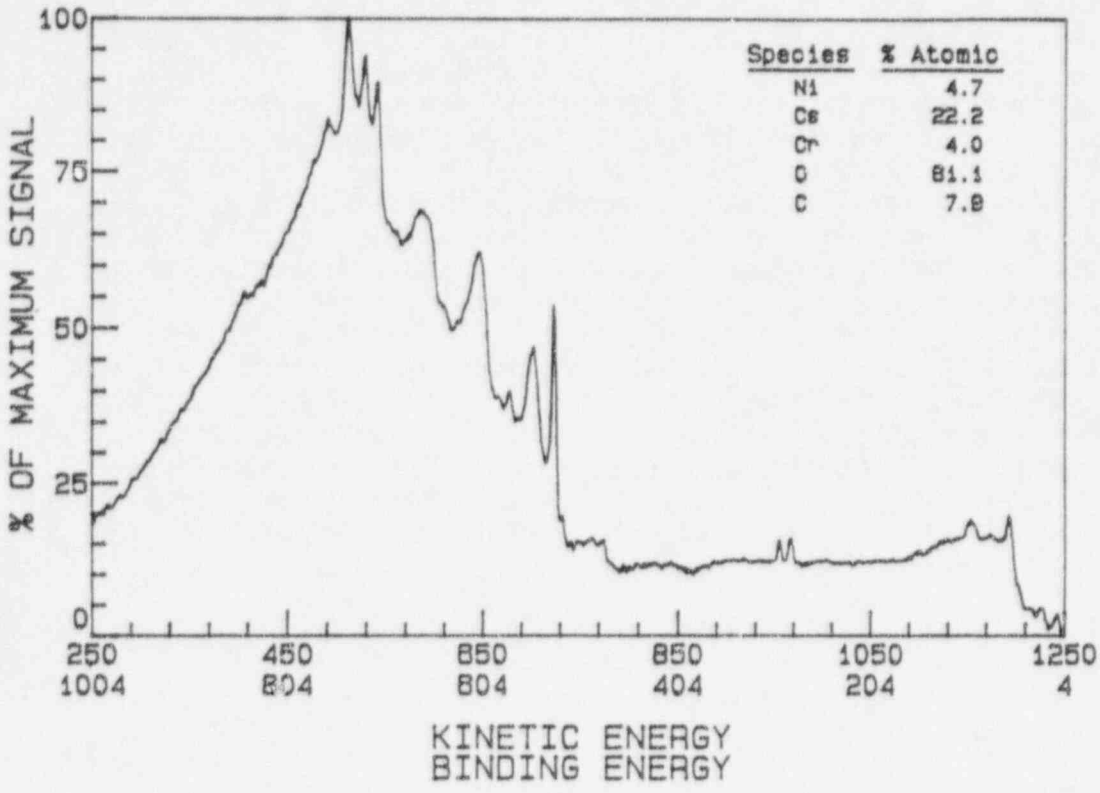

Figure 3.16 ESCA Spectrum of Reaction Surface

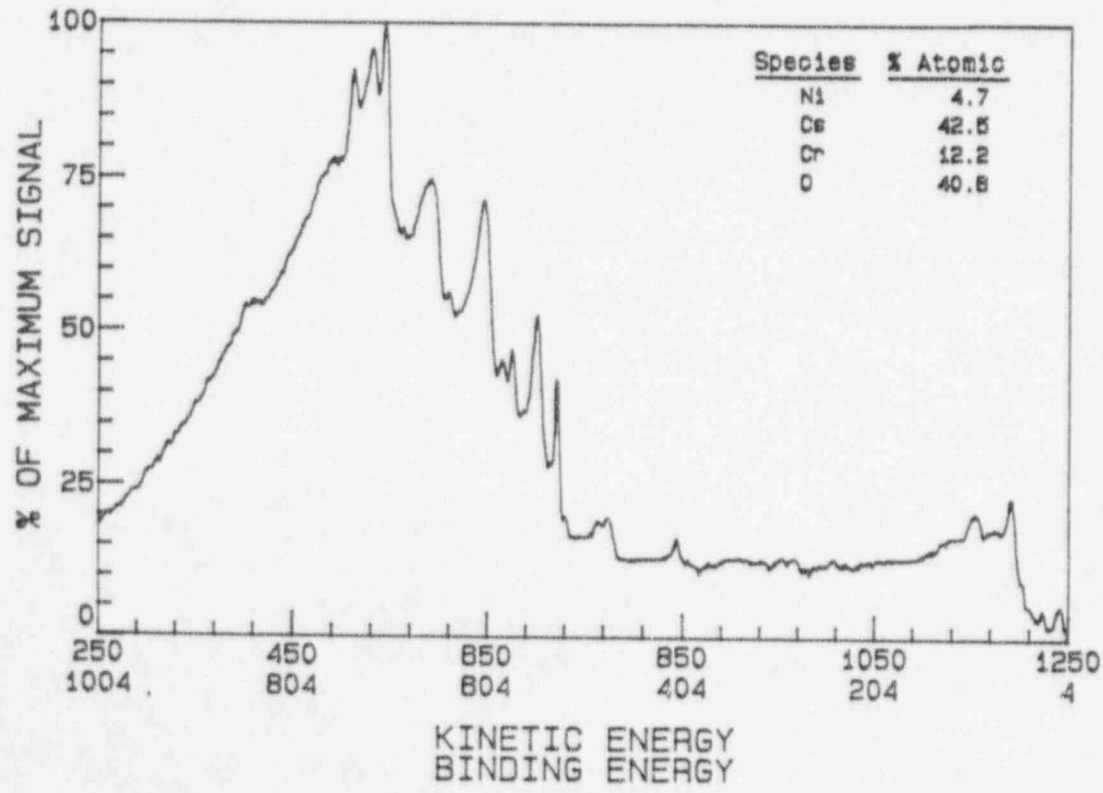

Figure 3.17 ESCA Spectrum 50 Å Under Top of Surface

with a 4:1 ratio. This ratio occurs because a thick layer of Cs built up on the surface.

The surface inside the top of the reaction cell where the vapor emerges through the orifice was also examined by an ESCA scan. Figure 3.18 is a scan of the inside lid of the reaction chamber. It shows a small traceable quantity of Cs on the surface. The largest signal was due to C. There was a small amount of deposition on the lid of the reaction chamber, as indicated by the high concentration of C. The C on the surface is possibly due to the oxidation of C in the stainless steel. During vaporization, CsOH tends to clog the orifice and interrupt the experiment. Because there was only a small amount of condensed material on the lid (where the orifice is located), the concern over the orifice clogging and interfering with the intensity measurements was resolved by an ESCA analysis. This ESCA test confirmed that this reaction cell showed no clogging from CsOH condensation on the surface.

The last region of interest is the skimmer surface. The skimmer is not a removable part of the mass spectrometer. A powder sample from the skimmer surface was scraped off and placed on a copper-surfaced ESCA sample holder. Cu was chosen because none of the elements expected to be detected would react with Cu, and the Cu Auger lines would not interfere with the Cs lines. Figure 3.19 is a spectrum from analysis of a sample taken from the skimmer of the mass spectrometer. As expected, both Cs and B were identified on the surface in addition to C.

The results from the experiment conducted using the mass spectrometer to revaporize any materials that may have deposited onto the inner walls of the partially melted reaction cell showed Cs revaporization. Elemental Cs was observed to be the only revaporized product. The mass spectrometer was used to scan for the same products detected during the volatilization experiment, and there were no such species detected other then Cs. After examination of the stainless steel surface by ESCA, it appeared that all the Cs deposits on the surface failed to revaporize. This ESCA scan also detected Cr on the surface. The inference can be drawn that it is possible some of the molecules may have chemically combined to the oxide layer or the stainless steel surface, or both, and will not revaporize.

3.5 Conclusions

The results of the reaction cell experiment were presented in this chapter. A combination of CsOH, B_2O_3, steam, H_2, and the oxidized stainless steel layer were heated to selected temperatures and measurements were made of the gaseous chemical products formed. The intensity of the signals was converted to vapor pressure for the analysis.

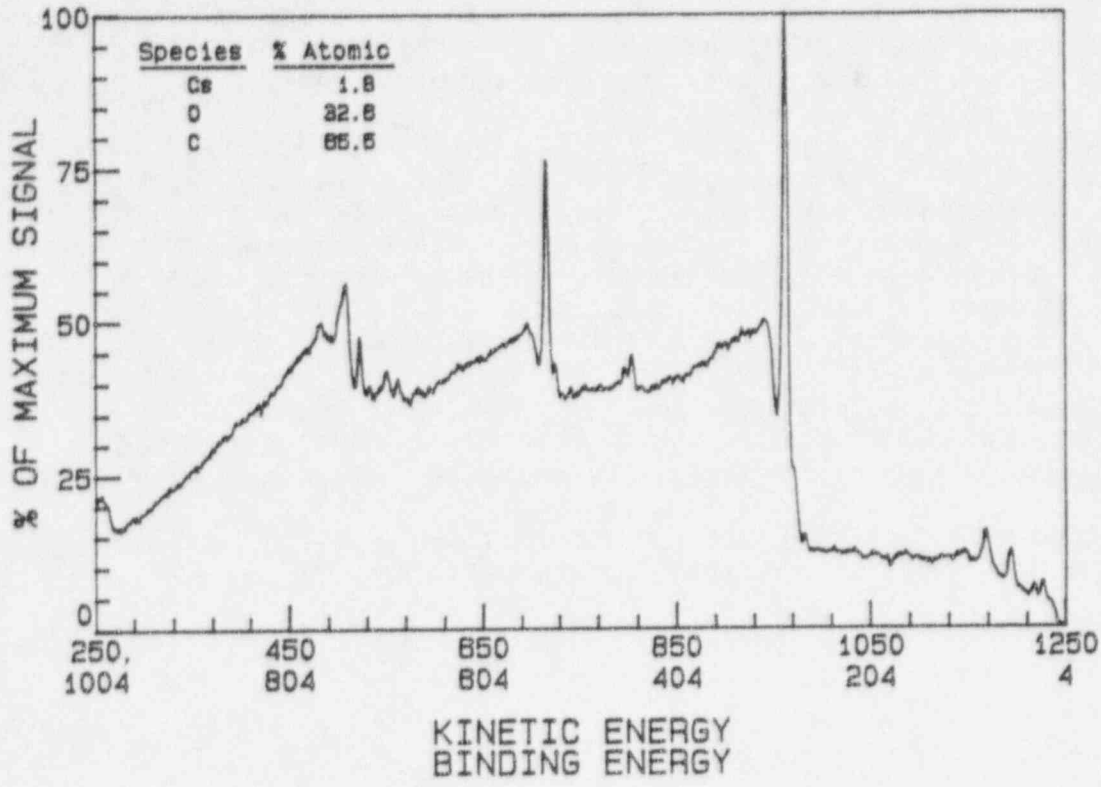

Figure 3.18 ESCA Spectrum of the Inside Lid of Reaction Cell

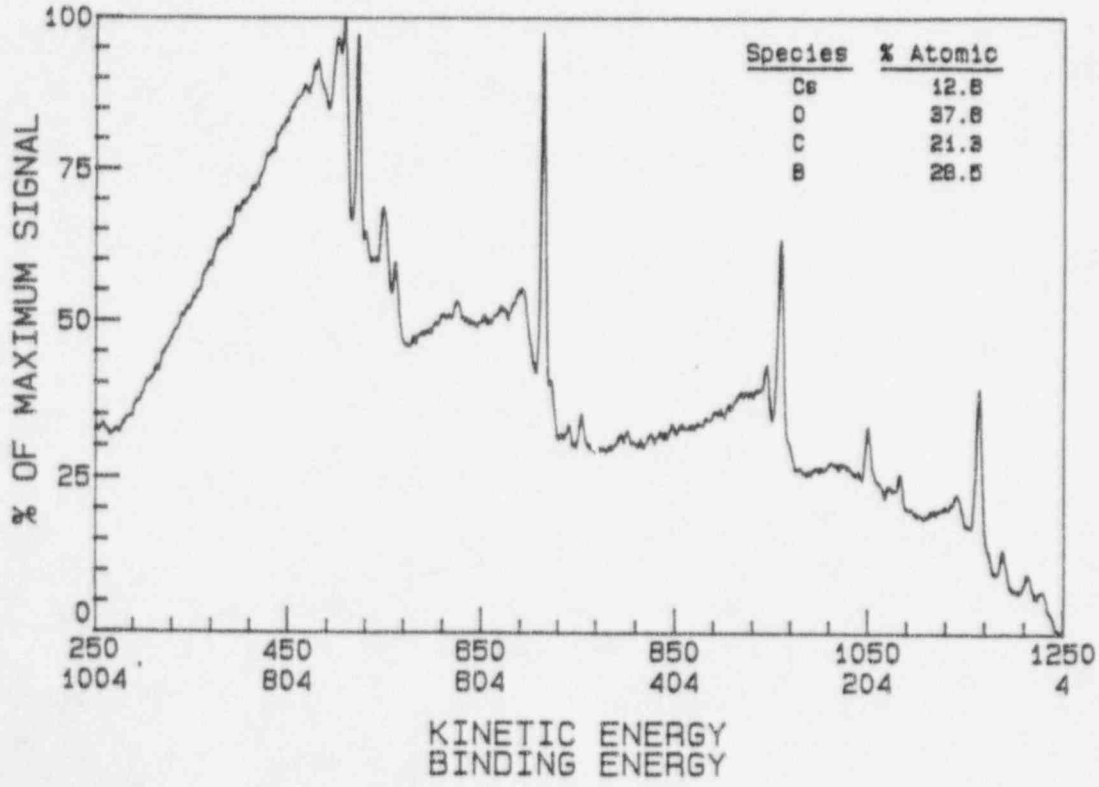

Figure 3.19 ESCA Spectrum of a Sample of Deposit on Skimmer

The analysis of the vapor pressure of six different species, CsOH, H_3BO_3, $CsBO_2$, Cs, HBO_2, and CsO were presented on Arrhenius plots. The equilibrium constants from the reactions involved are also shown on Arrhenius graphs.

According to the ideal gas laws, the vapor pressure of a gas increases when the temperature increases if the gas does not react with other materials. There are temperature regions in the graphs that show a decrease in the vapor pressure when the temperature increases. This indicates that not all the products from the reactions taking place are in the vapor form. Non-ideal chemistry behavior occurs on the surface of the reaction cell. It appears that a portion of the products are forming compounds on the surface. To understand the surface interactions, a further investigation of the surface is needed.

In the next chapter, a different experiment, which investigated the surface effects more directly, is described.

CHAPTER 4

MASS BALANCE MEASURING SYSTEM AND EXPERIMENTS

The decision to perform this set of experiments arose from the indications of unexpectedly significant chemical reactions with the surface of the reaction cell in the mass spectrometer experiments. The objective of these experiments was to determine the rate of deposition of Cs onto an oxidized stainless steel surface in the presence and absence of H_3BO_3. The variables in an environment that affect the deposition of materials in the cell are temperature, pressure, the physical and chemical form of the materials in the cell, and the chemical environment on the surface. An understanding of the effect of these variables motivated the different experiments conducted in this investigation.

An experimental apparatus was constructed that contains a reaction chamber to provide the testing environment for mass change measurements of an oxidized stainless steel sample. The walls of the reaction chamber were made of Ni, since the materials under investigation are not expected to react with Ni. CsOH, H_3BO_3, steam, and H_2 were admitted into the reaction chamber, using H_2 as the carrier gas; the flow paths are shown in Figure 4.1. The flow rates were controlled to provide the hydrogen and steam desired environment. An apparatus was designed and constructed using a

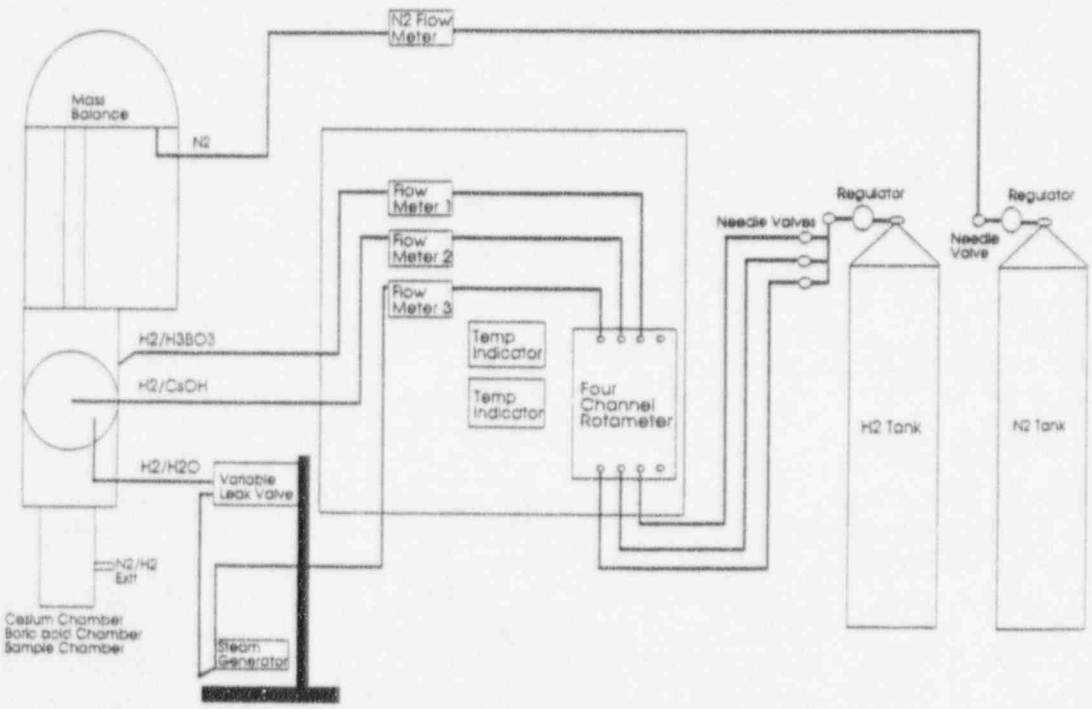

Figure 4.1 Schematic Representation of Hydrogen Flow Through System

torsion balance to measure the mass changes taking place on the oxidized stainless steel surfaces. A stainless steel cylinder was suspended from one arm of the torsion balance by a Ni chain in such way that the sample is located in the reaction chamber. The stainless steel was oxidized inside the reaction chamber by steam and H_2 before the other reactants entered. Measurements were made on the mass change of the oxidized stainless steel cylinder sample for four different environments.

An investigation of the deposition of Cs-bearing compounds was performed at two temperatures, 1028 and 1233 Kelvin. These temperatures were selected to be representative of those that are most important in the primary piping during a severe accident. The reaction chamber was heated to the selected temperatures. The reactants were permitted to flow into the reaction chamber and the mass change was recorded until there was no observable mass change.

An ESCA scan was later performed on the surface of the stainless steel to identify the deposits on the surface. This experiment showed the deposition of Cs-bearing compounds onto an oxidized stainless steel surface.

4.1 Mass Electrobalance Apparatus

An apparatus was constructed to utilize a mass balance to measure weight changes in the oxidized stainless steel during the experiment. The data recorded from the mass balance is a function of time. The electrobalance used in this experiment is a torsion balance and is sensitive to mass changes as small as 5×10^{-7} grams (g).

Figure 4.2 is a schematic drawing of the mass electrobalance system. A stainless steel sample, 5.08 cm long and 0.64 cm in diameter, suspended from the torsion balance by a nickel chain into the reaction chamber is balanced by tare weights, so that the balance is in equilibrium.

This drawing is a simplified representation of the system. The mass balance chamber was modified to provide the appropriate environment. The weighing unit can be operated under such different conditions as vacuum, flowing gas, or atmospheric conditions.

The sample chamber is in a condenser tube to condense any vapors that may leave the sample chamber (see Figure 4.3) and send the condensables to a liquid nitrogen cold trap. Figure 4.4 is a photograph of the sample chamber internals. The sample chamber has four large flanges attached to it, one each at the bottom and the top, and two parallel to the cell length. Each of these flanges has a port that provides the opening into the mixing chamber through which the vapors flow. The copper compression seals on flanges can be seen at the bottom of the photograph (Figure 4.3). On the right side is the H_3BO_3 line into the reaction chamber, and the CsOH and H_2 lines connected to the flange that is on the left

side. These connections lead the CsOH and H_3BO_3 vapors into the mixing chamber. This mixing chamber lies above the reaction chamber, and the mixed vapors flow into the reaction chamber.

The higher pressure maintained in this portion prevents any vapor from flowing into the torsion balance, and forces the vapors under investigation to remain in the reaction chamber pressurized to approximately 1.1 atm. If H_2 is flared at the capillary vent, then the pressure inside exceeds 1 atm. Figure 4.5 is a photograph of the top view of the reaction chamber with all the flanges connected. The inlet for CsOH has a heater coil wrapped on the outside surface to prevent clogging. At the top plane of the condenser tube are the ports where the volatilized CsOH, H_3BO_3, and the H_2 and steam enter the mixing chamber. The top portion of the

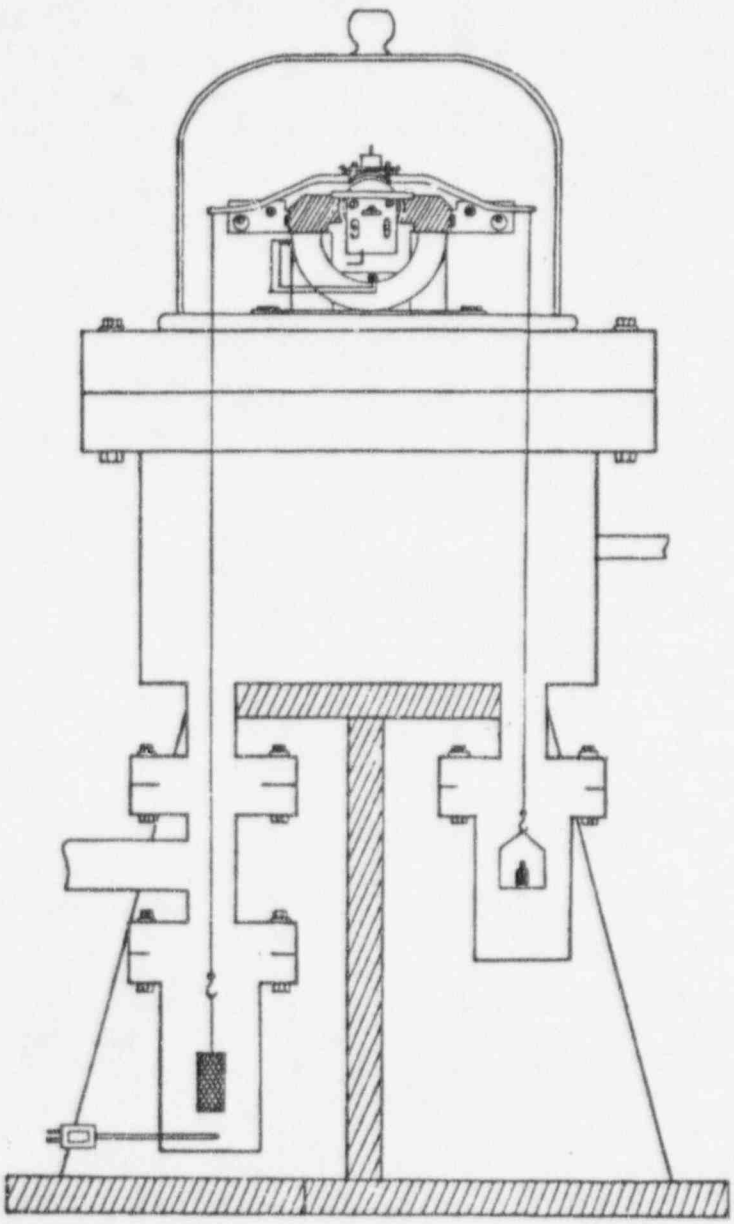

Figure 4.2 Schematic Representation of Mass Electrobalance System

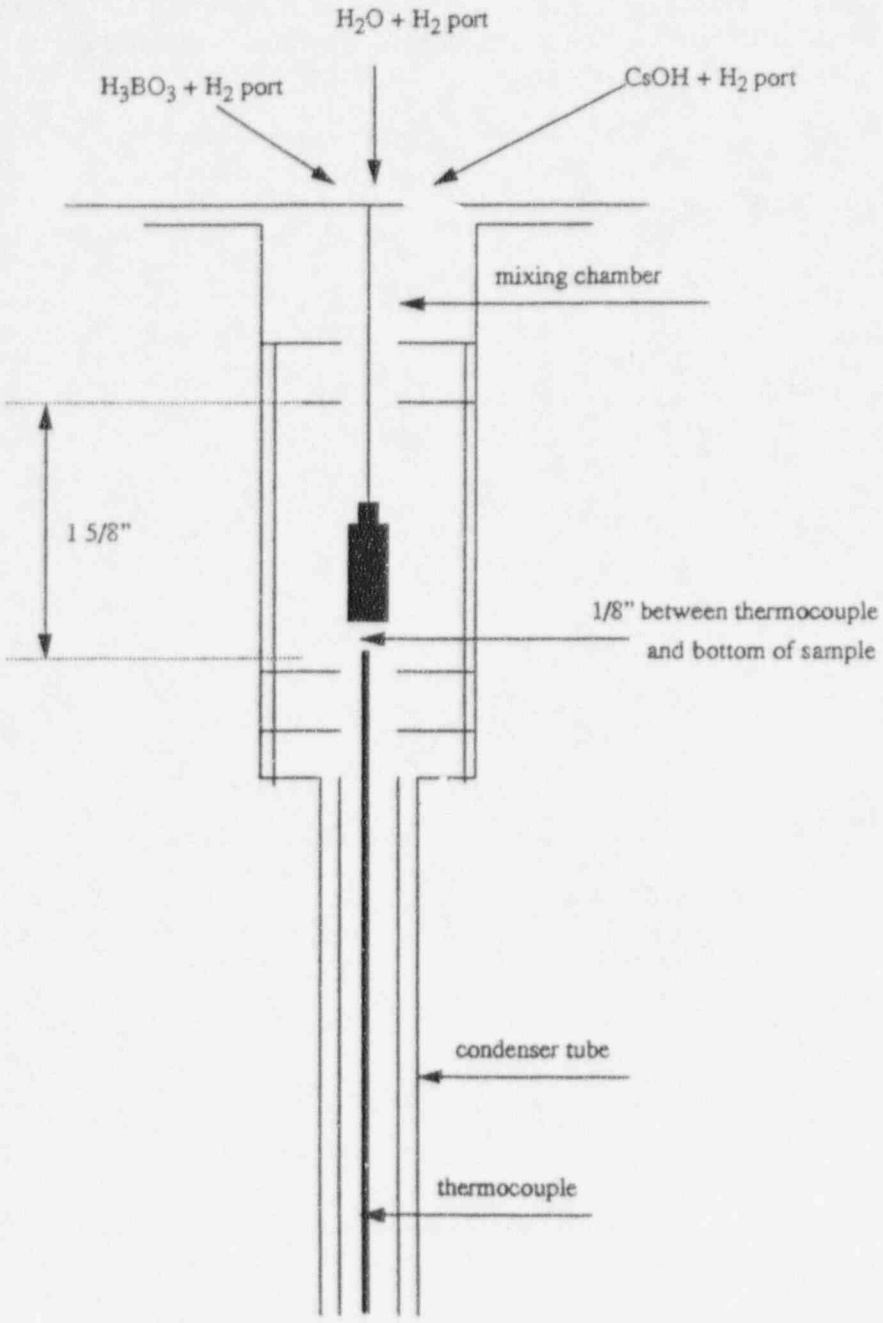

Figure 4.3 Sample Placement in Mass Electrobalance

apparatus from the torsion balance to the mixing chamber is pressurized by N_2 to slightly more than 1 atm. This configuration prevents the vapors in the mixing chamber from flowing upward into the torsion balance.

On the control panel shown in Figure 4.6, there is a six-channel digital indicator for temperature and a single-channel temperature indicator to monitor the sample temperature (these indicators are identified in Table 4.1). The temperature range of interest is

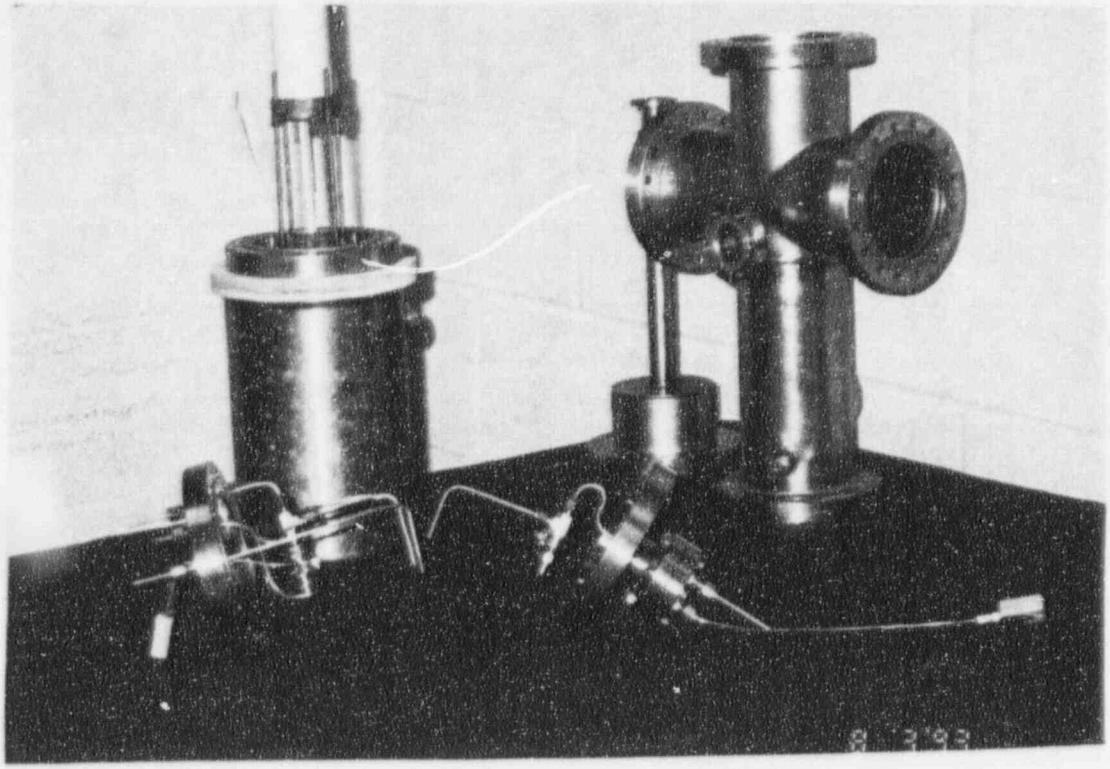

Figure 4.4 Photograph of Sample Chamber Internals

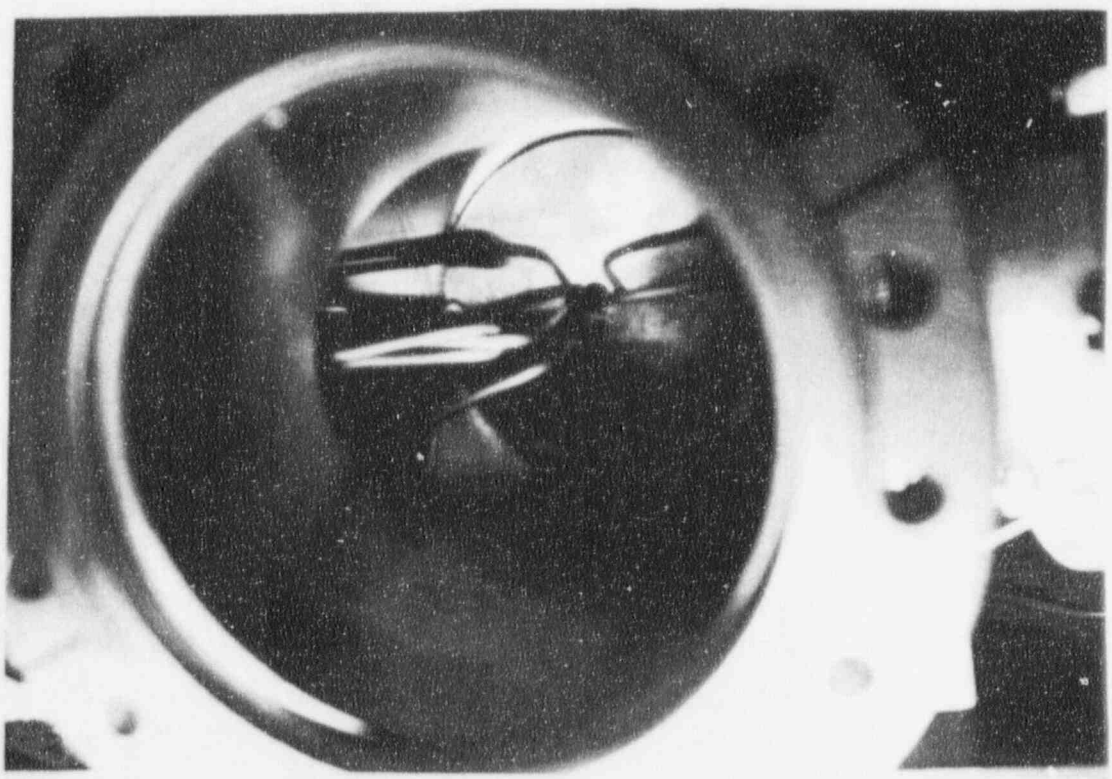

Figure 4.5 Top View of Inlet Lines to Reaction Chamber

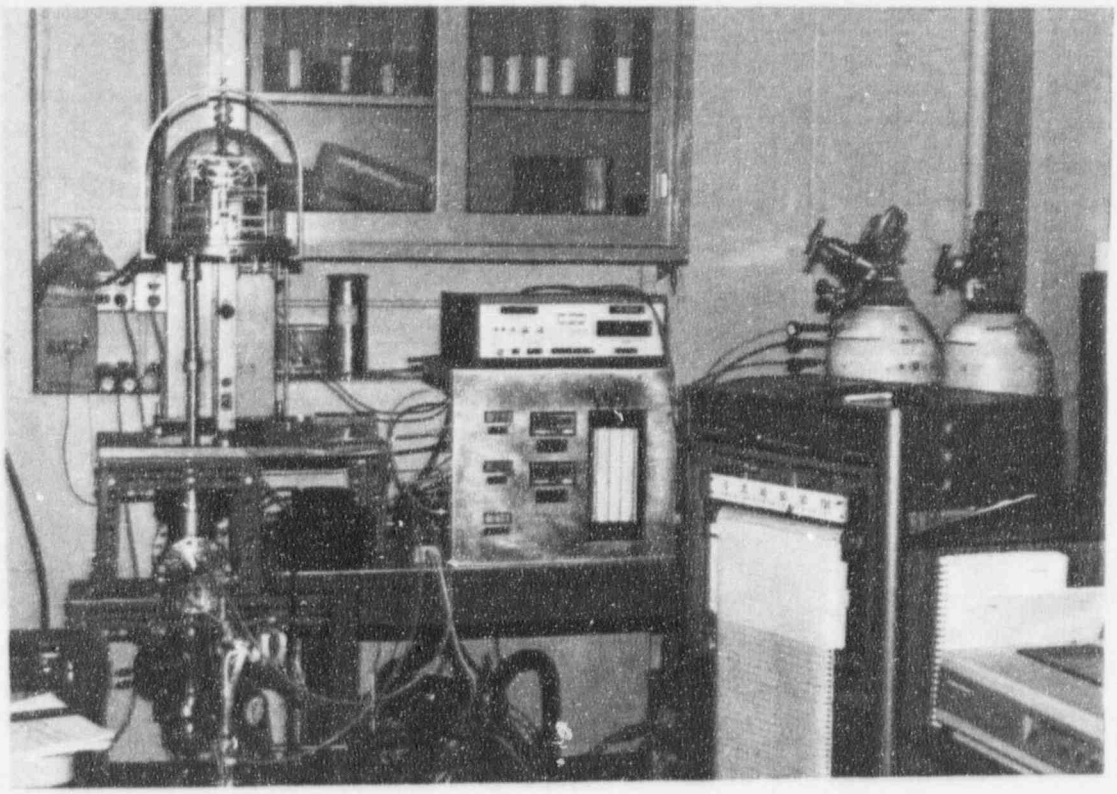

Figure 4.6 Mass Electrobalance Apparatus

between 700 and 1200 Kelvin. A Variac was used to control the chamber temperature. The temperature of the sample furnace was monitored by a separate gauge. Table 4.1 lists the thermocouple channels and the part of the system that is monitored. The temperature inside of the reaction chamber is separately monitored. The heater system is shown on the schematic drawing, Figure 4.7. There are four separate Variacs to control the heat for the sample chamber, steam generator, CsOH reservoir, and the hydrogen/ steam line into the sample chamber. Four separate Variacs are used to provide flexibility in the selection of temperature for the experiments. For example, the temperature of the CsOH controls its density and the rate at which it enters the mixing chamber. The mass change is recorded as a function of time on a strip chart. The strip chart is located in front of the N_2 and H_2 tanks in Figure 4.6.

Table 4.1 Thermocouple Channels

Thermocouple Channels	Area Monitored
1	Initial H_2O temperature
2	Leak valve temperature
3	Temperature outside sample
4	Temperature at top plate
5	CsOH temperature
6	H_3BO_3 temperature

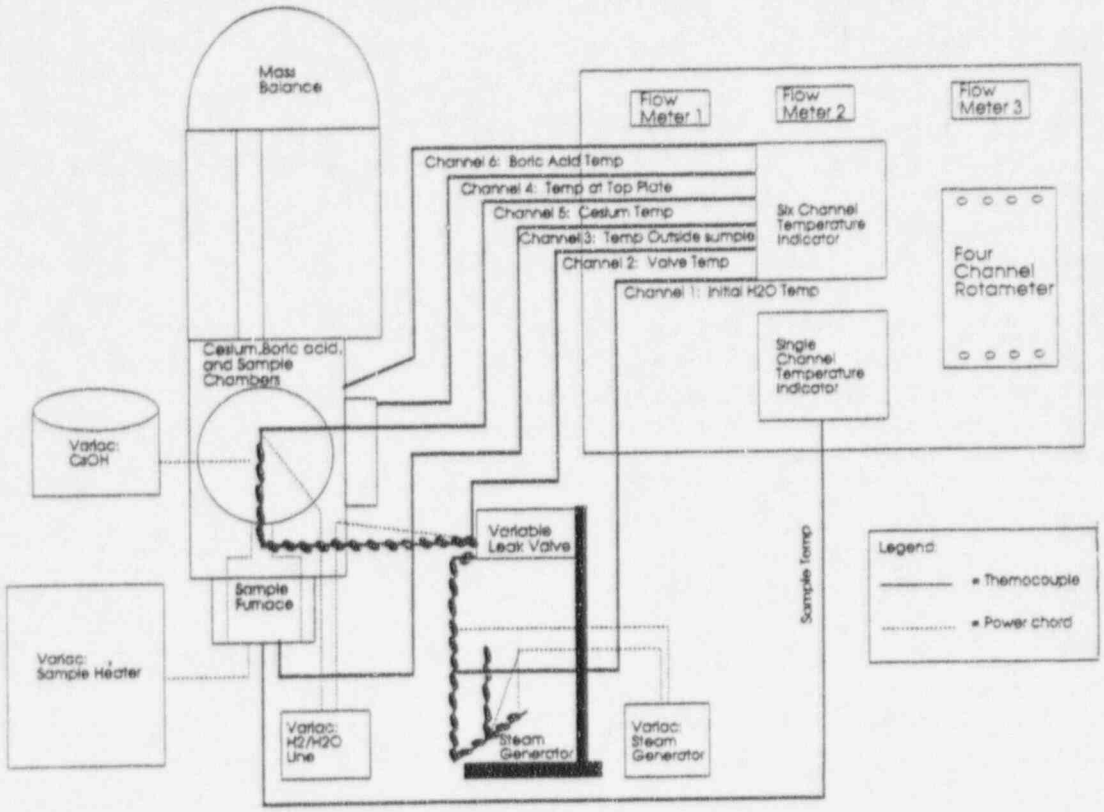

Figure 4.7 Schematic Representation of Heating System

4.2 The Selection of Gas Flow Rates

The flow rates of steam and hydrogen were selected at the beginning of the oxidation process when the stainless steel sample was placed inside the reaction chamber. The flow rates were carefully selected so that the suspended sample did not contact the walls of the reaction chamber when the gases flowed. When the flow rates are too high, the turbulence in the flow will cause the stainless steel sample to contact the walls, and the recording on the strip chart becomes meaningless for the experiment.

For this experiment, the pretreatment of the stainless steel cylinder took place inside the apparatus in which the experiment was to be conducted. For oxidation purposes, the hydrogen and steam were turned on slowly and their flow rates were controlled by the flow meter. When the chamber was heated to the temperature of interest, the hydrogen and steam valves were opened. Oxidation of the surface was considered to be complete (and its surface in equilibrium with the environment) when the observed weight change was negligible.

4.3 Description of the Experiments Conducted With the Mass Electrobalance

In the conduct of the experiment, the H_3BO_3 was admitted so that the stainless steel would be saturated by the vapor deposition. The CsOH was permitted to flow into the system after the H_3BO_3 was in equilibrium with the oxide layer. Equilibrium was assumed when there was no further total mass change in the sample. Weight changes were observed during the addition of CsOH.

The experiments conducted in the mass electrobalance apparatus are outlined below. For each experiment, a new stainless steel sample was oxidized using the same procedure. Each experiment was continued until there was no observable mass change of the stainless steel sample.

(1) A stream of CsOH, steam, and H_2 was fed into the reaction chamber. The temperature of the reaction chamber was controlled at 1028 Kelvin.

(2) A stream of CsOH, steam, and H_2 was fed into the reaction chamber. The temperature of the reaction chamber was controlled at 1233 Kelvin.

(3) A stream of H_3BO_3 was fed into the reaction chamber, coating the oxide layer with B_2O_3. When there was no further observable mass change, a stream of CsOH, H_2, and steam was fed into the reaction chamber. The temperature of the reaction chamber was controlled at 1233 Kelvin.

(4) A small cup was drilled into the top of an oxidized stainless steel cylinder sample and 0.095 g of pure B_2O_3 were placed in the cup. A stream of CsOH, steam, and H_2 was fed into the reaction chamber. The temperature of the reaction chamber was adjusted to 1023 Kelvin.

The results from these experiments are presented in Chapter 5, and the conclusions from these experiments and the reaction cell experiments are in Chapter 6.

CHAPTER 5

MEASUREMENTS USING THE MASS ELECTROBALANCE

For these experiments, the sequence of entry of the CsOH and H_3BO_3 into the mixing chamber, and the temperature of the reaction chamber were varied. The flow rates of both the H_3BO_3 and CsOH entering the reaction chamber were independently varied. The flow rate was varied between 13 cc/min and 26 cc/min. The flow rate of H_2 into the boiler is assumed to be the flow rate of the reactants into the mixing chamber. These flow values were selected so as to prevent collisions between the stainless steel sample and the walls of the reaction chamber. The mass changes during each experiment were recorded on a strip chart.

5.1 Data Collection and Analysis

In these experiments, the stainless steel surface was first oxidized. After oxidation, the temperature was increased in increments of approximately 100 °C until the selected temperature was reached. This was done in order to maintain the oxide layer in equilibrium with the gases in the chamber. Then, either CsOH was permitted to flow into the mixing chamber, or the surface was coated with H_3BO_3 followed by CsOH flow. Both of these experiments were performed in the presence of steam and H_2.

5.2 Cesium Deposition

When CsOH vapor enters the bulk gas composed of H_2 and H_2O at elevated temperatures, it dissociates. The reaction between CsOH and the steam/H_2 environment in the bulk gas in the mixing chamber is postulated as

$$CsOH + \frac{1}{2}H_2 = Cs + H_2O$$

This produces Cs which can deposit on the surface. Indeed, Cs is detected by ESCA on the oxidized stainless steel surface. ESCA analysis indicated that Cs formed a molecule with Cr (a chromium oxide on the surface).

5.2.1 Temperature Maintained at 1028 Kelvin

The Cs source entering the mixing chamber can be calculated from the conditions of the boiler temperature and the flow rate of the carrier gas from the boiler. CsOH enters the mixing chamber where it combines with the flows of H_2 and steam and then is directed to the reaction chamber where an oxidized stainless steel sample with a surface area of 5.0 ± 0.1 cm^2 is suspended. The temperature of the reaction chamber was maintained at 1028 Kelvin. A change in mass was observed and the mass increase was [30 ± 1.5] μg The mass change was followed for a period of 3500 sec, after which no further increase occurred. The experimentally observed deposition for these conditions was [8.57 ± 0.43] × 10^{-9} g/sec. The deposition rate per unit surface area was [1.71 ± 0.46] × 10^{-9} g/sec-cm^2.

In the CsOH reservoir, the temperature was 703 Kelvin, and the calculated partial pressure of CsOH was 2.5×10^{-5} atm. The vapor pressure for Cs and CsOH in the boiler can be calculated using the data of Cordfunke and Konings. Since dry H_2 is passed over CsOH, any H_2O in the chamber would be produced from CsOH. Therefore, as the system is at equilibrium, the vapor pressure of Cs is equal to that of the H_2O, inside the boiler. The vapor pressure of Cs is calculated to be 2.1×10^{-5} atm and the flow rate of the carrier gas into the reaction chamber was 25 cm^3/min.

The molecular density of Cs in the bulk was found using the ideal gas law and equilibrium conditions, $P = nkT$, and was 2.16×10^{14} molecules/cm^3. The Cs mass content in the vapor stream is due to Cs and CsOH and is 1.04×10^{-7} g-Cs/cm^3.

The flow rate can be converted into a mass flow rate by multiplying the flow rate of CsOH by the vapor density:

$$(26\ cm^3/min)\ (1.04 \times 10^{-7}\ g/cm^3 = 2.7 \times 10^{-6}\ g/min = 4.5 \times 10^{-8}\ g/sec$$

The weight gain experimentally observed was $[8.57 \pm 0.43] \times 10^{-9}$ g/sec. The Cs species available to react is 4.5×10^{-8} g/sec, so the percent reacted is

$$\frac{8.57 \times 10^{-9}\ g/sec}{4.50 \times 10^{-8}\ g/sec} = 19\%$$

The percent reacted is an average value in excess of 3500 seconds. Most of the weight addition is due to Cs interaction; however, a small part is due to increased oxidation on the surface of the cylinder.

5.2.2 Temperature Maintained at 1233 Kelvin

In this experiment, the reaction chamber was heated to a higher temperature than in the first experiment. A mixture of CsOH vapor and H_2 was fed into the reaction chamber as in the previous experiment.

A change in mass was observed and the mass increase was $[240 \pm 12]$ μg. The mass change was followed for a period of about 1800 sec to ensure no further mass increase was occurring. The experimentally observed mass rate increase was then $[1.33 \pm 0.07] \times 10^{-7}$ g/sec. The surface area of the sample was 5.0 ± 0.1 cm^2, so the observed deposition is $[2.66 \pm 0.14] \times 10^{-8}$ g/sec-cm^2.

The CsOH reservoir conditions were: temperature = 733 Kelvin, vapor pressure of CsOH = 7.0×10^{-5} atm, and vapor pressure of Cs = 6.1×10^{-5} atm. The flow rate was 26 cm^3/min.

The vapor densities of Cs in the stream for Cs and CsOH were calculated to be 1.33×10^{-7} g/cm^3 and 1.52×10^{-7} g/cm^3, respectively. The vapor density of the total Cs species in the stream

was 2.85×10^{-7} g-Cs/cm^3. The amount of cesium entering the reaction chamber was

$$(2.85 \times 10^{-7}\ \text{g-Cs/cm}^3)\ (26\ \text{cm}^3/\text{min} = 7.41 \times 10^{-6}\ \text{g/min} = 1.24 \times 10^{-7}\ \text{g/sec}$$

The Cs in the vapor stream entering the reaction chamber was 7.96×10^{-8} g/sec, and the weight gain observed was $[1.33 \pm 0.07] \times 10^{-7}$ g/sec. Essentially all the Cs species reacts with the surface. The large mass gain indicates that in addition to the Cs reaction with the surface, other reactions are taking place, perhaps increased oxide layer growth. This is addressed further in the conclusions.

5.3 Chemical Reactions for the Boric Acid-Cesium System

5.3.1 Boric Acid Deposition

H_2 is the carrier gas for moving the H_3BO_3 vapor into the mixing chamber. H_3BO_3 forms HBO_2 vapor and B_2O_3 solid in the presence of steam and H_2 at elevated temperatures (>1000 Kelvin). These products are a net result of the reaction with steam and H_2; there are intermediate reactions. The two reactions that can occur are represented below.

The first reaction forms H_3BO_3:

$$H_3BO_{3(g)} = \frac{3}{2}H_2 + \frac{3}{2}O_2 + B_{(c)}$$

$$\frac{1}{2}H_2 + O_2 + B_{(c)} = HBO_{2(g)}$$

$$H_2 + \frac{1}{2}O_{2(g)} = H_2O$$

The net result is $H_3BO_{3(g)} = HBO_{2(g)} + H_2O$. H_3BO_3 also forms B_2O_3:

$$2H_3BO_{3(g)} = 3H_2 + 3O_2 + 2B_{(c)}$$

$$2B + \frac{3}{2}O_2 = B_2O_{3\,(c)}$$

$$3H_2 + \frac{3}{2}O_2 = 3H_2O$$

The net result is $2H_3BO_{3(g)} = B_2O_{3(g)} + 3H_2O$.*

*Private communication from C. Alexander, 1993.

The temperature in the reaction chamber was held at 700 Kelvin when B_2O_3 coated the surface. The H_3BO_3 vapor continuously enters the reaction chamber and the stainless steel cylinder gains weight until the surface became saturated with B_2O_3. After the H_3BO_3 was deposited, the following experiments were conducted.

5.3.2 Cesium Interaction With the Boric Oxide Layer

The average thickness of the B_2O_3 layer is 0.100 ± 0.005 mg/cm^2 (from mass measurements). CsOH was permitted to enter the chamber and, during a 93,300-sec time period, the experimentally observed mass change was 5.18 ± 0.26 mg and the mass rate increase was [5.55 ± 0.28] × 10^{-6} g/sec. The surface area of the sample was 5.0 ± 0.1 cm^2, yielding a deposition rate of Cs onto the B_2O_3 layer of [1.11 ± 0.06] × 10^{-6} g/sec-cm^2.

The conditions in the Cs reservoir were as follows: temperature = 733 Kelvin, the calculated vapor pressure of CsOH = 7 × 10^{-5} atm, and the calculated vapor pressure of Cs = 6.1 × 10^{-5} atm. The total gas flow rate into the reaction chamber was 14.7 cm^3/min. The temperature of the reaction chamber was 1233 Kelvin when the Cs-steam vapor stream was introduced into the chamber.

The Cs and CsOH vapor densities in the carrier gas stream were calculated to be 1.33 × 10^{-7} g-Cs/cm^3 and 1.52 × 10^{-7} g-Cs/cm^3. The vapor density of Cs-containing species in the stream was 2.85 × 10^{-7} g-Cs/cm^3. The mass flow rate into the chamber was 6.98 x 10^{-8} g/sec. The percent of Cs that interacted with the oxidized stainless steel surface in the presence of B_2O_3 was

$$\frac{\text{experimentally observed}}{\text{cesium species available}} = \frac{5.55\times10^{-8}\,\text{g/sec}}{6.98\times10^{-8}\,\text{g/sec}} = 80\%$$

5.3.3 Cesium Deposition for the Case of Boron Oxide Evaporated Onto the Sample Surface

This experiment utilized a steam-oxidized stainless steel cylinder with a cup drilled into the top plane to act as a crucible for B_2O_3. This experiment is performed so that the reaction of CsOH with the surface can be investigated in an environment that does not contain H_3BO_3. The B_2O_3 was evaporated from the crucible and permitted to coat the oxidized stainless steel sample until there was no further observable mass change. At 1023 Kelvin, a mass loss of 0.140 ± 0.007 mg in 900 sec or [1.56 ± 0.08] × 10^{-7} g/sec was observed. The steam flow rate was 13 cm^3/min. The temperature in the CsOH reservoir was 705 Kelvin and the flow rate was 26 cm^3/min. The temperature of the reaction chamber was 1023 Kelvin.

The total Cs vapor pressure was calculated to be 4.6 × 10^{-5} atm. The density of Cs in the stream was 1.04 × 10^{-7} g-Cs/cm^3. The flow entering the reaction chamber was 4.5 × 10^{-8} g/sec.

The molar rate of Cs entering the reaction chamber was 3.4 × 10^{-10} mole/sec. If 2 moles of Cs remove 1 mole of B_2O_3 by the reaction

$2Cs + H_2O + B_2O_3 = 2CsBO_2 + H_2$, then the molar loss of B_2O_3 would be 1.7×10^{-10} mole/sec. The mass loss rate would be 1.18×10^{-8} g/sec.

This is the maximum weight loss possible in this system that could be due to $CsBO_{2(g)}$ leaving the surface. The actual observed loss rate was $[1.56 \pm 0.08] \times 10^{-7}$ g/sec. Therefore, another mechanism is at least partially responsible for this weight loss.

Consider the reaction for production of H_3BO_3 vapor: $3H_2O_{(g)} + B_2O_{3(c)} = 2H_3BO_{3(g)}$. The equilibrium constant for this reaction is calculated using the values of Cordfunke and Konings and experimentally measured values:

$$4.22 \times 10^{-4} = \frac{(pH_3BO_3)^2}{(pH_2O)^3(aB_2O_3)}$$

B_2O_3 is at unit activity, and the vapor pressure of H_2O was approximately 0.1 atm (pressure was read from pressure gauge on steam generator outlet). By substituting these values into the equilibrium expression, the vapor pressure of H_3BO_3 was found to be equal to 6.5×10^{-4} atm.

The steam pressure drives this reaction. The vapor density of H_3BO_3 in moles/sec was 7.64×10^{-9} mole/sec. Two moles of H_3BO_3 are formed from 1 mole of B_2O_3 at a rate of 3.82×10^{-9} mole/sec. The mass loss rate would be 2.67×10^{-7} g/sec.

This reaction can cause a mass removal rate of 2.67×10^{-7} g/sec. Again, the actual mass loss observed was $[1.56 \pm 0.08] \times 10^{-7}$ g/sec. The implication is that other reactions are either interfering with the removal of B_2O_3 from the surface or deposition of some species may be occurring, or a combination of both.

5.4 Reaction With Cesium Hydroxide, Boric Acid, and No Steam

When the oxidized stainless steel system was coated with B_2O_3 and CsOH was permitted to flow into the chamber together with H_2 in the absence of steam, no weight gain was observed.

There is insufficient oxidation potential in the atmosphere to form $CsBO_2$ without steam to provide an oxidizing condition.

5.5 Electron Spectroscopy Chemical Analyzer (ESCA)

The ESCA was used to analyze the surface of the stainless steel cylinder employed in the mass balance experiments. The results from the ESCA scan (Figure 5.1) show Cs, B, C, and Cr on the surface. The Cr is part of the oxidation layer; it is characteristic of the Cr in reactor grade stainless steel to migrate to the surface during an oxidation process.

B_2O_3 was also detected on the surface from an ESCA analysis. Thus, B_2O_3 was found to deposit on the surface as B_2O_3.

5.6 Summary

The experiments with H_3BO_3, steam, and H_2 show that B_2O_3 deposition on an oxidized stainless steel surface reaches saturation, even in the presence of continued H_3BO_3 flow.

The reaction of Cs, H_3BO_3, steam, and H_2 is much more reactive when all the species are in the gas phase together. When B is present on the surface and Cs is introduced to the system in the gas phase in the absence of H_2O, the mass loss is negligible. Cs does deposit on the B_2O_3 surface when H_2O is present; however, there is a weight loss due to at least two mechanisms if the vapor is free of H_3BO_3. In the event that the vapor contains H_3BO_3, from which the B_2O_3 is deposited, a mass gain due to Cs deposition is observed.

The "getterring" rate of Cs on stainless oxide layer was established. There is a strong Cs attraction to the oxidized surface when it is set down without H_3BO_3 present.

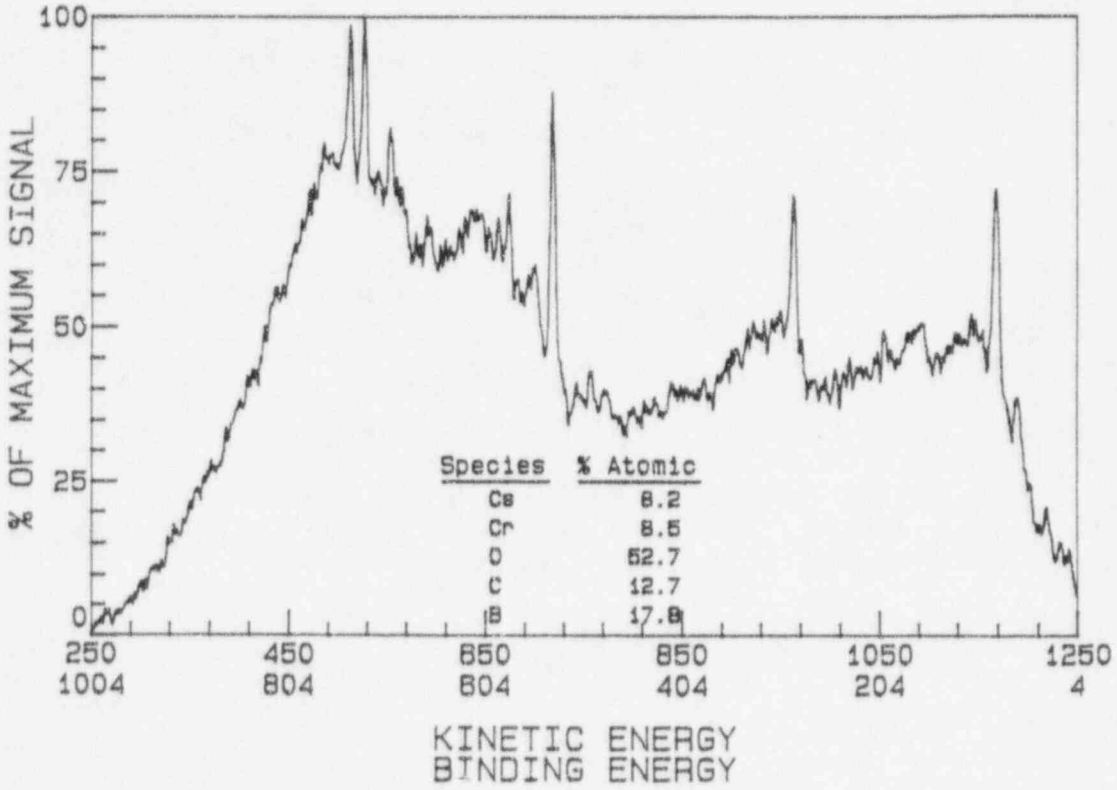

Figure 5.1 ESCA Spectrum Showing the Presence of Chromium on the Surface

CHAPTER 6

DISCUSSION AND CONCLUSIONS

An important finding of these experiments is that the oxidized stainless steel sample retained Cs species on its surface even though the conditions were such that complete revaporization of the $CsBO_2$ should have taken place. This is true even after accounting for the change in equilibrium during the course of the experiment between the H_3BO_3 and the B_2O_3 layer due to the increased production of H_2O from the CsOH. An investigation of the surface of the reaction cell by ESCA analysis showed the presence of Cs and Cr. This is coupled with the finding in the mass electrobalance experiments conducted without the introduction of H_3BO_3, that cesium chromite ($Cs_2Cr_2O_4$) was formed on the stainless steel oxide surface. This latter finding was not reported in the literature. This leads to the conclusion that even in the case where B_2O_3 coats the surface, the Cs interacts not only with the B_2O_3 but also with the Cr in the stainless steel. This result shows that Cs will react the same way with the Cr contained in the oxide layer, independent of the presence of B. The following model is proposed for the "getterring" action of the Cr to account for the retention of a fraction of the Cs inventory on the surface.

The Model for "Getterring" of Cesium by Chromates

Cr is a component of the stainless steel and has a tendency to migrate to the surface when the stainless steel is oxidized. In order to elucidate a model, there are two possibilities presented for the reaction of Cs with chromium oxide at 1000 Kelvin. The determination of the most likely possibility results from an investigation of the equilibrium of $Cs_2O_{(g)} + Cr_2O_{3(c)} = Cs_2Cr_2O_{4(c)}$.

The equilibrium constant for this reaction was calculated using the Gibbs free energy values in Cordfunke and Konings (recall that these values are for the assumption of an ideal gas):

$$K = 9.66 \times 10^{-10} = (pCs)^2 (pO_2)^{\frac{1}{2}}$$

A possibility that could be considered is the reverse of the reaction

$$2Cr + \frac{3}{2}O_2 = Cr_2O_3$$

However, the forward reaction is highly favored so that formation of O_2 from the dissociation of the chromium oxide is unlikely. It is more likely that O_2 in contact with the surface would cause some of the unoxidized Cr which has migrated to the surface to oxidize.

Instead, it may be assumed that the reaction that controls the equilibrium of the equation $CsOH_{(g)} + HBO_{(g)} = CsBO_{2(g)} + H_2O$ is

$$2Cs + \frac{1}{2}O_2 = Cs_2O_{(s)}$$

For this reaction, under the assumption of the ideal gas law, the vapor pressure of Cs is found as 3.77×10^{-4} atm. A comparative experiment was performed in the reaction cell of the mass spectrometer in the absence of H_3BO_3. The partial vapor pressure of Cs found in this experiment was 4.0×10^{-4} atm; this value was interpolated from a series of measurements performed in the mass spectrometer simulating the conditions of the mass electrobalance. This is in excellent agreement with the model calculation. Thus, the overall reaction by which cesium chromite ($CsCr_2O_4$) is formed on the surface is represented by the following set of equations:

In the vapor form:

$$CsOH_{(g)} + \frac{1}{2}H_2 = Cs_{(g)} + H_2O$$

$$CsOH_{(g)} = CsO_{(g)} + \frac{1}{2}H_2$$

$$CsO_{(g)} + CsO_{(g)} = 2Cs_{(g)} + O_2$$

$$2Cs_{(g)} + \frac{1}{2}O_2 = Cs_2O_{(g)}$$

On the surface:

$$2Cs + \frac{1}{2}O_2 = Cs_2O$$

$$Cs_2O + Cr_2O_3 = Cs_2Cr_2O_4$$

Additional support for this model is provided by the observation of the intermediate species, CsO, in the mass spectrometer experiments.

$Cs_2Cr_2O_4$ vapor was not observed in experiments conducted in the mass spectrometer up to approximately 1230 Kelvin. The formation of $CsCr_2O_4$ and its stability suggests a decrease in the predicted radiocesium source term during the transient initiation phase and late in-vessel release.

The primary finding of this investigation was the partial removal of Cs by the chromates in the oxide layer. In addition, other findings should be mentioned:

(1) The partial vapor pressures of CsOH, $CsBO_2$, Cs, and CsO do not agree with the predictions in VICTORIA.

(2) The results of the mass spectrometer and mass electrobalance experiments are in agreement with the prediction of Powers and

Bieniarz that $CsBO_2$ does replace part of the Cs inventory in the vapor form.

(3) Cr_2O_3 virtually arrests revaporization of Cs once it is bound to the surface.

Recommendations for Future Work

(1) The activity values for the species obtained in these experiments should be verified in other experiments and incorporated into the VICTORIA code. Benchmark calculations should be performed for validation of these measurements.

(2) Experiments such as are reported here should be carried out for Cd and In (speculated to act as gettering agents) for both Cs and perhaps I, another of the radiobiologically harmful fission products.

REFERENCES

Ackermann & Rauh, 1972 — R. J. Ackerman and E.G. Rauh, "The Thermodynamics and Vaporization of Thorium, Hafnium, and Zirconium," Journal of Chemical Thermodynamics, 4:521-532, 1972.

Ackerman et al., 1975 — R.J. Ackermann, E.G. Rauh and C.A. Alexander, "The Thermodynamic Properties of $ZrO_{2(g)}$," High Temperature Science, 7:304-316, 1975.

Alexander et al., 1985 — C.A. Alexander, J.S. Ogden, R.W. Wright, and L. Chan, "Matrix Stripping and Fission Product Release at High Temperatures," Proceedings of an International Symposium on Severe Accidents in Nuclear Power Plants, Vienna: International Atomic Energy Agency and Organization for Economic Cooperation and Development, pp. 179-184, 1985.

Alexander et al., 1986 — C.A. Alexander, J.S. Ogden, and L. Chan, "Actinide Release From Irradiated Fuel at High Temperatures," Source Term Evaluation for Accident Conditions, Vienna: International Atomic Energy Agency, pp. 77-88 1986.

Alexander et al., 1993 — C.A. Alexander, J.S. Ogden, and C.H. Dye, "Evaluation of Oxidic Films on the Surface of Inconel 600," Columbus, Ohio: Battelle Memorial Institute, 1993.

Alexander & Ogden, 1987 — C.A. Alexander and J.S. Ogden, "Real Time Mass Spectrometric Evaluation of Fission Product Transport at Temperature and Pressure," Proceedings of the Symposium on Chemical Phenomena Associated With Radioactivity Releases During Severe Nuclear Power Plant Accidents, Held at Anaheim, California, September 8-12, 1986, U.S. Nuclear Regulatory Commission, NUREG/CP-0078, June 1987.

Alexander & Ogden, 1990 — C.A. Alexander and J.S. Ogden, Vaporization of UO_2 at High Temperatures and High Pressures. A Generic Relation for Volatization," High Temperatures - High Pressures, 21:149-156, 1990.

Ball et al., 1993 — R.G.J. Ball, B.R. Bowsher, E.H.P. Cordfunke, S. Dickinson, and R.J.M. Konings, "Thermochemistry of Selected Fission Product Compounds," Journal of Nuclear Materials, 201:81-91, 1993.

Baston et al., 1985 — V.F. Baston, K.J. Hofstetter, and A.P. Malinauskas, "Circulation Within the Primary System at TMI-2 With Lowered Coolant Level and at Atmospheric Conditions," Nuclear Technology, 69:308-318, June 1985.

Behrens & Rinehart, 1980 — R.G. Behrens and G. H. Rinehart, "Vapor Pressure and Sublimation Enthalpy of Elemental Technetium," Journal of the Less-Common Metals, 75:241-254, 1980.

Bowsher et al., 1987 — B.R. Bowsher, S. Dickinson, S.R. Grubb, J.S. Ogden and N.A. Young, "The Interaction of Caesium Iodide With Boric Acid Under Severe Reactor Accident Conditions," Proceedings of the Symposium on Chemical Phenomena Associated With Radioactivity Releases During Severe Nuclear Plant Accidents, Held at Anaheim, California, September 8-12, 1986, U.S. Nuclear Regulatory Commission, NUREG/CP-0078, June 1987.

Camp, 1984 — W.J. Camp, "Release of Fission Products From Fuel During the In-Vessel Phases of Severe Nuclear Reactor Accidents," European Applied Research Reports, 5(6):1605-1637, 1984.

Chupka et al., 1963 — W.A. Chupka, J. Berkowitz, and D.J. Mesch, "Mass Spectrometric Studies of High Temperature Systems," Advances in Mass Spectrometry, 2:99-109, 1963.

Cordfunke & Konings, 1990 — E.H.P. Cordfunke and R.J.M. Konings, Thermochemical Data for Reactor Materials and Fission Products, Amsterdam: North Holland, 1990.

Craig, 1992 — N.C. Craig, Entropy Analysis: An Introduction to Chemical Thermodynamics, New York: VCH Publishers, Inc., 1992.

Cubicciotti, 1981 — D. Cubicciotti, "A Model For Release of Fission Gases and Volatile Fission Products From Irradiated UO_2 in Steam Environment," Nuclear Technology, 53:5-6, April 1981.

Drowart & Goldfinger, 1967 — J. Drowart and P. Goldfinger, "Investigation of Inorganic Systems at High Temperature by Mass Spectrometry," Angewandte Chemie International Edition, 6:581-648, 1967.

Elrick & Sallach, 1987 — R.M. Elrick and R.A. Sallach, "Importance of Environment on High Temperature Reactor Accident Chemistry," Proceedings of the Symposium on Chemical Phenomena Associated With Radioactivity Releases During Severe Nuclear Power Plant Accidents, Held at Anaheim, California, September 8-12, 1986, U.S. Nuclear Regulatory Commission, NUREG/CP-0078, June 1987.

Gotzmann, 1993 — O. Gotzmann, "Thermochemical Considerations in Source Term Evaluation," Journal of Nuclear Materials, 201:267-277, 1993.

Halliday & Resnick, 1988 — D. Halliday and R. Resnick, Fundamentals of Physics, Third Edition Extended, New York: John Wiley & Sons, 1988.

Hobbins et al., 1987 — R.R. Hobbins, A.W. Cronenberg, S. Langer, D.E. Owen, and D.W. Akers, "Insights on Severe Accident Chemistry From TMI-2," Proceedings of the Symposium on Chemical Phenomena Associated With Radioactivity Releases During Severe Nuclear Power Plant Accidents, Held at Anaheim, California, September 8-12, 1986, U.S. Nuclear Regulatory Commission, NUREG/CP-0078, June 1987.

Hobbins et al., 1991 — R.R. Hobbins, D.A. Petti, D.J. Osetek, and D.L. Hagrman, "Review of Experimental Results on Light Water Reactor Core Melt Progression," Nuclear Technology, 95:287-307, September 1991.

Hultgren et al., 1963 — R. Hultgren, R.L. Orr, P.D. Anderson, and K.K. Kelley, Selected Values of Thermodynamic Properties of Metals and Alloys, New York: John Wiley & Sons, Inc., 1963.

Inghram & Drowart, 1960 — M.G. Inghram and J. Drowart, "Mass Spectrometry Applied to High Temperature Chemistry," High Temperature Technology, New York: McGraw-Hill Book Company, Inc., 1960.

Kanno et al., 1988 — M. Kanno, M. Yamawaki, T. Koyama, and N. Morioka, "Thermodynamic Activity Measurements of U-Zr Alloys by Knudsen Effusion Mass Spectrometry," Journal of Nuclear Materials, 154:154-160, 1988.

Kazikowski et al., 1987 — S. Kazikowski, L.G. Johansson, U. Malmestrom, and O. Lindqvist, "Corrosion and Deposition Studies of Stainless Steel Exposed to Aerosols Containing Te, Cs, I, Sn,Mn, Ag, and B_2O_3 at 300-1000 °C in a Reducing ($H_2/H_2O/N_2$) Environment," Proceedings of the Symposium on Chemical Phenomena Associated With Radioactivity Releases During Severe Nuclear Plant Accidents, Held at Anaheim, California, September 8-12, 1986, U.S. Nuclear Regulatory Commission, NUREG/CP-0078, June 1987.

Kittel & Kroemer, 1980 — C. Kittel and H. Kroemer, Thermal Physics, San Francisco: W.H. Freeman and Company, 1980.

Klotz & Rosenberg, 1986 — I.M. Klotz and R.M. Rosenberg, Chemical Thermodynamics Basic Theory and Methods, Fourth Edition, Menlo Park, California: Benjamin/Cummings Publishing Company, Inc. 1986.

Lewis & Randall, 1923 — G.N. Lewis and M. Randall, Thermodynamics and the Free Energy of Chemical Substances, New York: McGraw-Hill Book Company, Inc., 1923.

Matsui, 1993 — T. Matsui, "Vaporization Study on M_2Zr (M=Fe and Cr) by a Mass-Spectrometric Method," Journal of Nuclear Materials, 201:278-283, 1993.

Minato, 1991 — K. Minato, "Thermodynamic Analysis of Cesium and Iodine Behavior in Severe Light Water Reactor Accidents," Journal of Nuclear Materials, 185:154-158, 1991.

NUREG-0772 — U.S. Nuclear Regulatory Research, "Technical Bases for Estimating Fission Product Behavior During LWR Accidents," NUREG-0772, June 1981.

NUREG-1150 — U.S. Nuclear Regulatory Research, "Severe Accident Risks: An Assessment for Five U.S. Nuclear Power Plants," NUREG-1150, December 1990.

NUREG/CR-4173 — U.S. Nuclear Regulatory Commission, "CORSOR User's Manual," NUREG/CR-4173, March 1985.

NUREG/CR-5214 — U.S. Nuclear Regulatory Commission, "Analysis of Natural Circulation During Surry Station Blackout Using SCDAP/RELAP-5," NUREG/CR-5214, October 1988.

NUREG/CR-6193 — U.S. Nuclear Regulatory Commission, "Primary System Fission Product Release and Transport: A State-of-the Art Report to the Committee on the Safety of Nuclear Installations," NUREG/CR-6193, June 1994.

Paul, 1951 — M.A. Paul, Principles of Chemical Thermodynamics, New York: McGraw-Hill Book Company, Inc., 1951.

Powers & Bieniarz, 1987 — D.A. Powers and P.P. Bieniarz, "Influence of Chemical Form on Cesium Revaporization From the Reactor Coolant System," Proceedings of the Symposium on Chemical Phenomena Associated With Radioactivity Releases During Severe Nuclear Plant Accidents, Held at Anaheim, California, September 8-12, 1986, U.S. Nuclear Regulatory Commission, NUREG/CP-0078, June 1987.

Quick et al. [n.d.] — D. Quick, T. Szymanski, A. Oxfurth, and P. Harmon, Fundamentals Course--Pressurized Water Reactors Manual, U.S. Nuclear Regulatory Commission, I&E Training Center, not dated.

Smith & Van Ness, 1975 — J.M. Smith and H.C. Van Ness, Introduction to Chemical Engineering Thermodynamics, New York: McGraw-Hill Book Company, Inc., 1975.

Steiner, 1941 — L.E. Steiner, Introduction to Chemical Thermodynamics, New York: McGraw-Hill Book Company, Inc., 1941.

Stull & Prophet, 1971 — D.R. Stull and H. Prophet, "JANAF Thermochemical Tables," Washington, D.C.: Office of Standard Reference Data, National Bureau of Standards, 1971.

Thorn & Winslow, 1957 — R.J. Thorn and G.H. Winslow, "Vaporization Coefficient of Graphite and Composition of the Equilibrium Vapor," Journal of Chemical Physics, 26:186-200, January 1957.

Wang & Olander, 1993 — Wei-E Wang and D.R. Olander, "U-O and Zr-O Thermochemistry From the Pure Metal to the Dioxide and Application to Core-Concrete Interactions in Severe Fuel Damage Accident Analysis," Journal of Nuclear Materials, 201:231-237, 1993.

APPENDIX A

THEORY AND APPLICATION OF CHEMICAL THERMODYNAMICS

The effects of various species in a chemical reaction with each other at a given temperature and the rates of reaction are determined by chemical thermodynamics. Assumptions made in the equations of state for the ideal gas laws are very important in understanding the analysis in this work. This appendix provides a theoretical basis for these assumptions, as well as a discussion and application of the theories employed here.

A.1 The Laws of Thermodynamics

Thermodynamics is based on empirical energy relationships. The first law of thermodynamics establishes the principle of conservation of energy. In 1840, Joule (Steiner) did the experimental work to carry out the foundation of the first law that energy may be converted to other forms of energy but that it cannot be created or destroyed. The second law, formulated by Carnot in 1824 (Paul), shows that heat energy at one temperature can be transferred to another system at a different temperature, which shows that systems have a general tendency toward equilibrium. The third law fixes the absolute value of entropy at absolute zero. This principle, which means that the standard state entropy is zero, was formulated by Nernst in 1906 (Paul) to permit the calculation of chemical equilibrium from purely thermal data.

A.2 Nature of an Ideal Gas in the Mass Spectrometer

To describe the state of a system for an ideal gas, or a gas that behaves like one, the equation $PV = Rt$ must be satisfied. In this equation P = pressure, V = total volume occupied by the gas, R = gas constant, and T = absolute temperature for 1 mole of gas. At a given temperature and pressure, the volume of a gas is proportional to its mass or to the number of moles (N) in the system, so the equation can be modified to represent more than 1 mole, as follows: $PV = NRT$.

In a mixture of ideal gases, it is assumed that each gas behaves as if it were the only gas in the closed system. A single ideal gas will not react with another one. The partial pressure (p) of any gas in the system would be the same as if the gas occupied the volume alone: $pV = NRT$. In this equation p_i = partial pressure of gas i and N_i = number of moles of gas i present in the system.

Since each gas will independently exert its own pressure in the system, the total pressure (P) of the closed system is equal to the sum of the partial pressures:

$$P = \sum_i p_i$$

The gas constant (R) is directly related to the Boltzmann constant (k), which is a constant from the kinetic theory of gases. The gas constant can be substituted by kN_A, where N_A is Avogadro's number (the number of atoms per mole). With this substitution, the ideal gas law becomes $PV = NkN_AT$.

Because the volume is defined as the volume occupied by a gas, the number of moles divided by the volume can be one quantity, and the partial pressures can be represented in terms of the concentration of atoms per unit volume (n), as follows:

$$\frac{(N_j)(N_A)}{V} = n$$

where

N_j = number of moles
N_A = number of atoms per mole
n = number of atoms per unit volume
V = volume

So, the ideal gas law can be modified further as $P = nkT$.

The principles discussed in the next section are all derived from the ideal gas laws in this section. Various derivations of these ideal gas laws can be implemented to determine the vapor pressure of a substance in equilibrium by applying data collected using a mass spectrometer.

For this application, the mass spectrometer signal (I) is proportional to the number density (n) and the number of ionizable species per unit volume (N_j). For ions formed by electron impact, the intensity measured on the collector in the mass spectrometer can be calculated. By relating machine characteristics and the intensity signals from the strip chart connected to the mass spectrometer, the vapor pressure of a species can be determined.

The intensity recorded by the strip chart is derived from characteristics of the overall mass spectrometer system. The relationship for intensity is $I_j = N_j l g \rho_j \eta$

where

I_j = intensity of ionizing electrons
l = effective path length of the electrons
g_j = multiplier gain
σ_j = cross section for ionization by electron impact for energy used
η = transmission factor, the ratio of the number of ions formed to those collected

In the ideal gas law ($PV = NRT$), a simple substitution for the molecular concentration, $n = N/V$, can establish a relationship for pressure in the mass spectrometer (as derived in $P = SIT$). The

effective partial pressure (P_j) can be related to the ion source using N_j and the modified gas law ($P = nkT$). In the gas law, n is the number of atoms per unit volume in the system, k is the Boltzman constant, and T is the absolute temperature.

The ideal gas law relates the intensity signal recorded by the mass spectrometer and the vapor pressure of each species in the vapor matrix. The following set of equations shows the derivation and the relationship to thermodynamics for the vapor system: $P_j = nkT$; $I_j = ng\rho_j il\eta$.

The current (i), effective path length (l), and transmission factor (η) can all be combined into one machine constant (C), which can be included the machine constant in the derivation where $I_j = Ng\rho C$; $C = il\eta$ to solve for the number of atoms (N_j), as follows:

$$N_j = \frac{I_j}{g_j \sigma_j C}$$

Further, it is possible to define a variable, S, that includes all of the machine characteristics and specific values used during calibration, and substitute the derived value of N_j from the mass spectrometer as follows:

$$S = \frac{k}{g_j \sigma_j C};\ P_j = NkT;\ \frac{P_j}{S} = I_j T$$

The final result is the partial pressure of an ideal gas in a matrix of gases that are ideal or behave like an ideal gas at a constant temperature at a fixed volume: $p_j = SI_jT$.

The only condition that must be applied to this equation is that the system must be in thermodynamic equilibrium during the initial and final states of the process.

A.3 Chemical Phase Equilibria Process

In thermodynamics, the physical properties of a system are classified as extensive or intensive. The extensive properties are mass and volume, which depend on the quantity of matter in the system. The intensive properties are characteristic of the substance and do not depend on the amount present in the system. Pressure and temperature, the variables measured by the mass spectrometer, describe the state of a thermodynamic system.

The equilibrium of a system depends only on the state of the system, and implies that there is no change of material properties over time at a constant pressure, volume, and temperature. The definition of an equilibrium state for a closed system notes that equilibrium is that state in which the total Gibbs free energy (G) is a minimum with respect to all the possible changes at a given temperature and pressure. The decrease in the free energy in an isothermal system is a measure of the maximum work obtained from that change in state. For an isothermal reversible process, the

values of work and heat transferred depend only on the initial and final states, and it includes all forms of work performed on or by the system. This is true for a system consisting of multiple phases, as long as the system is closed and the mass remains constant. The equations apply to the system as a whole (not to the individual phases), although changes may take place among the phases.

The definition of a reversible change is $\Delta S = 0$ for an isolated system. For systems undergoing an irreversible change ($\Delta S > 0$), if a spontaneous change occurs in an isothermal system, there is no external force to counteract the change. When a system is at equilibrium, small departures from equilibrium are opposed by the natural tendency of the system to return to its equilibrium state as stated by the second law of thermodynamics.

In an isothermal system at constant temperature and pressure for each measurement, all reactions are reversible and the Gibbs free energy criterion for equilibrium is $\Delta G = \Delta H - T\Delta S = 0$.

A system not in equilibrium will tend to change irreversibly, lowering the free energy until no further change is possible. At this point, the system's free energy is a minimum and the system is at equilibrium while at constant pressure and temperature. Because the Gibbs free energy function is the only criterion of equilibrium for the system at this stage, only the behavior of the system needs to be considered. The surrounding systems are not figured into the calculations because any reactions in the outside environment will go from a high-energy state to a low-energy state and will proceed spontaneously. A process outside the reaction cell in the mass spectrometer that proceeds from a low chaos probability to a higher one will also proceed spontaneously.

A system in thermal contact with a reservoir that allows the exchange of heat between the system and its surroundings can be considered an isolated system.

A solid existing in equilibrium with a vapor is represented by the Gibbs free energy function (G). The Gibbs free energy function is equal to the difference in the change of enthalpy (H) and the spontaneous change of temperature (T) and entropy (S), as follows: $\Delta G = \Delta H - TS = 0$.

The differential change in free energy is for macroscopic changes.

$$\Delta G = \Delta H - \Delta(TS) = 0$$

$$\Delta G = \Delta H - T\Delta S - S\Delta T$$

$$\Delta G = T\Delta S + V\Delta P - T\Delta S - S\Delta T$$

$$\Delta G = V\Delta P - S\Delta T$$

The criterion for an equilibrium state is $\Delta G = 0$ at constant pressure and temperature. When temperature and pressure are kept constant, the free energy will still change.

For a substance existing in two phases that are in equilibrium with each other, $G_1 = G_2$ for a new equilibrium established at a temperature and pressure different from that of the original equilibrium. An expression for vapor pressure can be derived from that principle, and the incremental free energy change is $G_1 + \Delta G_1 = G_2 + \Delta G_2$.

The following quotation from Lewis and Randall (p. 161) on thermodynamic equilibrium is the theoretical foundation for the calculations in this study:

> If no reaction at constant temperature and pressure is thermodynamically possible, no reaction whatever can occur. For suppose that some spontaneous process could occur in such a way as to produce inequalities of temperature and pressure within the system, or to produce a difference between the temperature and pressure of the system and the temperature and pressure of the environment; then this process could be followed by another obviously spontaneous process, consisting in the equalization of pressure and temperature. But these two processes together would be the equivalent of a spontaneous process occurring at constant temperature and pressure.

The partial pressure and activity of materials varies with temperature. The free energy of an ideal gas is represented by the Gibbs equation (Klotz & Rosenberg; Craig) as in an empirical form:

$$\Delta G^0 = \sum \Delta G^0(\text{products}) - \sum G^0(\text{reactants})$$

where ^{0} denotes the standard state of a substance.

The standard state of all reactants is the form in which it existed before any experiments; and this state is considered the reference. The following equation is used to interpret the data from the mass spectrometer because it represents the equilibrium vapor pressure of an ideal gas:

$$\Delta G^0 = \Delta G - RT \ln\left[\frac{P(\text{products})}{P(\text{reactants})}\right]; \quad \Delta G = 0; \quad \Delta G^0 = -RT \ln K$$

where

K = the temperature-dependent equilibrium constant
$\Delta G = 0$ because the system is in equilibrium.

Since ΔG^0 is the change in free energy under certain specified conditions, it must have a fixed value at a given temperature. The equilibrium constant (K) is calculated for each temperature to provide information about the spontaneity of the reaction.

A.4 Vapor Phase Equilibrium

All of the equilibrium criteria are derived from the second law of thermodynamics. The particular criterion chosen in practice is selected because of convenience, not because it is more valid or less valid than any other criterion.

The analysis for this work is based on the assumption that the vapors and condensed species are in equilibrium with each other. Analytically, this means that $\Delta G = 0$. Since ΔG is the change in free energy and ΔG equals zero, the temperature (T) and pressure (P) are constant for each measurement made by the mass spectrometer. This is the equilibrium criterion.

Application of the first and second laws of thermodynamics to an isothermal system shows the derivation of the Clausius—Clapeyron equation. Given pressure and temperature corresponding to an equilibrium condition for that transition, the Clausius—Clapeyron equation permits calculation of the entire coordinated set of temperatures and pressures. The assumptions underlying this equation are only true at low pressure (Craig) for a system in equilibrium. Every solid or gas has a vapor pressure at a given temperature. All of the equilibrium states for that transition (described by the Clausius—Clapeyron equation) are for the solid and vapor phases. In describing the state of a gas, its partial pressure is specified as well as its temperature.

The derivation of vapor pressure at constant pressure and temperature is as follows (assuming vapor behaves like an ideal gas, and P and T are constant):

$$V_1 - S_1\Delta T = V_2\Delta P - S_2\Delta T;\ \Delta T(S_2 - S_1) = \Delta P(V_2 - V_1);\ \Delta T\Delta S = \Delta P\Delta V$$

where

V = total volume occupied by the gas
S = entropy
T = absolute temperature
P = pressure

For differential changes in pressure and temperature

$$\Delta H\frac{dT}{T} = RT\frac{dP}{P};\ \Delta H\int\frac{dt}{T^2} = R\int\frac{dp}{P};\ \frac{-\Delta H}{RT} + b = \ln P$$

where b is a constant of integration. If $\ln P$ is plotted against $1/RT$, the slope of a fitted data set is equal to ΔH, and the y-intercept (represented by b in the derivation) is S.

Local thermodynamic equilibrium exists at each temperature; however, regions in the reaction cell of the mass spectrometer may not have reached equilibrium at the same time. The most important information derived from this analysis is the equilibrium magnitude and temperature dependence.

Consider a general equilibrium vapor-phase reaction involving gases:

$$aA_{(g,P_A)} + bB_{(g,P_B)} = cC_{(g,P_C)} + dD_{(g,P_D)}$$

where the lowercase letters represent the stoichiometric coefficients.

To further expand on the equation and the relationship to free energy and equilibrium, the partial pressures are related by

$$\Delta G = nRT \ln\left(\frac{P}{P^0}\right)$$

where P^0 is the standard state of the partial pressure, which in most cases is equal to 1 atm. The standard is a reference pressure arbitrarily chosen at any temperature for all reactants, but must remain the same throughout a series of analysis.

From thermodynamics, the extent to which the reactants (A and B) react to yield the products (C and D) can be defined by the difference in standard states of the free energies (ΔG^0) for both reactants and products, as follows: $\Delta G(\text{reaction}) = (G_C + G_D) - (G_A + G_B)$.

The following derivation applies equation

$$\Delta G = nRT \ln\left(\frac{P}{P^0}\right)$$

to equation ΔG (reaction) = $(G_C + G_D) - (G_A + G_B)$ which is the foundation for most of the analysis in the vapor phase when the system is in equilibrium:

$$\Delta G = \Delta G^0 + \Delta G_A + \Delta G_B + \Delta G_C + \Delta G_D$$

$$\Delta G_A = aRT \ln\left(\frac{P_A}{P^0}\right)$$

$$\Delta G_B = bRT \ln\left(\frac{P_B}{P^0}\right)$$

$$\Delta G_C = nRT \ln\left(\frac{P_C}{P^0}\right)$$

$$\Delta G_D = nRT \ln\left(\frac{P_D}{P^0}\right)$$

$$\Delta G = \Delta G^0 + nRT \ln\left(\frac{P_C}{P^0}\right) + nRT \ln\left(\frac{P_D}{P^0}\right) - \left[nRT \ln\left(\frac{P_A}{P^0}\right) + nRT \ln\left(\frac{P_B}{P^0}\right)\right]$$

If the reactants are taken in their equilibrium concentrations and converted to the products in their equilibrium concentrations, then $\Delta G = 0$.

The concentration quotient is only true if the pressures (P_A, P_B, P_C, and P_D) are the values that exist at equilibrium. When a reaction reaches equilibrium, the free energy of the products equals the free energy of the reactants. The standard state pressures are all chosen at 1 atm, and the equilibrium constants are represented herein in the following form:

$$K = \ln\left[\frac{P_A P_B}{P_C P_D}\right]$$

A.5 Condensed Phase Equilibrium

Activity is a measurement that defines the equilibrium constant (K) as a function of temperature for a gas-solid mixture at a fixed temperature and pressure. If one substance in a solution exists in two different phases at the same temperature, activity is the measure needed to define that quantity. The activity of a component may have any positive value depending on the conditions for the standard state chosen. The standard partial pressure (P^0) is defined as unity at constant temperature and 1 atm, and the activity standard state uses these same conventions. The expression that defines the equilibrium constant (K) is the same expression used to calculate activity on the surface. Activity can be calculated after comparing the experimental vapor pressure with published thermochemical data. The difference between the Gibbs free energies (ΔG) of the products and reactants applies only to substances that are in their standard states at the temperature and pressure defined for the given system. For an ideal gas, activity is represented as

$$a_i = \frac{P_i}{P^0}$$

For each reaction, the substances are in their pure state at atmospheric pressure; therefore, the standard state is equal to unity and $a^0 = 1$ at atmospheric pressure.

In a solution, activity can be determined from the vapor pressure of the pure solvent and the solvent in solution when the vapor behaves like an ideal gas. From the definition of the standard state of activity, P^0 is the vapor pressure of the pure solvent at a system temperature and pressure, and P_i is the measured vapor pressure. The activity of the solvent remains constant, independent of the concentration of solute. The vapor and condensed phases of a species are in equilibrium for the entire system.

The thermodynamic link between the condensed phase and the vapor phase is given by activities. Activities of condensed phase components can be expressed in terms of partial vapor pressures with reference to the standard state pressure. Measurement of the vapor phase can provide activity data for the condensed phase.

The condensed components of the reaction is the activity (a) which is directly related to the Gibbs free energy by $\mu = G^{\circ} + RT\ln a$ where ^{0} denotes the standard state of the species at the temperature of the system at a fixed pressure, and μ is the chemical potential.

The activity value is a measure of the interaction of the condensed phase species attraction/interaction on the surface. The activity coefficient can be derived from the Gibbs relationship and defined as $\ln K = -RT\ \ln(a_i)$ where $a_i = N_i\gamma_i$.

The molality of a molecular species is γ; it is used to define the molecular quantity of a species which may be present.

There are three possibilities for the activity coefficient:

(1) If $\gamma<1$, there is a strong interaction between the condensed phase species and the surface.
(2) If $\gamma>1$, there is a weak interaction with the surface.
(3) If $\gamma=1$, there is no interaction with the surface.

The fission product deposition and revaporization predictions can be estimated on the basis of the results of the activity calculations. The pressure values are used to calculate the equilibrium constants.

A.6 Vapor Pressure Determination by Knudsen Effusion

Not all molecules of a gas in a closed system have the same energy. Statistical mechanics shows a distribution at each temperature where the total energy of a gas among the other molecules is more probable than any other distribution.

In a system with N molecules that do not attract or repel each other, such as an ideal gas, the energy of any molecule at any specific instant will have a certain energy (E_i). The kinetic energy (E) of a molecule is defined as $E = \frac{1}{2}\ mv^2$. The number of molecules in the lowest state is N_0, and N_i is the number of molecules in the state E_i. If the gas follows Boltzman statistics, the most probable distribution of molecules at a constant volume and absolute temperature is

$$N_i = N_0 e^{-\frac{E_i}{kT}}$$

To find the average speed of the molecules, the Maxwell speed distribution for gases in equilibrium is integrated (Halliday & Resnick), as follows:

$$P(V) = 4\pi\left(\frac{m}{2\pi RT}\right)^{\frac{3}{2}} v^2 e^{-\frac{mv^2}{2RT}}$$

The product of $P(v)dv$ is the fraction of molecules characterized by a speed in the range of v to $v + dv$. From a table of integrals, the average speed is

$$\bar{v} = \sqrt{\frac{8kT}{m\pi}}$$

where

$\bar{v}$ = mean speed of molecules
k = the Boltzmann constant
T = absolute temperature (Kelvin)
m = mass of a molecule.

The reaction chamber is where all of the gas molecules collide with the surface. The rate at which molecules strike a unit surface area per unit time (Kittel & Kroemer) is

$$J_n = \frac{n\bar{v}}{4}$$

where

J_n = flux total number of molecules per unit time-unit area

n = number of molecules per unit volume

$\bar{v}$ = mean speed of molecules

If the gas obeys ideal gas laws, the flux (J_n) can be expressed as:

$$Z = M\left(\frac{J_n}{6.02 \times 10^{23}}\right)$$

where M is the molecular weight and 6.02×10^{23} is Avogadro's number.

Substituting the definition of J_n into the preceding equation produces

$$P = nkT$$

$$J_n = n\sqrt{\frac{kT}{2\pi m}}$$

$$J_n = P\sqrt{\frac{1}{2\pi mkT}}$$

Hertz derived the molecular effusion relationship from Maxwell's distribution for molecular velocity, expressing the flux (J_n) in grams effusing from the reaction chamber instead of molecules. Using that derivation, it is possible to define a variable (Z) to represent the flux in terms of grams of a substance using J_n:

$$Z = \frac{PM}{6.02 \times 10^{23}} \sqrt{\frac{1}{2\pi mkT}}$$

The values for the constants can be substituted into the preceeding equation so the effusion (Z) can be represented in terms of pressure, molecular weight, and temperature as follows:

$$Z = \frac{PM}{6.02 \times 10^{23}} \sqrt{\frac{1}{(2)(3.14)(1.6 \times 10^{-24})M(1.38 \times 10^{-16})(T)}}$$

$$Z = \frac{PM}{6.02 \times 10^{23}} \sqrt{\frac{7.21 \times 10^{38}}{MT}}$$

$$Z = 4.458 \times 10^{-5} P \sqrt{\frac{M}{T}}$$

The pressure in the equation is expressed in dynes, while the pressure convention in this study is calculated in atmospheres where p (dynes) = P (atm) × 1.013×10^6.

Thus, the preceding equation becomes

$$Z = 44.3 P(\text{atm}) \sqrt{\frac{M}{T}}$$

The molecular effusion formula and experimental mass rate of effusion of a dilute vapor form a method of measuring the vapor pressures. This information leads to the free energies of vaporization of volatile substances independent of the vapor mechanism. The preceding equation represents the mass loss of the species due to effusion related to the partial pressure of the substance by the Hertz-Knudsen equation (Drowart & Goldfinger).

The Knudsen experimental method is the most suitable for vapor pressure measurements at high temperatures. The experiment is carried out in a high vacuum system, and material is transported from the Knudsen cell by pressure differential between the effusion cell and the rest of the system. In the Knudsen cell, the sample is contained inside an inert crucible that has a thin small orifice for the sample vapor to enter the detector. Because the orifice is

contained inside an inert crucible that has a thin small orifice for the sample vapor to enter the detector. Because the orifice is small, equilibrium is established inside the crucible and the rate of effusion through the orifice is fixed by the vapor pressure, temperature, molecular weight of the effusing species, and dimensions of the orifice.

With this technique, the sample is enclosed in a nonvolatile cell with a small orifice. Ideally, the equilibrium vapor pressure builds up within the Knudsen cell, and the area of the orifice acts as the effective area of the sample from which the vapor molecules escape at the equilibrium rate. The amount of material transported from the Knudsen cell is measured by the loss in mass of the crucible and sample, and indicates the vapor pressure of the vapor in the cavity. The vapor composed of the species in the cell flows from an isothermal container into an evacuated space. The experimental aspects of this method are appealing and straightforward.

The measurement of weight loss over a known period of time at a constant temperature, combined with a knowledge of the relative concentrations of the molecular species, supplies the input to calculate the partial pressures of the species with the effusion formula. The vapor effuses into a vacuum with nearly collision-free paths, and the effusing material is allowed to condense on the stainless steel material. To ensure that the vaporization phase is time invariant and the effusion rate is independent of the vaporization process, the rate of evaporation of the experimental substance must be much greater than the rate of effusion. This is accomplished by controlling the size of the orifice, which controls the effusion rate (the rate at which the material leaves the crucible).

A.7 Summary

The ideal gas laws will be used in the analysis of the chemical system in these experiments. The experimental system is isothermal and isobaric during each measurement; therefore, the Gibbs free energy relationships are utilized for equilibrium analysis. The analysis is based on the reasonable assumption that the gas and condensed phases of species are in equilibrium with one another. If they are not in equilibrium, the discrepancy will be revealed on the Arrhenius plot.

APPENDIX B

SOURCES OF SYSTEMATIC ERRORS IN THE MASS SPECTROMETER AND UNCERTAINTY ANALYSIS

The settings of all instruments remain constant during the experiment, such as vacuum pressure; however, there are a few systematic errors in the experiment that cannot be controlled, and some are not quantifiable.

There is an uncertainty associated with the temperature measurements for each intensity. The reaction chamber is heated by a resistor heater and blackbody shielding. There is one thermocouple inside the shielded container and four around the reaction chamber. Their locations are on top of the reaction cell, the bottom of the reaction cell, at the gas inlet for steam and hydrogen, and the cesium hydroxide heater. The thermocouples inside the blackbody heated chamber could read a temperature higher than the actual temperature in the region, but not one that is lower because the heat flows from a high temperature region to a lower one only. The temperature inside the blackbody region will be sightly higher than the temperature of the thermocouples because heat travels from a high region to a lower one. There is only a negligible temperature gradient in the region measured by the thermocouple. The uncertainties associated with the temperature measurements are as follows:

Temperature	Uncertainty
≤ 1000 ^{0}K	±2 ^{0}K
1200 ^{0}K	±4 ^{0}K
1600 ^{0}K	±6 ^{0}K
≥ 2000 ^{0}K	±8 ^{0}K

The uncertainty was estimated by taking temperature measurements in the empty Knudsen cell and evaluating the reproducibility of the measurements. The uncertainty values in this study are reasonable compared with some of the uncertainties reported in the literature. Matsui reported an uncertainty in thermocouple readings from the mass spectrometer up to 13 percent of the temperature measurement. Inghram and Drowart suggest that, with the regulation of power, the cell temperatures can remain constant over small ranges within ±10^0 at the high-temperature regions.

There is also an uncertainty from the strip charts which is estimated as 0.5 percent of each intensity. The same percentage applies to the intensity peaks independent of their size. There is a traceover uncertainty due to the nature of the pen on the strip chart. The pen will draw to the top of a peak then go back to the zero position. At the peak, the pen traces over part of the peak.

The uncertainty in the pressure can be derived using a propagation of errors analysis with $P = SIT$. The quantity of interest is the

natural logarithm of the pressure. The intensity (I) is equal to the voltage (V) multiplied by the number of divisions in the strip chart (D). So $P = SVDT$; in terms of natural logarithms, this equation is equal to $\ln P = \ln S + \ln V + \ln D + \ln T$

There is little uncertainty in the voltage (V) reading because it is read from a dial with only four well-calibrated settings. The sensitivity constant of the machine includes all the uncertainties from the other instrument uncertainties because it is a number derived from the calibration to set the lower limit of the vapor pressure detectability. The uncertainty in the natural logarithm of P is

$$\sigma^2_{\ln P} = \left(\frac{d(\ln P)}{dS}\right)^2 \sigma_s^2 + \left(\frac{d(\ln P)}{dD}\right)^2 \sigma_D^2 + \left(\frac{d(\ln P)}{dV}\right)^2 \sigma_V^2 + \left(\frac{d(\ln P)}{dT}\right)^2 \sigma_T^2$$

$$\frac{d\ln P}{dD} = \frac{SVT}{D}; \quad \frac{d\ln P}{dT} = \frac{SDV}{T}$$

$$\sigma^2_{\ln P} = \left(\frac{1}{D}\right)^2 \sigma_D^2 + \left(\frac{1}{T}\right)^2 \sigma_T^2$$

$$\sigma_{\ln P} = \left[\left(\frac{1}{D}\right)^2 \sigma_D^2 + \left(\frac{1}{T}\right)^2 \sigma_T^2\right]^{\frac{1}{2}}$$

Again, the uncertainty expressed by $\sigma_{\ln P}$ is representative of the uncertainty in the measurement due to systematic errors.

NRC FORM 335 (2-89) NRCM 1102, 3201, 3202

U.S. NUCLEAR REGULATORY COMMISSION

BIBLIOGRAPHIC DATA SHEET

(See instructions on the reverse)

1. REPORT NUMBER (Assigned by NRC. Add Vol., Supp., Rev., and Addendum Numbers, if any.)

NUREG-1519

2. TITLE AND SUBTITLE

Surface Interactions of Cesium and Boric Acid with Stainless Steel

3. DATE REPORT PUBLISHED

MONTH	YEAR
August	1995

4. FIN OR GRANT NUMBER

5. AUTHOR(S)

N. Grossman-Canfield

6. TYPE OF REPORT

Technical

7. PERIOD COVERED *(Inclusive Dates)*

8. PERFORMING ORGANIZATION – NAME AND ADDRESS *(If NRC, provide Division, Office or Region, U.S. Nuclear Regulatory Commission, and mailing address; if contractor, provide name and mailing address.)*

Division of Systems Technology
Office of Nuclear Regulatory Research
U.S. Nuclear Regulatory Commission
Washington, D.C. 20555-0001

9. SPONSORING ORGANIZATION – NAME AND ADDRESS *(If NRC, type "Same as above"; if contractor, provide NRC Division, Office or Region, U.S. Nuclear Regulatory Commission, and mailing address.)*

Same as above.

10. SUPPLEMENTARY NOTES

11. ABSTRACT *(200 words or less)*

In this report, the effects of cesium hydroxide and boric acid on oxidized stainless steel surfaces at high temperatures and near one atmosphere of pressure are investigated. This is the first experimental investigation of this chemical system. The experimental investigations were performed using a mass spectrometer and a mass electrobalance. Surfaces from the different experiments were examined using a scanning electron microscope to identify the presence of deposited species, and electron spectroscopy for chemical analysis to identify the species deposited on the surface.

The analysis couples vaporization, deposition, and desorption of the compounds formed under conditions similar to what is expected during certain nuclear reactor accidents.

Cesium deposits on an oxidized stainless steel surface at temperatures between 1000 and 1200 Kelvin and on stainless steel surfaces coated with boric oxide in the same temperature ranges. The mechanism for such deposition involved the chemical reaction between cesium and chromate. Some revaporization in the cesium hydroxide-boric acid system was observed. Under the conditions given, boric acid will react with cesium hydroxide to form cesium metaborate. A model is proposed for this chemical reaction.

12. KEY WORDS/DESCRIPTORS *(List words or phrases that will assist researchers in locating the report.)*

boric acid
cesium hydroxide
chemical thermodynamics
chemistry
containment bypass
deposition and revaporization
light water reactors
oxidized stainless steel
severe accident chemistry
severe accident source terms
severe accidents
source terms
thermochemical data
VICTORIA

13. AVAILABILITY STATEMENT

Unlimited

14. SECURITY CLASSIFICATION

(This Page)
Unclassified

(This Report)
Unclassified

15. NUMBER OF PAGES

16. PRICE

Federal Recycling Program

UNITED STATES
NUCLEAR REGULATORY COMMISSION
WASHINGTON, DC 20555-0001

OFFICIAL BUSINESS
PENALTY FOR PRIVATE USE, $300

SPECIAL FOURTH-CLASS MAIL
POSTAGE AND FEES PAID
USNRC
PERMIT NO. G-67

120555139531 1 1AN
US NRC-OADM
DIV FOIA & PUBLICATIONS SVCS
TPS-PDR-NUREG
2WFN-6E7
WASHINGTON DC 20555